Technical and Economical Evaluation of Measures Decreasing Inductive Interference of Metallic Pipelines

PhD Thesis
submitted by

René Braunstein

Institute of Electrical Power Systems
Graz University of Technology

Supervisors:
Univ.-Prof. DI Dr. techn. Lothar Fickert
DI Dr. techn. Ernst Schmautzer

Reviewers:
Univ.-Prof. DI Dr. techn. Lothar Fickert
Graz University of Technology

Assoc. Prof. Petr Toman, PhD
Brno University of Technology

Head of Institute: Univ.-Prof. DI Dr.techn. Lothar Fickert

A - 8010 Graz, Inffeldgasse 18-I
Phone: (+43 316) 873 – 7551
Fax: (+43 316) 873 – 7553
http://www.ifea.tugraz.at
http://www.tugraz.at

Graz / January – 2012

TU Graz Graz University of Technology – Erzherzog Johann-University

Acknowledgements

This PhD thesis was written during my time as university assistant at the Institute of Electrical Power Systems at Graz University of Technology.

I would like to thank Prof. Lothar Fickert for his willingness to supervise this thesis, his help and his support. I will never forget our carried out investigation regarding a data centre in Romania.

I would like to thank Prof. Toman for his acceptance to rewiew this thesis, the discussions and the hints for this thesis.

I would like to thank Ernst Schmautzer for having the possibility to work on the field of inductive pipeline interference independently. Thanks for confirming me in carrying on the road. Pipeline interference projects where sometimes time-critical, but at the end of the day they contributed to the impact of this thesis. Many thanks for being a reliable contact partner during the years.

Many thanks go to Prof. Herwig Renner for the interests in this work. He never lets young scientists forget to go on with their scientific work.

I would like to thank my colleague Katrin Friedl. We often were in the same position and had a good cooperation.

Sincere thanks go to Beti Trajanoska for her openness, support and interest especially at the end of my studies.

I would like to thank my colleague Emanuel Fuchs for the numerous conversations which helped each other to keep on the path.

I would like to thank my former colleague Werner Friedl who helped me especially during my start of work.

I would like to thank the guys from the earthing measurements, especially Martin Lindinger, Werner Brandauer and Mario Ölz. I will always remember our measurements in Rodund and in Dürnrohr.

Special thanks go to Josef Gugerel from EVN Netz GmbH for the possibility to carry out measurements on an EVN pipeline and for the useful hints regarding specific costs of pipeline interference voltage mitigating measures.

Without the within the progress of this work supervised bachelor- and master theses, some in this thesis derived conclusions would not be possible. Therefore I want to thank Michael Muffat and Thomas Mayer. Special thanks go to Mario Ölz and Christian Wahl.

I want to thank my friend Thomas. Thanks for the numerous discussions that I do not want to miss. Thanks for explaining life and jobs to each other.

I want to thank my friends Mario and Walter for our time in Graz. I cherish the way you see things in life.

I also want to thank my family. They were always calm and never doubted that I will finish this thesis.

My final word of thanks goes to my fiancé Corina. We have gone through thick and thin and will continue the path.

Abstract

Based on growing infrastructure more and more metallic oil- or natural gas pipeline systems reach the interfering area of high-voltage overhead lines and electric railway systems.

This PhD thesis deals with the inductive interference of metallic pipelines by high-voltage overhead lines and electric railway systems.

In addition to the limits of the pipeline interference voltage regarding personal safety in normal operation as well as short-circuit situations of the interfering systems, it is nowadays a matter to keep a voltage limit regarding AC corrosion likelihood whereas a current density criterion at coating holidays has to be observed.

In addition to that computational models for simulating the pipeline interference voltages under consideration of pipeline interference voltage mitigating measures such as AC earthing systems, isolating joints and compensation conductors, are developed within this PhD thesis.

With the help of the developed computational models, as well as with measurements carried out in the context of this thesis, the functionalities of the most important pipeline interference voltage mitigating measures are described, including an analysis of the dependency of the pipeline reduction factor on the horizontal distance.

The comparison between the impacts of electric railway systems and high-voltage overhead lines on pipeline interference voltages shows different results for the vicinity and the far area.

Based on practical experiences in the area of mitigating inadmissible interference voltages by AC earthing systems, algorithms for the optimum positioning of AC earthing systems are developed within this thesis. The functionality of algorithms as well as the effectiveness of the investigated pipeline interference voltage mitigating measures are investigated and evaluated economically and technically on the basis of a representative case study including solution scenarios in which the impact of seasonal varying specific soil resistivity is included.

Keywords: AC corrosion, inductive interference, galvanic interference, coating holidays, earthing systems, isolating joints, compensation conductors, pi-circuits, digital simulation, comparison and evaluation of measures

Kurzfassung

Aufgrund der wachsenden Infrastruktur gelangen immer mehr metallische Öl- oder Erdgasleitungssysteme in den Einflussbereich von Hochspannungsfreileitungen und elektrischen Bahnsystemen.

Die vorliegende Dissertation beschäftigt sich mit der induktiven Beeinflussung metallischer Rohrleitungen durch Hochspannungsfreileitungen und elektrische Bahnanlagen.

Neben den Grenzen der Rohrleitungsbeeinflussungsspannung zur Wahrung des Personenschutzes im Normalbetrieb als auch im Fehlerfall der beeinflussenden Systeme gilt es heutzutage im Normalbetrieb auch Spannungsgrenzen in Bezug auf die Wahrscheinlichkeit des Auftretens von Wechselstromkorrosion einzuhalten, wobei ein Stromdichtekriterium an Umhüllungsfehlstellen der Rohrleitung gilt.

Des Weiteren werden in dieser Dissertation Berechnungsmodelle zur Simulation von Beeinflussungsspannungen unter Berücksichtigung von beeinflussungsspannungs-reduzierenden Maßnahmen wie Wechselstromerdungsanlagen, Isolierkupplungen und Kompensationsleitern entwickelt. Mit Hilfe der entwickelten Berechnungsmodelle sowie von im Zusammenhang mit dieser Arbeit durchgeführter Messungen werden die Funktionaltäten der wichtigsten Maßnahmen zur Reduktion von Beeinflussungsspannungen entlang induktiv beeinflusster Rohrleitungen beschrieben, wobei auch auf die Analyse der Abhängigkeit des Rohrleitungsreduktionsfaktors vom Horizontalabstand eingegangen wird.

Der Vergleich der Auswirkungen von elektrischen Bahnsystemen und Hochspannungsfreileitungen auf die Beeinflussungsspannungen induktiv beeinflusster Rohrleitungen zeigt unterschiedliche Ergebnisse für den Nah- und den Fernbereich.

Anhand praktischer Erfahrungen auf dem Gebiet der Reduktion von unzulässigen Beeinflussungsspannungen durch Wechselstromerdungsanlagen, werden in dieser Arbeit Algorithmen zur optimalen Standortwahl von Wechselstromerdungsanlagen entwickelt. Die Funktionalität der Algorithmen als auch die Wirkungsweise der untersuchten beeinflussungsspannungsreduzierenden Maßnahmen werden untersucht und anhand von einer repräsentativen Fallstudie mit möglichen Lösungsszenarien wirtschaftlich und technisch bewertet, wobei auch die Auswirkungen jahreszeitlichen Schwankungen des spezifischen Erdwiderstandes miteinbezogen wird.

Schlagwörter: Wechselstromkorrosion, induktive Beeinflussung, ohmsche Beeinflussung, Fehlstellen, Erdungsanlagen, Isolierkupplungen, Kompensationsleiter, Pi-Schaltungen, digitale Simulation, Vergleich und Bewertung von Maßnahmen

STATUTORY DECLARATION

I declare that I have authored this thesis independently, that I have not used other than the declared sources / resources and that I have explicitly marked all material which has been quoted either literally or by content from the used sources.

…… ……..

date (signature)

Contents

1 Introduction

1.1 Overview

Due to spatial planning measures, it comes in the area of natural gas- oil and district heating pipelines to increased approaches with high voltage transmission lines as well as with electric railway systems which lead to electromagnetic interference. In general inductive, capacitive and conductive interferences cumulate to electromagnetic interference [4]. In the case of buried metallic pipelines, capacitive interference plays a minor role because there is a shielding effect of the electric field by earth.

Conductive interference means the galvanic coupling of currents, through the flow field in earth. The galvanic influence is to be examined above all in fault conditions [4].

Inductive interference stands for the magnetic coupling of a current carrying conductor and a pipeline, which has to be examined especially for long parallel courses of influencing and influenced systems. The inductive interference is the most important type of interference, in the area of pipeline network interference. Induced voltages along influenced pipelines may cause dangerous touch voltages and propagate AC corrosion [4].

There exist several measures to reduce induced pipeline interference voltages. It is a scope of this thesis to investigate selected measures in detail in order to simplify future electromagnetic pipeline interference investigations and optimisation tasks to minimize pipeline interference voltages.

1.2 Motivation

This thesis was developed during the author's employment as scientific university assistant at the Graz University of Technology, Institute of Electrical Power Systems. Based on the increasing infrastructure more and more pipelines are over several kilometres in the vicinity of high-voltage lines and electric railways. As a consequence AC corrosion got a real topic for Austrian pipeline operators. As a result a proper cathodic corrosion protection and an accurate pipeline coating are nowadays a must. In addition to these measures, there exist active, constructional measures to reduce the pipeline interference voltages such as earthing of the pipeline, the installation of isolating joints and the burying of compensation conductors. Motivation for this thesis is to establish knowledge for the efficiency of these measures and to provide comprehensible strategies for a sustainable reduction of the pipeline interference voltage. The main ideas for this thesis were developed by dealing with national and partly cross-border (Italy, Germany) projects regarding pipeline interference. The constant work on this topic enabled additional projects and implicated important topics on the institutes teaching agenda.

1.3 Research Problem

The problem of inductively interfered pipelines exists in almost every country. The mitigation of pipeline interference voltages is treated differently. The technical problems are mostly solved by engineering companies or university institutes. Most of them use complete commercial software packages for computing conductive and inductive interference. It's the main objective of this thesis to develop adequate models and tools to simplify future pipeline interference investigations and optimisation tasks in order to be independent and to have the possibility to implement tools and features to comply with future and upcoming tasks. Pipeline interference mitigating measures like AC earthing systems, isolating joints as well as compensation conductors are integrated in the simulation model. The effectiveness of these measures are investigated and evaluated at which general statements should be developed. The preferred fields of application of each mitigation measure is analysed in order to get new information for future discussions with pipeline operators and operators of high-voltage lines as well as electric railways.

AC corrosion is a recent keyword regarding pipeline interference. There are a lot of parameters influencing the AC corrosion likelihood, such as the humidity of the soil, the pH-value of the soil, the specific soil resistivity, the coating holiday[1] diameter etc. The electrical parameters that nowadays are associated with AC corrosion (for example coating holiday diameter, coating holiday resistance, current densities at coating holidays) are examined in this thesis to compare differences between the voltage and the current density criteria's for the AC corrosion likelihood.

Nowadays pipeline interference voltages should be reduced by a combination of passive elements such as AC earthing systems, isolating joints and compensation conductors. The impacts of these measures are evaluated technically and economically in this thesis, whereas the optimisation of AC earthing systems along an influenced pipeline with the help of algorithms is considered.

[1] Small defects of the isolating pipeline coating are denominated as coating holidays.

1.3.1 Research Questions

Based on the mentioned research problem, the following research questions are formulated:

Research questions	Chapters
Why do AC earthing systems have to be low impedant (≤ 1Ω) to reduce pipeline interference voltages to acceptable values?	2.2.3, 4.1
Under which circumstances are the current densities at coating holidays below the threshold limits of 100 A/m^2 and 30 A/m^2 ?	3.5, 3.7
How do reduction factors of compensation conductors change with varying horizontal distances between compensation conductor and pipeline?	4.3
Which interfering system (400 kV overhead lines/ electric railways) has a greater influence on pipeline interference voltages?	5.4
What role does the seasonal changing of the specific soil resistivity play in planning and operation processes of effective earthing systems?	6.1, 7.2
Which benchmark for an economical comparison of pipeline interference voltages mitigating measures is derivable?	7.3
What are the preferred pipeline interference voltage mitigating measures, and where are they applied?	4, 7.4
How can practical optimisation procedures for achieving optimal locations of AC earthing systems be described with algorithm?	8.2, 8.3

Table 1.1: Research Questions

1.3.2 Research Tasks

Based on the mentioned research questions, the following concrete research tasks are identified:

1. Development of a model for computing the pipeline interference voltages along inductively interfered pipelines.

2. Integration of the possibilities of AC earthing systems and isolating joints in the simulation model.

3. Investigation of the electrical conditions for AC corrosion from an electrical engineering point of view as for example the correlation between the size of coating holidays, specific soil resistivity, current densities at coating holidays and AC corrosion likelihood.

4. Investigation of the influence of compensation conductors and developing a tool for computing the reduction factor of compensation conductors. Investigation of the impact of varying compensation conductor positions. Stating the impact of different phase conductor arrangements.

5. Investigation and comparison of the influences of 400 kV overhead lines and electric railways on pipelines and AC corrosion.

6. Performance of statistical analyses based on long-term measurements of the specific soil resistivity and performing.

7. Technical as well as economical evaluation of mitigating measures of the pipeline interference voltage. Working out the preferred fields of application of the investigated measures for the mitigation of pipeline interference voltages.

8. Developing algorithms for an automated application of AC earthing systems at the most advantageous connection points.

1.4 Scope of the Research

In thesis mainly the inductive interference of metallic pipelines is treated. In the case of the investigation of coating holidays there are some considerations regarding conductive interference. In this thesis primarily low frequency (16.7 Hz, 50 Hz) interference is investigated. Considerations regarding pipeline impedances for high frequencies complete this investigation.

1.5 Research Methods

The mutual impedances for calculation of the induced pipeline voltages are calculated with the infinite series of Carson and Pollaczek. The pipeline interference voltage distribution is calculated with the within this thesis developed Matlab®-based programme PipePotentials which bases on the pipeline impedance formulas of Michailow and Rasumov and the solution of the nodal admittance matrix. Specific soil resistivities for the dimensioning of earthing systems are measured by the Wenner-method. Statistical methods are applied for investigating the seasonal changes of the specific soil resistivity. The measures to mitigate pipeline interference voltages are evaluated with the help of a characteristic case study including four solution scenarios. The economic evaluation of these measures is based on the approach of stating € per reduced Volt.

1.6 Previous Work

Induced pipeline voltages due to long parallel routes between pipelines and high voltage systems or electric railway systems are a well-known problem since the early 1960ies. In these times in Austria several publications of Richard Muckenhuber (for example [31], [32], [33]) appeared. Muckenhuber referred to the infinite series of Carson [17] and Pollaczek [18]. These formulas are used up to now for calculating induced pipeline voltages in longitudinal direction. By now there exist some modifications, with more or less members for increasing accuracy or different frequencies. Nowadays they can be found in technical literature regarding Electrical Power Systems and in calculation directives, for example in [29] and [46]. The 1990 by Ernst Schmautzer, a student and later assistant of Prof. Muckenhuber, published dissertation [3], deals with the automated calculation of the mutual impedances for any type of geometrical situation (parallel, angular etc.) between pipeline and interfering system. Schmautzer introduces the formulas of Michailow and Rasumov [5] that enable to calculate pipeline impedances in shunt- and in longitudinal direction. In a publication of 1994 [22] the hint of using Monte-Carlo algorithms for optimising locations of AC earthing systems can be found. Subsequent and actual references (for example [13], [30], [22]) show how the same problem occurs in different countries as for example in Germany, Poland and Egypt. In

2004 at Graz University of Technology the diploma thesis of Werner Friedl [34] was published. Within Friedl's thesis a Simulink® based model was developed in order to calculate pipeline interference voltage distributions. The elements of the Pi-circuits were generated with the help of the power systems toolbox. Under some circumstances, for example for input parameters like higher specific coating resistivities than 100 $k\Omega m^2$ or large pipelines with more than 100 km, the computation oscillates and doesn't reach a solution. These problems of this valuable previous work can be avoided by using the concept of the nodal admittance matrix, which was implemented in this work.

In 2006 the effectiveness of buried compensation conductors was well discussed in Germany. Some calculation results and experiences with compensation conductors as pipeline interference voltage mitigating measures are found in [36]. In 2007 a 7-km long test compensation conductor was buried in the same route with an Austrian pipeline. This makes it possible to investigate the influence of the compensation conductor in detail within this thesis.

A new focus is to analyse AC corrosion processes. Therefore electrochemical analyses from Büchler, Schöneich et al. (for example [11], [24]) have to be mentioned. Valuable and practicable elaborations are found in the Cigré Technical Brochure Nr. 290 [1] of 2006 and in a Technical report [15] of Graz University of Technology and Vienna University of Technology, where electrochemists modelled together with electrical engineers the electrochemical processes at coating holidays. The CEN/TS 15280 prestandard [9] delivers reference values for the AC corrosion risk and concludes the list of relevant ground- and frameworks for this thesis.

1.7 Scientific Contribution

This thesis builds on previous and actual works. A lot of research colleagues nowadays use commercial software packages for Electromagnetic Fields- and Interference problems. Within the scope of this thesis the MATLAB®-program PipePotentials was developed in order to calculate interference voltage distributions of any pipeline configuration for user-defined earthing systems and isolating joints. Therefore independent simulations and interpretations are possible and contained in this work. This thesis creates new concepts of view such as the "moving fault location" of high voltage lines, described by Muckenhuber [31], [32], for instance is picked up and used in a new context to show a new method for calculating and interpreting the influence of moving, electric railways. In this work new concepts (pipeline interference voltage, one side-, balanced- and unbalanced earthing) are introduced and effects are named like the "self-earthing-effect" of an inductively interfered pipeline. Within this thesis it is shown that in regions with higher soil resistivities possibly higher pipeline

interference voltages can be accepted according to the admissible current densities for evaluating AC corrosion risk. In this thesis it is shown that the assumption of the maximum inducing current along the whole approach of a railway system and a pipeline demonstrates a worst-case. Accordingly for future investigations also relevant load flow situations of interfering high-voltage lines should be taken into account in order to evaluate AC corrosion risks. Within the context of this PhD thesis the experimental setup of the measurement of the impact of the first Austrian scientific test compensation conductor and the proof of the best compensation conductor switching scenarios are developed.
In this thesis it is shown that the pipeline reduction factor depends on the horizontal distances between compensation conductor, pipeline and interfering system, consequently usually applied constant reduction factors don't reflect realistic conditions.
Within the scope of this thesis the influence of the seasonal varying specific soil resistivity on earthing systems and consequently on the pipeline interference voltage was demonstrated.
Within this thesis two new algorithms are designed in order to simulate the practical optimisation steps of an expert.

1.8 Outline of the Thesis

After Chapter 1 („Introduction") the Chapter 2 of this thesis describes standards and recommendations concerning admissible interference voltages and current densities as well as the theoretical computation background regarding differential equations, mutual impedances and the equivalent network of inductively interfered pipelines.

In chapter 3 the AC corrosion process at coating holidays and cathodic corrosion protection are described. Moreover chapter 3 deals with the correlation between coating holiday diameter, specific soil resistivity, induced voltages, current densities and AC corrosion likelihood.

In the chapter 4 the function and impact of the in this thesis investigated pipeline interference voltage mitigating measures AC earthing systems, isolating joints and compensations conductors as well as a brief description of measures like the increasing of the horizontal distance between interfering and interfered system, varying phase conductor arrangements as well as partial and full (active) compensation are described.

In chapter 5 the impacts of the most interesting origins of inductively interference- electric railways and 400 kV overhead lines are investigated and compared with each other for the normal operation and the short-circuit situation.

In chapter 6 the seasonal changes of the specific earth resistance for the upper and deeper layers are quantified, based on an annual measuring series of the specific soil resistivity.

Within the in chapter 7 carried out case study the impact of the seasonal varying specific soil resistivity on AC earthing systems and consequently on pipeline interference voltages is quantified. Furthermore the specific costs of the in this thesis investigated pipeline interference voltage mitigating measures are evaluated.

Chapter 8 describes the present calculation- and optimisation procedures as well as two algorithms in order to simulate the practical optimisation procedures of an expert to achieve optimal locations of AC earthing systems along inductively interfered pipelines.

2 Pipeline Interference Voltages

In the first part of this chapter actual limiting values for induced pipeline voltages regarding risk of hazard as well as AC corrosion likelihood are described. In the second part of this chapter all necessary calculation steps for receiving pipeline interference voltage distributions are shown. After discussing induced pipeline voltages with differential equations, it is especially gone into the numerical solution which means the connection of mutual impedances, pipeline parameters and nodal network admittance matrix. The basic pipeline interference voltages for the full parallel approach or the partial parallel approach between interfering system and pipeline conclude this chapter.

2.1 Admissible Pipeline Voltages

An investigation of the inductive interference on inadmissibly high touch voltages in buried pipelines has usually to be investigated for high-voltage lines with rated voltages higher than 110 kV, as well as for railway systems [4].

Due to the magnetic field of the interfering systems, AC currents are flowing along interfered pipelines. These currents lead to potential differences along the pipeline to *reference earth* [13]. The in the following introduced relevant guidelines [1], [7], [8], [9], unequally use the terms *induced voltages* or *pipeline potentials*.

In [8] a comprehensible declaration is written: ”The *interference voltage* is due to inductive, conductive and capacitive coupling and occurs between pipeline and *remote earth* (*reference earth*).*”*

Based on this explanation the notations *interference voltage, („Beeinflussungsspannung”)*, and *pipeline interference voltage distribution, („Rohrleitungsbeeinflussungsspannungsverteilung”)* are further used in this thesis.

2.1.1 Risk of Hazard

With the following criteria an overview, under which conditions no inadmissibly high touch voltages in pipelines are to be expected and in which cases a special investigation of the possible interference is necessary, is given.

limiting values for pipe potential U_P	type of interference	Measures for the protection against inadmissible touch voltages
$U_P \leq 65$ V	**long-term**	**none**
$U_P > 65$ V	**long-term**	- Connection of earthing systems, to reduce the pipe potential below 65 V (TE30, chapter 4.1.1) or - Potential grading to reduce touch voltage below 65 V (TE30, chapter 4.1.2)
$U_P \leq 500$ V	**short-term**	**none**
$U_P > 500$ V	**short-term**	- Measures according to TE30, chapter 4.1.3 (improved insulation), and TE30, chapters 4.2 (insulating joints), 4.3, 5.2 and 5.3 or - Connection of earthing systems according to TE30, chapter 4.1.1 to reduce the pipe potential below 500 V or - Potential grading or rather Isolation of location to reduce touch voltage below 500 V according to TE30, chapter 4.1.3

Table 2.1: Limiting values for pipe potential as well as protective measures against inadmissible touch voltages. Extracts from TE 30 [7]

According to TE 30 [7] and AfK Nr. 3 [8] it is principally distinguished between long-term interference and short-term interference. Simplistically a long-term interference can be understood by everlasting interferences as for example in normal operation modes of electric railways and high-voltage lines. One understands by short-term interference an interference with durations smaller than 0.5 seconds like it appears, for example in short-circuit modes. Therefore in normal operation mode pipeline interference voltages below 65 V have to be addressed. Under short-circuit conditions a pipeline interference voltage below 500 V has to be kept [7].

2.1.2 Risk of AC Corrosion

Boundary values regarding pipeline interference voltages are arranged in CEN/TS 15280 [9]. In it, the following definitions can be found:

“To reduce the AC corrosion likelihood on a buried pipeline, the pipeline AC voltage should not exceed at any time:

- 10 V where the local soil resistivity is bigger than 25 Ωm;

- 4 V where the local soil resistivity is less than 25 Ωm;

These values should be considered as threshold limits which significantly reduce AC corrosion likelihood; they are based on long-term practical experience of European pipeline operators [9]”. Practical experiments [11], [24] show that under certain circumstances up to 15 V can be tolerated in case of suitable settings of the cathodic protection potential.

In addition to the AC voltage-criterion, there exists an additional criterion regarding current densities at coating holidays. Referring to European standards and recommendations [9], [25] a pipeline can be considered as sufficiently protected from AC corrosion, if the rms AC current density is lower than 30 A/m^2. Medium AC corrosion likelihood exists for current densities between 30 A/m^2 and 100 A/m^2. Very high AC corrosion risk occurs for current densities higher than 100 A/m^2.

Procedures at coating holidays of inductively interfered pipelines and the correlation between specific soil resistivity, coating holiday diameter, interfering voltage and current density on coating holidays are investigated and described in chapter 3.

2.2 Calculation of Induced Interference Voltages

2.2.1 Differential Equations

The pipeline interference voltages can be calculated with the help of differential equations. Therefore the common lattice equivalent network of a conductor (see figure 2.1) with a galvanic shunt addmitance g_L and an impedance in longitudinal direction Z_L are used. The interfering system carries the current I. The variable zg stands for the mutual impedance between the interfering system and the pipeline (see chapter 2.2.2 for the detailed calculation). The pipeline is terminated with the resistances R_1 and R_2 at its ends.The following equations and procedures in the formulas (1) - (13) are taken from the literature [33].

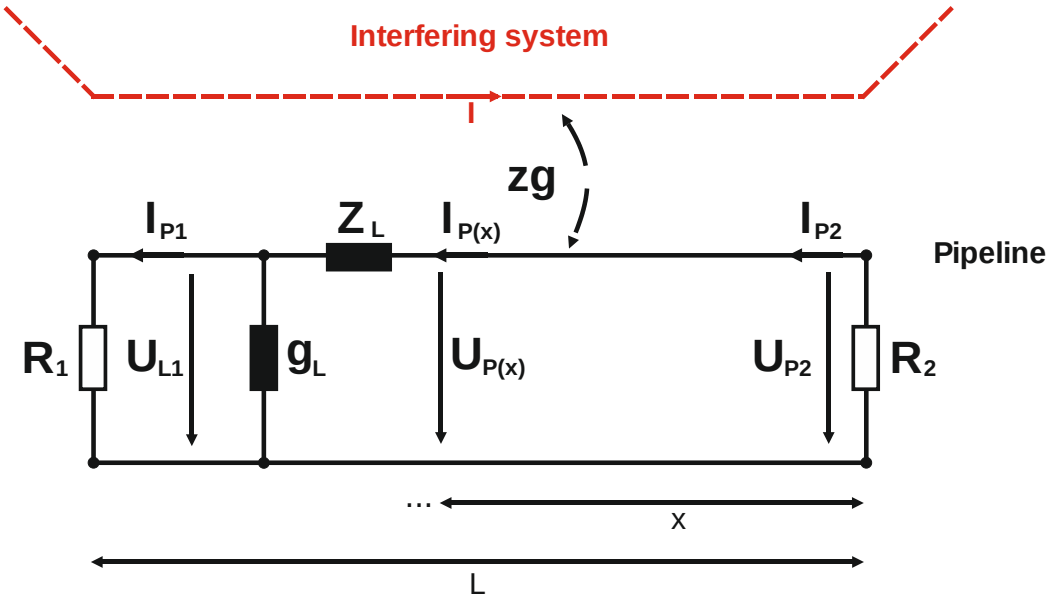

Figure 2.1: Inductive interference of a conductor [33], modified

The complex transfer constant γ, the coupling factor κ and the characteristic wave impedance W (see formulas (1) – (3)) are introduced before setting up the differential equations for the pipeline interference voltages.

$$\gamma = \sqrt{Z_L \cdot g_L} \quad (1)$$

γ	Complex transfer constant
Z_L	Longitudinal direction impedance (Ω/km)
g_L	Galvanic conductance per unit length (S/km)

$$\kappa(x) = \frac{zg(x)}{Z_L} \quad (2)$$

κ	Coupling factor
zg(x)	Mutual impedance between interfering system and pipeline (Ω/km)

$$W = \sqrt{\frac{Z_L}{g_L}} \quad (3)$$

W	Characteristic wave impedance

The differential equations for the interfering problem in figure 2.1 can be stated as:

$$\frac{d^2U_P}{dx^2} = \gamma^2 \cdot U_P + \gamma \cdot W \cdot \kappa'(x) \cdot I \quad (4)$$

$$\frac{d^2I_P}{dx^2} = \gamma^2 \cdot [I_p - \cdot\kappa(x) \cdot I] \quad (5)$$

I	Interfering current (A)

The differential equations can be solved with the method of the variation of the constants, assuming no parallel approach, which means that the mutual impedance zg and the coupling factor κ are functions of the distance x, the pipeline interference voltages and currents can be formulated with the equations (6) and (7).

$$U_{P(x)} = U_{P2} \cdot \cosh(\gamma \cdot x) - W \cdot I_{P2} \cdot \sinh(\gamma \cdot x) + \gamma \cdot W \cdot I \cdot \int_0^L \kappa(\xi) \cdot \cosh(\gamma) \cdot (x - \xi)\, d\xi \quad (6)$$

$$I_{P(x)} = I_{P2} \cdot \cosh(\gamma \cdot x) - \frac{U_{P2}}{W} \cdot \sinh(\gamma \cdot x) - \gamma \cdot I \cdot \int_0^L \kappa(\xi) \cdot \sinh(\gamma) \cdot (x - \xi)\, d\xi \quad (7)$$

As it is shown in the introduced case (figure 2.1), the pipeline is terminated with the resistances R_1 and R_2. Therefore the boundary conditions (8) and (9) are introduced:

$$U_{P1} = R_1 \cdot I_{P1} \quad (8)$$

$$U_{P1} = -R_2 \cdot I_{P2} \quad (9)$$

By the boundary conditions, the system of equations is complete and can be solved. The pipeline interference voltages U_{P1} and U_{P2} at the beginning and the end of the lattice network result to:

$$U_{P1} = \gamma \cdot I \cdot R_1 \cdot \left(1 - \frac{1}{\cosh(\gamma \cdot L) + \frac{W}{R_2} \cdot \sinh(\gamma \cdot L)} \right) \cdot \int_0^L \kappa(\xi) \cdot \frac{\sinh(\gamma \cdot \xi) + \frac{W}{R_2} \cdot \cosh(\gamma \cdot \xi)}{\cosh(\gamma \cdot L) + \frac{W}{R_2} \cdot \sinh(\gamma \cdot L - 1)} \, d\xi \quad (10)$$

$$U_{P2} = -\gamma \cdot I \cdot R_2 \cdot \left(1 - \frac{1}{\cosh(\gamma \cdot L) + \frac{W}{R_1} \cdot \sinh(\gamma \cdot L)} \right) \cdot \int_0^L \kappa(\xi) \cdot \frac{\sinh(L - \xi) + \frac{W}{R_1} \cdot \cosh(I - \xi)}{\cosh(\gamma \cdot L) + \frac{W}{R_1} \cdot \sinh(\gamma \cdot L - 1)} \, \xi \quad (11)$$

In case of a pure parallel approach (constant coupling factor κ), the terms (10) and (11) for U_{P1} and U_{P2} are simplified to:

$$U_{P1} = \kappa \cdot I \cdot R_1 \cdot \left(1 - \frac{1}{\cosh(\gamma \cdot L) + \frac{W}{R_2} \cdot \sinh(\gamma \cdot L)} \right) \quad (12)$$

$$U_{P2} = -\kappa \cdot I \cdot R_2 \cdot \left(1 - \frac{1}{\cosh(\gamma \cdot L) + \frac{W}{R_1} \cdot \sinh(\gamma \cdot L)} \right) \quad (13)$$

When considering non parallel approaches or distributed earthing systems along the pipeline, the setting up and the solution of the introduced differential equations gets rather complex. Therefore within the scope of this work a numerical approach is preferred. For that purpose the calculation of the mutual impedances, the electrical pipeline parameters as well as the setting up and the solution of the nodal admittance matrix are needed. The necessary procedures are described in the following subchapters 2.2.2 – 2.2.4.

2.2.2 Mutual Impedances

The calculation and analysis of the inductive interference of the concerned pipelines due to operational and short-circuit currents occurs in a first step by determination of the inductive coupling by calculating the mutual impedances due to the infinite series of Carson and Pollaczek [17], [18]. The next figure 2.2 shows the mirror model of two conductors with earth return, which is crucial for the calculation of the mutual impedances.

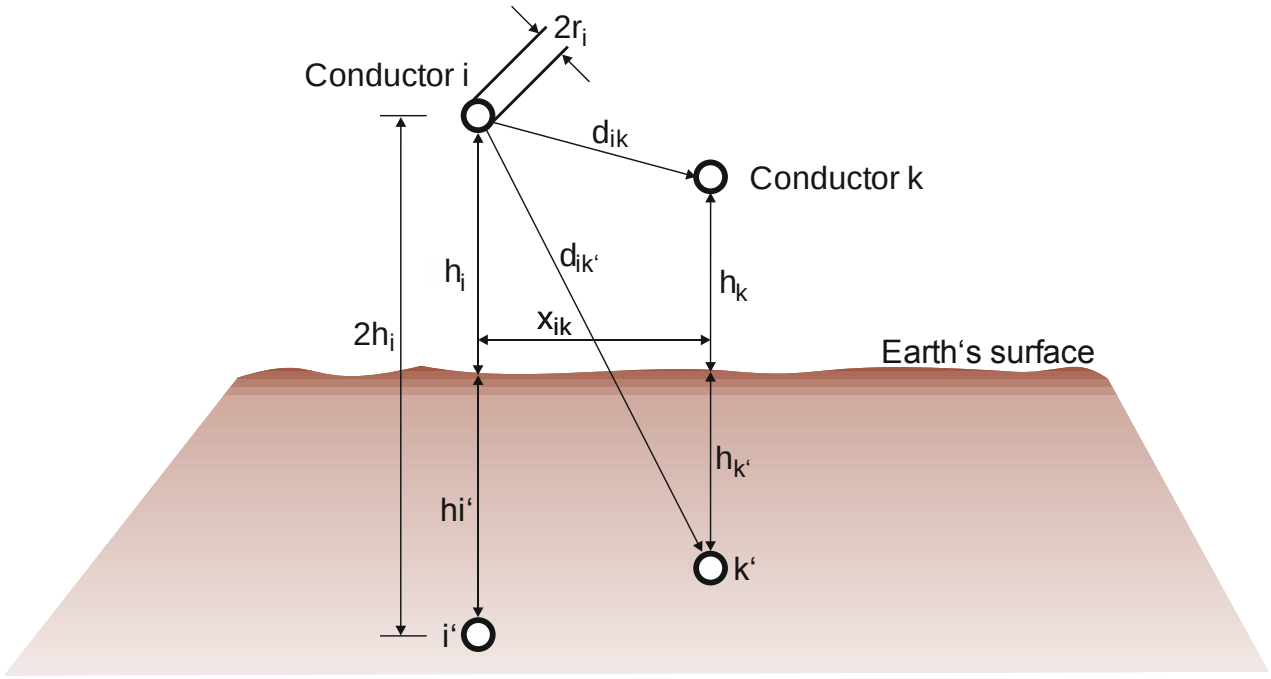

Figure 2.2: Mirror-model for calculating mutual impedances between two conductors [29], modified

Simplified formulas for the mutual impedances can be found in technical literature regarding Electrical Power Systems [29] and in international calculation directives [46]. In the following simplified Carson formulas (13) – (22) are quoted from [29]. The geometrical parameters r_i, h_i, x_{ik}, d_{ik}, $d_{ik'}$ and h_k are shown in the figure 2.2. The other important parameters are described directly below the formula.

Self-impedances Z_{ii} per unit length:

$$Z_{ii} = R_i + \frac{\omega \cdot \mu_0}{8} + j \cdot \frac{\omega \cdot \mu_0}{2\pi} \left(\frac{1}{4} + \ln \frac{D_E}{r_i} \right) \quad (14)$$

R_i: Resistance per unit length of conductor I (Ω/m)
ω: Angular frequency
ω=2πf (1/s)
f: Interfering signal frequency (Hz)
μ_0: Magnetic field constant, $\mu_0 = 4\pi 10^{-7}$ (Vs/Am)

D_E Depth of equivalent earth return conductor (m)

$$D_E = \frac{\sqrt{2e}}{\gamma}\,\delta_e = \frac{\sqrt{2e}}{\gamma}\sqrt{\frac{2\rho}{\omega\mu_0}} = \frac{\sqrt{2}}{\alpha_e} = 658.80\sqrt{\frac{\rho}{f}}\ \ (m)\ \ (15)$$

e: Euler's number 2.718

γ: Bessel constant 1.781

$\delta_{E:}$ Penetration depth in earth (m)

ρ: Specific soil resistance (Ωm)

Mutual impedances Z_{iK} per unit length above earth's surface (h_i and $h_k \geq 0$ m)

$$Z_{ik} = \frac{\omega \cdot \mu_0}{8} + j \cdot \frac{\omega \cdot \mu_0}{2\pi} \cdot \ln\frac{D_E}{d_{ik}} \quad (16)$$

According to [29], formula (16) is valid as long the Condition C_1 (formula 17) is smaller than 0.5.

$$C_1 = \frac{1.85}{D_E} \cdot \sqrt{(h_i + h_k)^2 + {x_{ik}}^2} \quad (17)$$

For a specific soil resistivity of ρ=100 Ωm and a frequency of f=50 Hz formula (16) is valid for a d_{ik} (horizontal distance between conductors) of approximately 300 m [29]. The dominant parameter of D_E amounts for f=50 Hz and ρ=100 Ωm to approximately 932 m and for f=16.7 Hz to approximately 1612 m. Formula (16) is applicable for the in this thesis carried out investigations because for the investigated high-voltage lines and railway systems (see chapter 5) C_1 is smaller than 0.5.

The borderline case of a conductor lying directly on the earth's surface (h_i or h_k=0) is covered by the following approximation formula (18):

$$Z_{ik} \approx \frac{\omega \cdot \mu_0}{4\pi} \cdot 1.17 \cdot \left(\frac{D_E}{d_{ik}}\right)^2 \quad (18)$$

According to [29], formula (18) is also valid if the Condition C_1 is greater than 3.5. For $0.5<C_1<3.5$ other accurate formulas have to be used.

Mutual impedances Z_{iK} per unit length under the earth's surface (h_i >0 and h_k < 0 m)

For horizontal distances (x_{ik}) between pipeline and interfering conductor of approximately 300 m the condition C_1 is valid and formula (16) has to be used.

For increasing horizontal distances the Conditions C_2 (19) and C_3 (20) get valid and formula (22) has to be used [29].

$$C_2 : \frac{h_i}{x_{ik}} << 1 \quad (19)$$

$$C_3 : \left| e^{j\frac{3\cdot\pi}{4}} \cdot \sqrt{\frac{\omega\mu_0}{\rho}} \right| > 4 \quad (20) \qquad \text{with} \qquad k = e^{j\frac{3\cdot\pi}{4}} \cdot \sqrt{\frac{\omega\mu_0}{\rho}} \quad (21)$$

$$Z_{ik} = \frac{j\cdot\omega\cdot\mu_0}{4\pi} \cdot \left(-4e^{-j\cdot k\cdot k_h} \cdot \frac{1\text{-}j\cdot k\cdot h_k}{k^2\cdot x_{ik}^{\ 2}} \right) \quad (22)$$

For very high distances (x_{ik}) between pipeline and interfering conductor ($x_{ik} > D_E$) C_1 gets greater than 3.5 and formula (18) can be used [29].

With the help of the mutual impedances and the interfering currents, the induced pipeline voltages in longitudinal direction Ud (figure 2.3) can be calculated:

$$\underline{U}d = \underline{z}_g . \ell . \underline{I} \quad (23) \text{ [3]}$$

I	Interfering currents of the electrical power system (A)
zg	Mutual impedance per unit length (Ω/km)
ℓ	Length of parallel course (km)

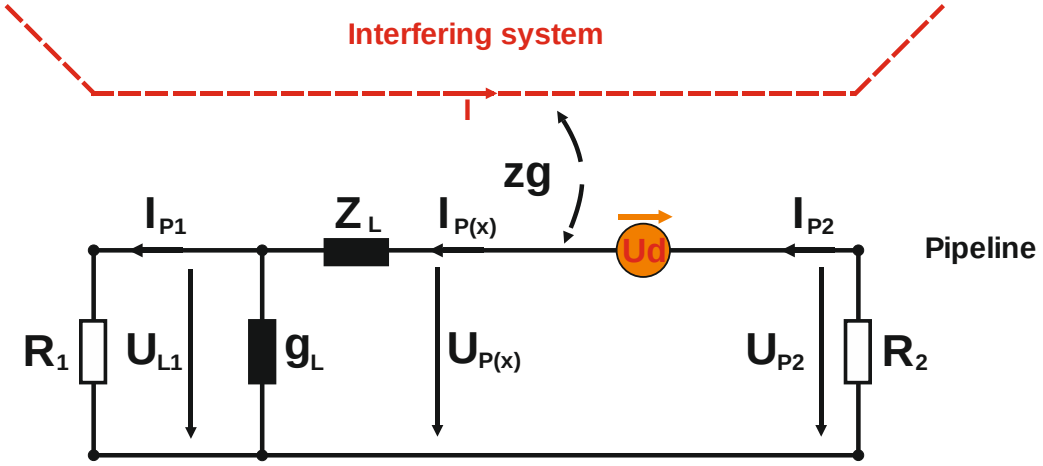

Figure 2.3: Inductive interfered pipeline with induced voltage in longitudinal direction [15], modified

For calculating the pipeline interference voltage distribution the pipeline parameters as the galvanic shunt conductance g_L and the impedance in longitudinal direction Z_L are necessary. The calculation procedures are described in the following subchapter 2.2.3.

2.2.3 Pipeline Parameters

In the following the longitudinal direction and shunt-axis parameters are calculated for a PE-isolated pipeline (r_u = 100.000 Ωm^2) with a radius of 250 mm and a specific soil resistivity of 100 Ωm. The fundamental frequency of the interfering system is assumed with 50 Hz. The pipeline longitudinal direction impedance per unit length (R_L, L_L) and the shunt-admittance per unit length (R_Q, C_Q) are calculated by the formulas of Michailow and Rasumov [3],[5]. The following formulas (24) - (30) and (33) - (34) in this subchapter are taken from [3].

Longitudinal direction-impedance Z_L per unit length:

The pipeline resistivity per unit length r_{L0} results from the resistivity of a full conductor regarding skin effect.

$$r_{Lo} = r'_{Lo} \cdot \left(\frac{R_L}{2\delta_L} + \frac{1}{4}\right) \cdot 10^3 = \frac{\rho_L}{R_L{}^2 \pi} \cdot \left(\frac{R_L}{2\delta_L} + \frac{1}{4}\right) \cdot 10^3 \quad (\Omega/\mathrm{km}) \quad (24)$$

r'_{L0} Pipeline resistivity per unit length without skin effect (Ω/km)
$r'_{Lo} = \rho_L/(\pi \cdot R^2) \cdot 10^3$ (Ω/km) (25)
R_L Pipeline radius (mm)
δ_L Skin depth(mm)

$$\delta_L = \sqrt{\frac{2\rho_L}{\omega \mu_0 \mu_r}} \quad (\mathrm{mm}) \quad (26)$$

ρ_L Specific resistance of the material, for steel approx. 0.16 Ωmm^2/m
f Interfering signal frequency (Hz)
μ_r Relative permeability, for steel approximately 200.

As one can see from formula (26), the skin effect has an impact on the longitudinal direction pipeline resistivity covering. In the supposed case, the skin depth in a steel-pipeline with a radius of 250 mm amounts for 16.70 Hz, which is the common frequency of Austrian railway systems, approximately 3.48 mm. For a fundamental frequency of 50 Hz the skin depth amounts approximately 2.01 mm. The pipeline resistivity covering in direct axis r_{L0} can be calculated to 0.051 Ω/km, for the fundamental frequency of 50 Hz. For the fundamental frequency of 16.7 Hz the pipeline resistivity covering in direct axis r_{L0} amounts to approximately 0.029 Ω/km.

The earth resistivity per unit length r_e is calculated with the following formula:

$$r_e = \frac{\omega \mu_0}{2\pi} \cdot \frac{\pi}{4} \cdot 10^3 \quad (\Omega/\mathrm{km}) \quad (27)$$

The self-resistance of the loop per unit length x_L can be calculated with the following equation:

$$x_L = \frac{\omega\mu_0}{2\pi} \ln\frac{D_e}{R_L} .10^3 \ (\Omega/\text{km}) \quad (28)$$

The inner reactance covering x_{iL0} can be calculated with the following equation:

$$x_{iLo} = x'_{iLo} \frac{2\delta_L}{R_L} .10^3 = r'_{Lo} \frac{R_L}{2\delta_L} = \frac{\rho_L}{2\pi R_L \delta_L} .10^3 \ \ (\Omega/\text{km}) \quad (29)$$

The whole longitudinal direction impedance per unit length Z_L' is calculated with:

$$Z_L' = (r_e + r_{L0}) + j \cdot (x_L + x_{iL0}) \ \ (\Omega/\text{km}) \quad (30)$$

The ohmic component in longitudinal direction r_L for a one kilometer pipeline segment can accordingly be calculated with:

$$r_L = (\text{real}(zL)) \cdot l \ \ (\Omega) \quad (31)$$

The inductive component in longitudinal direction l_L for a one kilometer pipeline segment can accordingly be calculated with:

$$l_L = \frac{(\text{imag}(zL))}{(2 \cdot \pi \cdot f \cdot l)} \ \ (\text{H}) \quad (32)$$

Shunt admittance Y_L' per unit length:

An inductively influenced pipeline can not only be simulated as an ideally isolated buried pipeline. Due to unavoidable coating holidays, and the spatial dimensions of buried pipelines the modelling of shunt elements has also be taken into account. The calculation of the shunt-elements, bases on the assumption of the ladder network as an equivalent network for an inductively influenced pipeline. The main difficulty is the determination of the coating resistance, which is taken by experiences or measurements [19].

The coatings of older pipelines, that were constructed approximately between 1960 and 1975, are made of bitumen with an inside glass fibre tissue. Today's pipeline coatings are principally made of Polyethylene (PE). The existence of coating holidays can never be completely avoided. In idealised considerations, a coating holiday can be seen as a steady galvanic conductance, which depends on the amount of pipeline coatings as well as on the specific soil resistivity. The galvanic conductance per unit length g_L can be estimated with following relation [3], [5]:

$$g_L = \frac{2 \cdot \pi \cdot R_L}{r_u} \cdot 10^3 \ \ (S/km) \ \ (33)$$

r_u On the surface related specific coating resistivity (Ωm^2)

The capacitive conductance per unit length b_L, which arises from the capacity from the pipeline to earth can be calculated with the following formula:

$$b_L = \omega \frac{2 \cdot \pi \cdot \varepsilon_{0.} \varepsilon_R}{\ln \frac{R_L + t_L}{R_L}} \cdot 10^3 \ \ (S/km) \ \ (34)$$

t_L Wall thickness of the metallic pipeline (mm), 3 mm in this example

The whole shunt-admittance per unit length Y_L' is calculated with:

$$Y_L' = g_L + j \cdot b_L \ \ (S/km) \ \ (35)$$

The shunt-ohmic component r_P for a pipeline segment with a length of one kilometre can accordingly be calculated with:

$$r_P = \left(\frac{1}{g_L} \right) / l \ \ (\Omega) \ \ (36)$$

The shunt-capacitive component c_P for a pipeline segment with a length of one kilometre can accordingly be calculated with:

$$c_P = \left(\frac{b_L}{2 \cdot \pi \cdot f} \right) \cdot l \ (F) \quad (37)$$

The whole pipeline impedance (pipeline-earth-loop) can be achieved by solving the quadripole (see also figure 2.6):

$$| Z_{Pipeline} | = | ((Y_L / 2)^{-1} + Z_L) / /(Y_L / 2)^{-1} | (\Omega) \quad (38)$$

To get an overview about the sensitivity of the equivalent pipeline network components for changing parameters as frequency and coating material, the parameters introduced in the formulas (24) – (38) are summarized in the following table 2.2 and in table 12.1 in the appendix of this thesis.

Network Element or derived term	**Bitumen-Coating** ru = 10 kΩm^2			**PE-Coating** ru = 100 kΩm^2			
	16.7 Hz	**50 Hz**	**150 Hz**	**16.7 Hz**	**50 Hz**	**150 Hz**	**Most Determining Factors**
r_{L0} (Ω/km)	0.029	0.051	0.088	0.029	0.051	0.088	f,R_L
r_e (Ω/km)	0.017	0.049	0.148	0.017	0.049	0.148	f
x_L(Ω/km)	0.039	0.083	0.144	0.039	0.083	0.144	f, R_L, ρ
x_{iL0} (Ω/km)	0.029	0.051	0.088	0.029	0.051	0.088	f, R_L
Z_L'(Ω/km)	0.046+ 0.068 j	0.100+ 0.133 j	0.240+ 0.232 j	0.046+ 0.068 j	0.100+ 0.133 j	0.240+ 0.232 j	f, R_L, ρ
|Z_L'|(Ω/km)	0.082	0.167	0.331	0.082	0.167	0.331	f, R_L, ρ
$r_{L\ 1km}$ (Ω)	0.046	0.100	0.236	0.046	0.100	0.236	f, R_L
$l_{L\ 1km}$ (mH)	0.651	0.424	0.246	0,651	0.424	0.246	f, R_L, ρ
g_L(mS/km)	157.1	157.1	157.1	15.71	15.71	15.71	r_u, R_L
b_L(mS/km)	2.40	7.33	21.98	2.40	7.33	21.98	f, R_L
Y_L'(mS/km)	157.1+ 2.45 j	157.1+ 7.33 j	157,1+ 21.98 j	15.71+ 2.45 j	15.71+ 7.33 j	15.71+ 21.98 j	r_u, f, R_L
$r_{p\ 1km}$ (Ω)	6.37	6.37	6.37	63.66	63.66	63.66	r_u, R_L
$c_{p\ 1km}$ (μF)	23.32	23.32	23.32	23.32	23.32	23.32	R_L
|$Z_{Pipeline}$|$_{1km}$ (Ω)	6.38	6.38	6.36	62.91	57.69	37.02	f, ru

Table 2.2: Sensitivity table for elements of pipeline equivalent network for low frequencies

As one can see from table 2.2, the most determining factors for the pipeline equivalent network parameters are the frequency f, the pipeline radius R_L, the specific soil resistivity ρ and the to the surface related specific coating resistivity r_u.

The impedance distribution along the pipeline is an interesting factor regarding induced voltage distribution. The figures in table 2.2 show that primarily the specific coating shunt-resistivity r_u is dominant. The specific coating resistivity r_u results from the coating material, the surrounding soil and the number of coating holidays. In the table 2.2 guideline values as 10000 Ωm^2 for Bitumen-coatings and 100000 Ωm^2 for PE-coatings are applied. The specific coating resistivity for newly constructed PE-pipelines is nowadays mentioned with about 1 MΩm^2 and above. The value of r_u is measured by the pipeline operators, whereas the pure pipeline voltage at switched off corrosion protection and the pipeline potential at switched on corrosion protection are taken into account [19].

A continuous contact to earth, which means a low soil resistivity over the full pipeline length and possible coating holidays lead to a decrement of the specific coating resistivity r_u during the years.

Being aware of the influence of the specific coating resistivity r_u, the following figure 2.4 shows the correlation between the shunt resistance r_P and the specific coating resistivity r_u for variable pipeline radii.

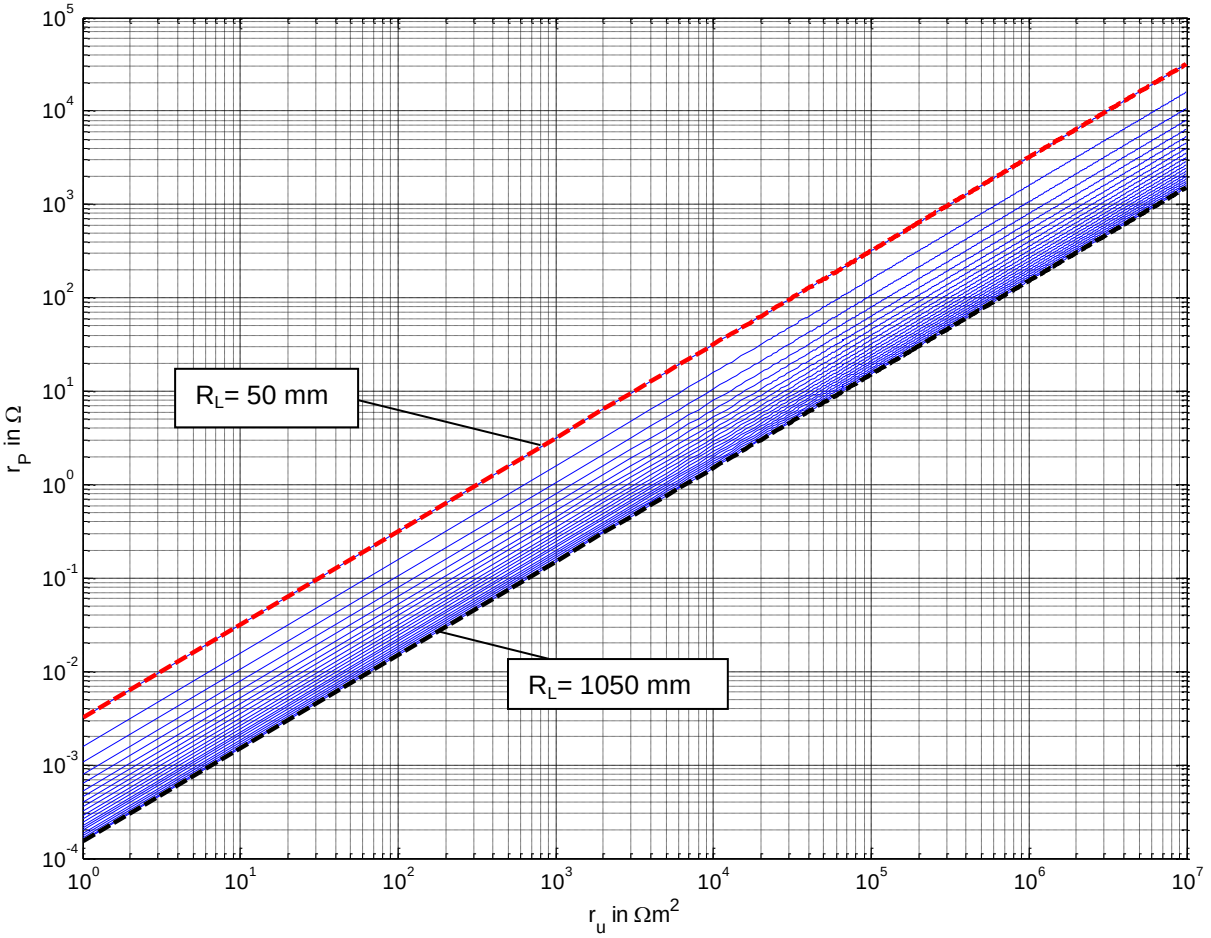

Figure 2.4: r_P plotted against r_u for variable pipeline radii

The figure 2.4 shows how the shunt resistance r_P rises with increasing specific coating resistivity r_u, for 1 km pipeline segments. The specific coating resistivity r_u is varied from 1 Ωm^2 to 10 MΩm^2. The figure 2.4 shows that r_P increases clearly with rising r_u, which underlines the effect of lower induced voltages in Bitumen isolated pipelines than in PE isolated pipelines.

The pipeline radius R_L is varied from 50 mm to 1050 mm in 50 mm steps. The R_L=50 mm series is dotted red; the series with the biggest pipeline radius of 1050 mm is dotted in black. The greater the pipeline radius, the smaller the shunt resistance as well as the induced pipeline voltage distribution.

With the help of Z_L' and Y_L' the whole impedance of the pipeline-earth-loop can be calculated. For the at the beginning of this subchapter introduced PE-isolated pipeline segment with 1 km the absolute value of the pipeline-earth loop $|Z_{Pipeline}|_{1km}$ is 57.69 Ω (see table 2.2). One can imagine that this leads to very low impedances of longer pipeline

networks due to the facts of the rising capacity with increasing pipeline length (formula 37) and the parallel connection indicated in figure 2.6. According to this, the pipeline-earth-loop impedance of a pipeline network consisting of as ten above mentioned 1-km PE-isolated segments is about 5.90 Ω. An equivalent pipeline-earth-loop of a 10-km Bitumen isolated pipeline amounts to approximately 0.88 Ω. As one can see from these explanations, the pipeline acts like a low impedant horizontal earthing conductor for itself. This effect is hereby be titled as self-earthing effect. Consequently pipeline interference voltages can only be significantly reduced by low impedant earthing systems because of this low impedant pipeline self-impedances.

In the appendix of this thesis (see table 12.1) the change of the equivalent network components for frequencies between 1 kHz and 50 kHz are shown. The results show clearly, that the Pipeline impedance gets lower with increasing frequency. The pipeline impedance in longitudinal direction (loop, inductivity) increases with growing frequency. The pipeline shunt impedance (capacity of pipeline-coating to surrounding earth) decreases with growing frequency. The consequence is that the influence of high frequency sources drains off earlier to ground, compared with the influence of low frequency (for example 16.7 Hz 50 Hz) sources.

2.2.4 The Nodal Admittance Modell

With the help of the in the previous subchapter described parameters, influenced pipeline pieces can be modelled as an equivalent network and the distribution of the pipeline interference voltage along an inductive interfered pipeline can be calculated.

To act on the assumption of a homogeneous pipeline, which means that pipeline- constants or the longitudinal direction-impedance per unit length Z_L as well as the shunt admittance per unit length Y_L are constant, an equivalent network can be used (compare figure 2.3). The pipeline is represented by a longitudinal direction-impedance ($r_L + j\omega l_L$) and shunt admittance ($r_p \,//\, 1/j\omega c_p$), at which it has to be mentioned that it can be distinguished between influenced and uninfluenced pipeline segments (figure 2.5) [4].

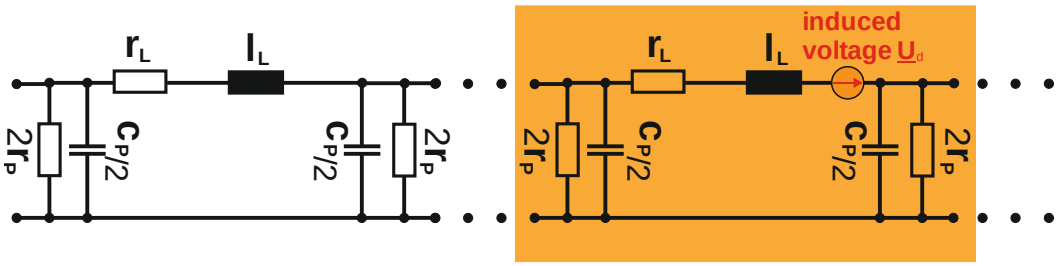

Figure 2.5: Pi-Circuit with influenced and uninfluenced pipeline segments [2], modified

The for the specific interference situation modelled lattice networks can for example either be solved by modelling the lattice network elements with Simulink® power systems toolbox or by solving the voltage-current-equations with the help of the nodal-admittance-matrix (figure 2.6, equation 39).

The elements of the main diagonal are build up with the positive sum of all conductivity values at the nodes of the main diagonal (Y_{11},Y_{22}… Y_{nn}). Elements outside the main diagonal (Y_{12},Y_{21}… Y_{mn}) are build up with the negative coupling conductivity values between two nodes [23]. The following figure 2.6 shows an example of the complex admittance matrix for a pipeline system with 6 nodes.

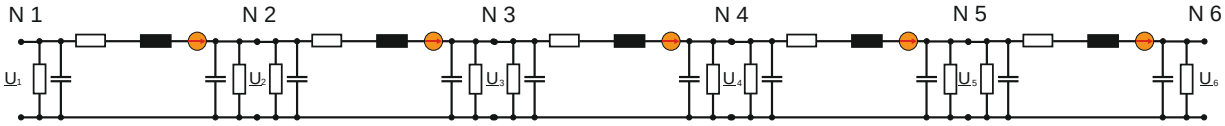

$$\underline{Y} = \begin{bmatrix} \underline{Y}_{11} - \underline{Y}_{12} & 0 & 0 & 0 & 0 \\ -\underline{Y}_{12} & \underline{Y}_{22} - \underline{Y}_{23} & 0 & 0 & 0 \\ 0 & -\underline{Y}_{32} & \underline{Y}_{33} - \underline{Y}_{34} & 0 & 0 \\ 0 & 0 & -\underline{Y}_{43} & \underline{Y}_{44} - \underline{Y}_{45} & 0 \\ 0 & 0 & 0 & -\underline{Y}_{54} & \underline{Y}_{55} - \underline{Y}_{56} \\ 0 & 0 & 0 & 0 & -\underline{Y}_{65} \quad \underline{Y}_{66} \end{bmatrix} \left(\frac{1}{\Omega} \right)$$

Figure 2.6: Example with 6 nodes and complex nodal network admittance matrix [2], modified

Based on the induced voltage, a longitudinal direction component, the nodal current vector $\underline{I}_n$ can be calculated. In a next step the pipeline interference voltage distribution can be calculated with the following formula:

$$\underline{U} = \underline{Y}^{-1} \cdot \underline{I}_n \quad (39) \text{ [2]}$$

$\underline{U}$	nodal voltages
$\underline{Y}$	nodal admittance matrix
$\underline{I_n}$	nodal currents (n… number of nodes)
N1..6	nodes

The conductivity values of possible interference voltage reducing AC earthing systems have to be considered within the main diagonal.

Within the scope of this thesis, the MATLAB®-programme PipePotentials was developed to calculate interference voltage distributions of any pipeline configuration for user-defined earthing systems and isolating joints.

2.3 Pipeline Interference Voltage

The figure 2.7 shows the interfering scheme of the full parallel approach between an interfering system and a pipeline. The appending pipeline interference voltage distribution is shown in figure 2.8. The beginning and the end of the approach is marked with a green dotted line in both figures. It is assumed that the pipeline has an uninfluenced course at the first and the last 20 % of its length. U_{P1} and U_{P2} are the pipeline interference voltages at the beginning and the end of the parallel approach.

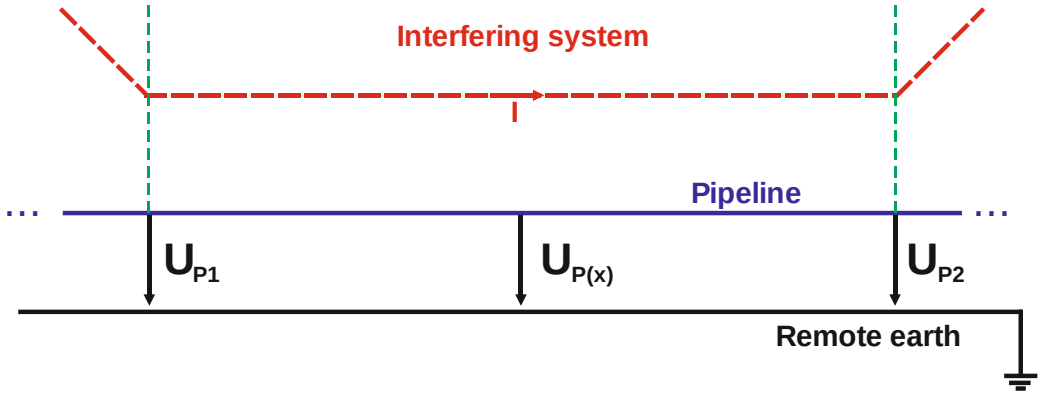

Figure 2.7: Interfering scheme of a full parallel approach

In the figure 2.8 the interference voltage distribution is shown with black points. U_{P1} and U_{P2} have based on the ladder network composition different directions (compare chapter 2.2.1). The absolute value of the pipeline interference voltage is shown in blue. Based on the shunt conductance the pipeline interference voltage reduces after the parallel approach. This effect can slightly be seen in figure 2.8.

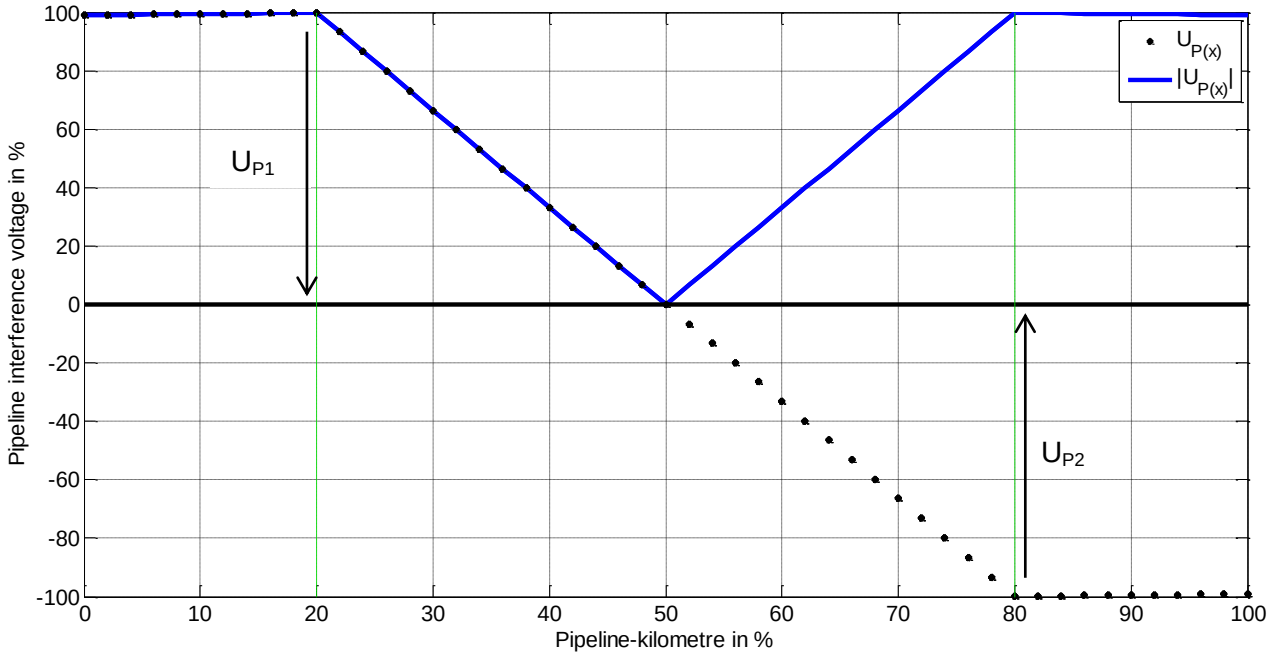

Figure 2.8: Pipeline interference voltage distribution for the full parallel approach

The figure 2.9 shows the interfering scheme of the partial parallel approach between an interfering system and a pipeline. The appending pipeline interference voltage distribution is shown in figure 2.10. The beginning and the end of the approach is marked with a green dotted line in both figures. It is assumed that the pipeline has an uninfluenced course at the first 20 % and the last 50 % of its length. U_{P1} and U_{P2} stand again for the pipeline interference voltages at the beginning and the end of the parallel approach.

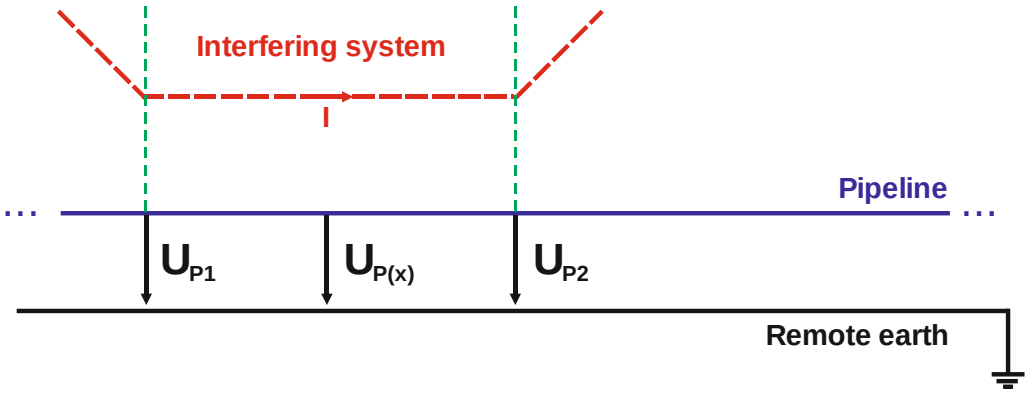

Figure 2.9: Interfering scheme of a partial parallel approach

In the figure 2.10 the interference voltage distribution is shown with black points. U_{P1} and U_{P2} have based on the ladder network composition different directions (compare chapter 2.2.1). Based on the shunt conductance the pipeline interference voltage reduces after the parallel approach. This effect can compared to figure 2.10 be better seen in figure 2.10. The representation of the absolute value (blue) is common use, therefore in further simulations only the absolute values of the pipeline interference voltages are shown.

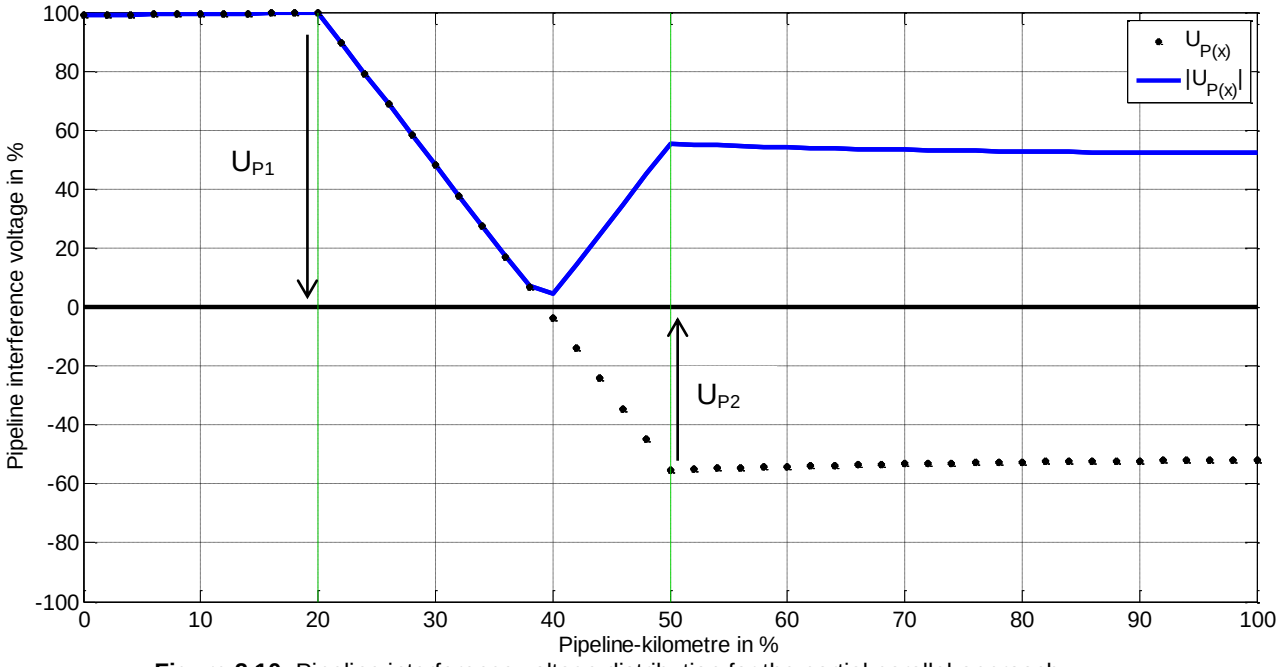

Figure 2.10: Pipeline interference voltage distribution for the partial parallel approach

3 AC Corrosion and Coating Holidays

This chapter describes the AC corrosion process and points the relevant factors for AC corrosion out. Furthermore AC corrosion protection measures and the necessary equipment are explained. In addition to that the correlation between coating holiday diameter, specific soil resistivity and current densities are investigated in order to evaluate the AC corrosion likelihood. At the end of this chapter the contribution of conductive interference at coating holidays to the AC corrosion likelihood is discussed.

3.1 AC Corrosion Process

AC corrosion in general is an electrochemical process, which takes place under certain circumstances. The following figure 3.1 shows a scheme of an isolated pipeline in earth with coating holidays.

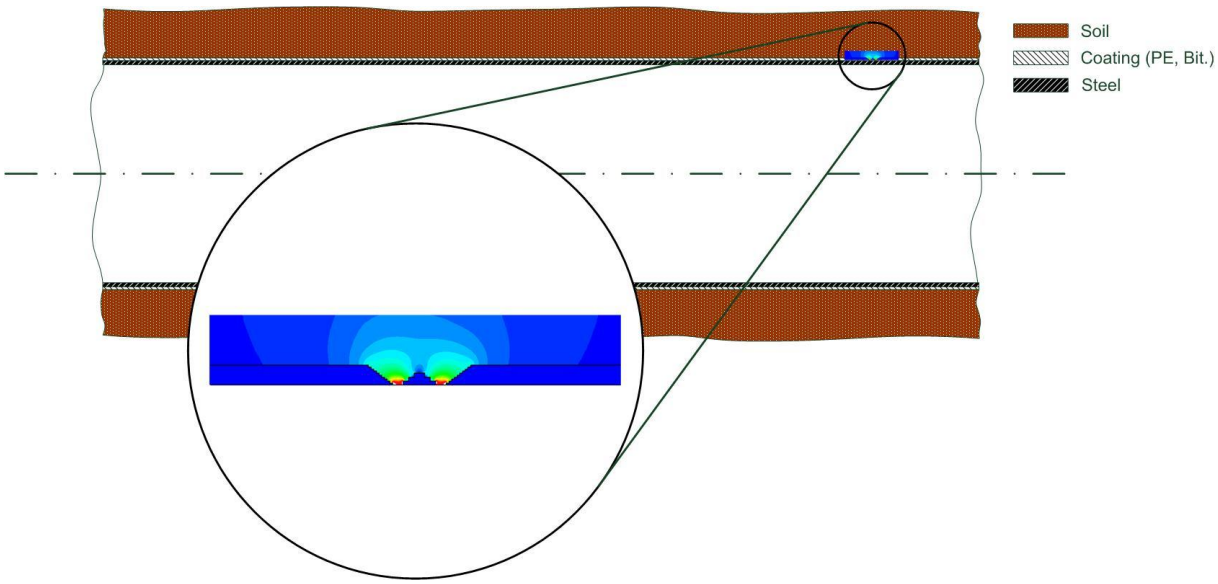

Figure 3.1: Scheme of an isolated pipeline in earth with coating holidays [14]

If the pipeline is inductively influenced and has at least one isolation defect (coating holiday) and lies in a humid soil all necessary requirements for AC corrosion (soil with oxygen, water, ions and salts) are given. The humid, salty or rich in oxygen soil can be seen as the electrolyte. The bare steel in the area of the coating holiday is the cathode. The electric circuit is given by the fact that the pipeline is inductive (or conductive) interfered. For AC corrosion two electrochemical processes are necessary. The first one is the reduction of water or oxygen (humid or oxygen-rich soil). A reduction process needs electrons which are taken from the earth contacting metal. Therefore the second necessary process starts with the oxidizing of the metal. Within this step metal ions (ferric) and electrons get free. The

metal ions react with other ions in the electrolyte. In the following rust-products (for example metal oxide) develop [1].

3.2 AC Corrosion Protection

Metallic oil-, gas-, and district heating pipelines are covered with an isolating coating. This first protection measure is also called primary corrosion protection [1]. If there are no coating holidays, the pipeline will be protected against AC corrosion. Figure 3.2 shows the installation of a natural gas pipeline. The pipeline could get some surface defects for example by stones lying under it at the moment the digger fills the gap. In case of inductive interference already small induced voltages of some 4-10 V can lead to high current densities (above 100 A/m^2) at small coating holidays (for example diameters < 10 mm, see also subchapter 3.5).

Figure 3.2: Burying of a natural gas pipeline, image by Ernst Schmautzer

For this reason there exists the secondary corrosion protection called cathodic corrosion protection [1]. In that case the pipeline is charged with a low (approx. -1.2 V_{DC} to -3.0 V_{DC}) negative DC-voltage. Because of the negative polarity of the protection voltage, positive metallic ions simply cannot leave the pipeline. The release of positive metal-ions and a consequently anodic attack on the metal can so be mitigated and retarded. Therefore the pipeline is split up into so called protection sections. The galvanic separations between protection areas is realised with isolating joints. The following figure 3.3 shows the separation of a cathodic protected pipeline into two protection areas [2].

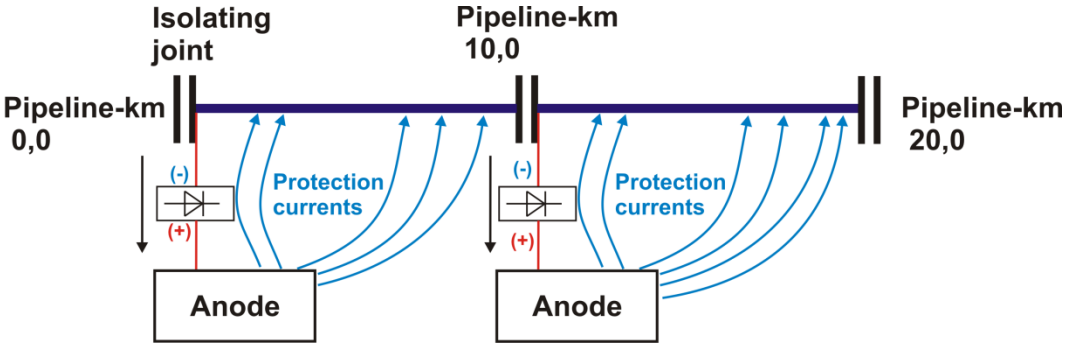

Figure 3.3: Cathodic corrosion protection along interfered pipeline [2]

3.3 Modelling Coating Holidays

Pipeline isolation defects can develop very easily, for instance during construction work. From an electrical point of view, coating holidays can be seen as a small, high-impedant pipeline AC earthing system connected to the pipeline.

There exist several publications and technical reports for example [1], [9], [25] in which the model of a coating holiday is discussed. In this thesis it is chosen the approach to assume the coating holidays as high impedant earthing systems of the pipeline. Generally speaking the total resistivity of a coating holiday is the sum of the polarisation resistance of the bare steel, the resistance of the medium inside the coating defect and the leakage resistance in the soil. In this context in literature the term spread resistance is often mentioned.

Assuming homogenous soil conditions inside and outside the coating defect, the coating holiday can be simplified as a circular plate earthing system. The amount of the polarisation resistance plays a minor role and is not taken into account for the following considerations. This can be done aware of the fact that for example the determination of the soil resistivity is always an assumption [14].

The resistivity of a circular coating holiday can be calculated for example with the approximate formula for a circular plate earthing system under the surface.

$$r_{ch} = \frac{\rho}{4 \cdot d}\left(1 + \frac{2}{\pi} \cdot \arctan\frac{r}{2 \cdot H}\right) \quad (40) \text{ [16]}$$

r_{ch}	resistivity of the coating holiday in Ω
ρ	specific soil resistivity in Ωm
d	diameter of circular coating holiday in m
r	radius of circular coating holiday in m
H	vertical distance from earth's surface to coating holiday in m

The following figure 3.4 shows the correlation between the resistivity of the coating holiday r_{ch}, the specific soil resistivity ρ and the diameter of the coating holiday d.

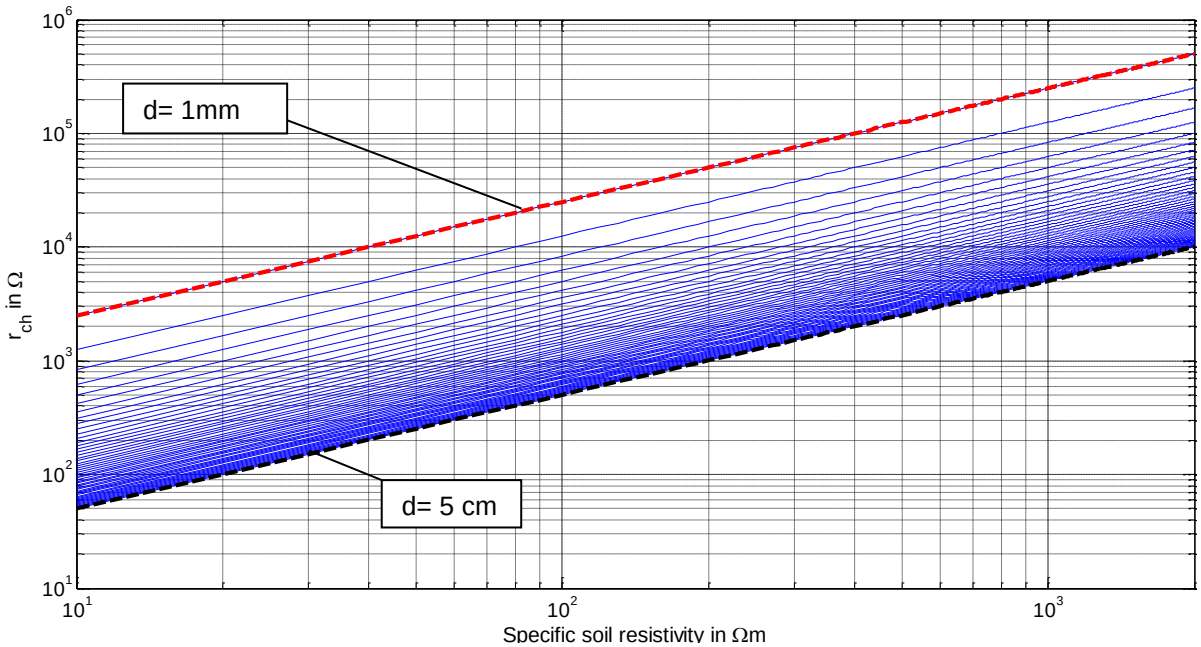

Figure 3.4: Coating holiday resistance r_{ch} plotted against ρ for variable coating holiday diameters [14], [1], modified

The figure 3.4 shows how the resistance of the coating holiday rises with increasing soil resistivity. The specific soil resistivity ρ is varied from 10 Ωm to 2000 Ωm in steps of 10 Ωm. The diameter of the coating holiday is varied from 1 mm to 5 cm in steps of 1 mm. The d = 1 mm series is dotted in red, the d = 5 cm series is dotted in black.

One can see that a coating holiday acts like a very high impedant earthing system (for example 1000 Ω for a coating holiday with d = 2.5 cm at 100 Ωm) to inductively interfered pipelines. As can be shown the earthing effect of such high impedant holiday earthing systems is much too low to reduce pipeline interference voltages of inductively interfered pipelines, because of the low pipeline self-impedance [14].

3.4 Currents over Coating Holidays

In a next step a relevant induced pipeline voltages of 10 V is assumed (the plots for the relevant voltages of 1 V, 4 V and 20 V can be found in the appendix – chapter 12.2). Based on the coating holiday resistivities shown in figure 3.4 and Ohm's law, the currents I_{ch} flowing over the coating holidays, for the chosen values of the soil resistivity ρ and the coating holiday diameter d can be calculated.

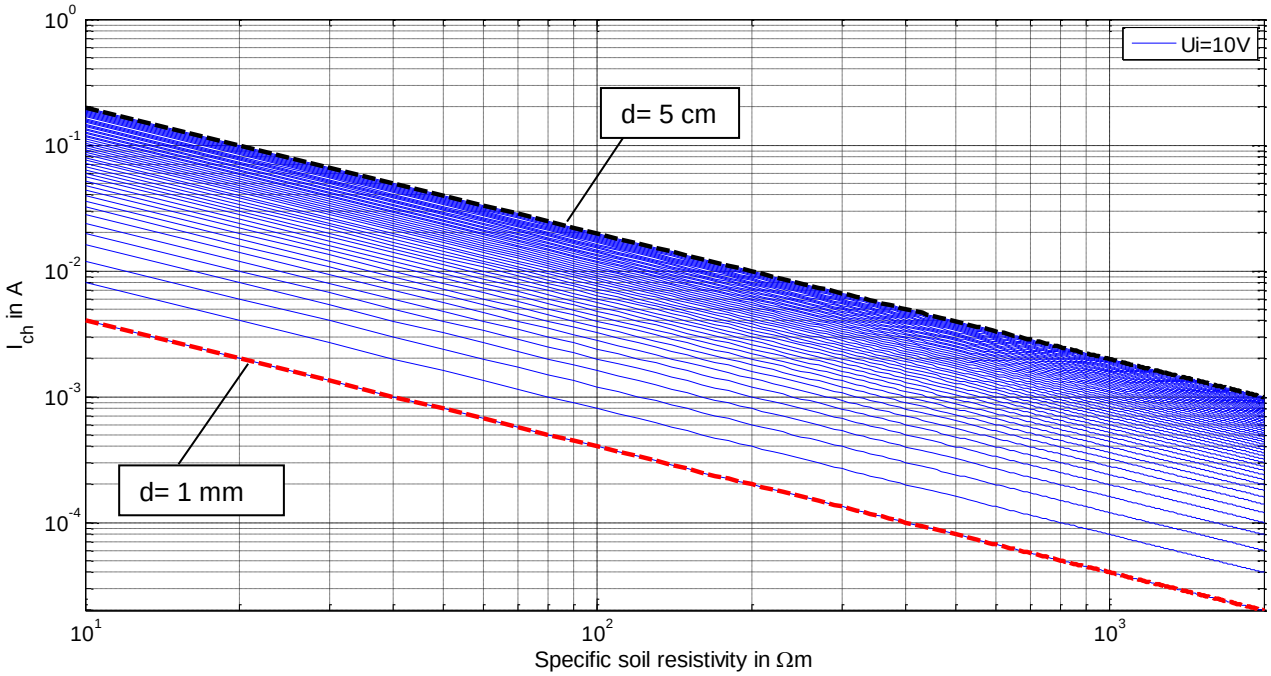

Figure 3.5: Coating holiday current I_{ch} plotted against ρ for variable coating holiday diameters and the reference pipeline interference voltage of 10 V

The figure 3.5 shows how the currents over coating holidays decrease with rising soil resistivity. This corresponds to relevant European recommendations [9], that state that for very low soils resistivities (ρ < 25 Ωm), the measured pipeline voltage towards remote earth should not exceed 4 V, to reduce AC corrosion likelihood. For greater soil resistivities (ρ > 25 Ωm) the pipeline voltage to remote earth should not exceed 10 V. These mentioned values base on long term practical experience of European pipeline operators [9].

The diameter of the coating holiday in figure 3.5 is again varied from 1 mm to 5 cm in steps of 1 mm. The d = 1 mm series is dotted in red, the d = 5 cm series is dotted in black. The currents leaving the coating holidays are relatively small. The highest current I_{ch} of approximately 0.4 A can be achieved with the maximum assumed interference voltage U_i = 20 V (see figure 12.2), the maximum assumed coating holiday diameter d = 5 cm and the minimum assumed specific soil resistivity ρ = 10 Ωm [14].

3.5 Current Densities at Coating Holidays

By dividing the currents over the coating holidays I_{ch} (see figures 3.5, 12.1 and 12.2) by the circular surfaces of the coating holidays, the current densities at the assumed coating holidays J_{ch}, for the assumed induced pipeline voltages can be calculated.

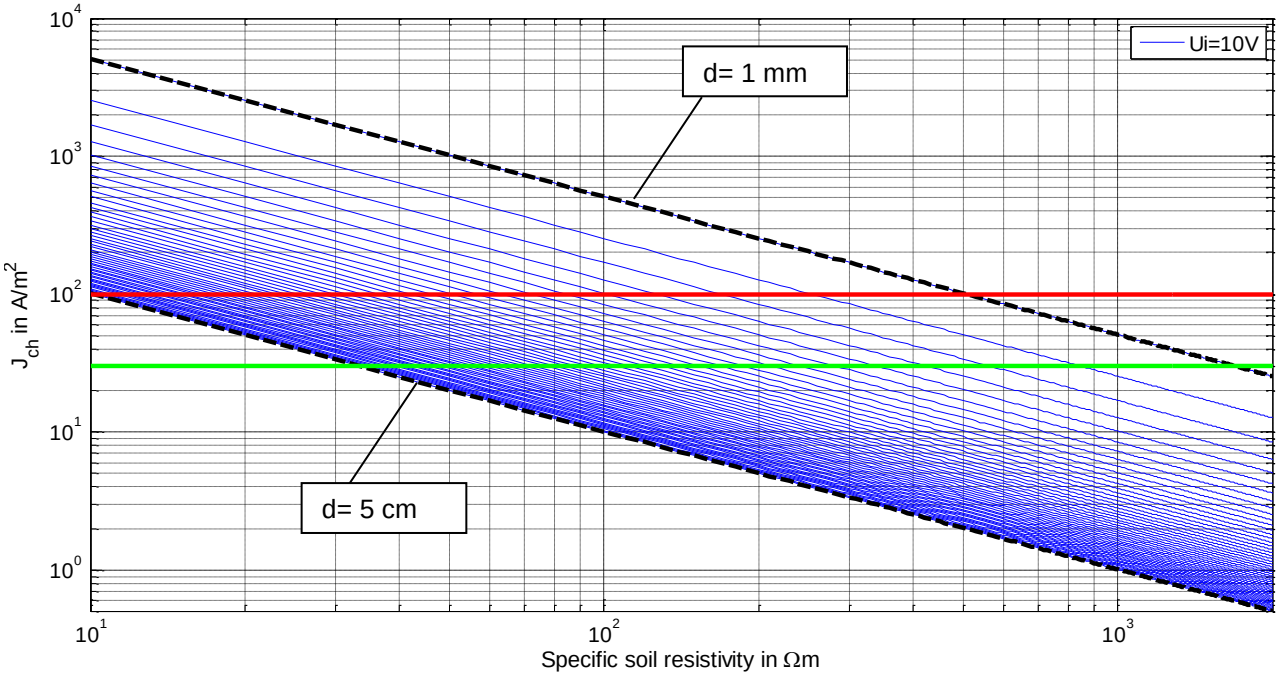

Figure 3.6: Current density at coating holidays J_{ch} plotted against ρ for variable coating holiday diameters and the selected reference pipeline interference voltage of 10 V, red line: 100 A/m^2 limit, green line: 30 A/m^2-limit

The figure 3.6 shows how current densities at coating holidays J_{ch} decrease with rising soil resistivities. At coating holidays with smaller diameters, the current densities are comparatively higher. Due to the relevant European recommendations [9] there exists no or a low likelihood of AC corrosion for current densities < 30 A/m^2. The 30 A/m^2 limit is plotted in green. For current densities between 30 A/m^2 and 100 A/m^2 there exists a medium AC corrosion likelihood. For current densities > 100 A/m^2 there exists very high AC corrosion likelihood. The 100 A/m^2 limit is plotted in red.

The calculations show that there already exist high AC corrosion risks for an assumed induced voltage of 1 V (see figure 12.1), knowing well that this occurs only for very low soil resistivities and very small coating holidays with diameters up to 5 mm. The small coating holidays (d~ 1mm) in this investigation demonstrate a borderline case [14].

In the following tables 3.1 – 3.3 some significant cases are represented. Current densities over 100 A/m^2 (very high AC corrosion likelihood) are marked in red. Current densities between 30 A/m^2 and 100 A/m^2 (medium AC corrosion likelihood) are marked in yellow. Current densities lower than 30 A/m^2 are marked in green.

	d=1mm	d=5mm	d=1cm	d=2cm	d=5cm
	J_{ch} in A/m^2				
Ui = 1V	509.21	101.78	50.84	25.38	10.11
Ui = 4V	2036.85	407.11	203.39	101.54	40.42
Ui = 10V	5092.14	1017.78	508.49	253.84	101.06
Ui = 20V	1018.42	2035.56	1016.97	507.68	202.11

Table 3.1: J_{ch} for selected induced pipeline voltages, selected coating holiday diameters and ρ = 10 Ωm

The cases of low or no AC corrosion likelihood are marked in green. The medium AC corrosion likelihood is marked yellow. Cases of high AC corrosion likelihood are marked red. The bigger the coating holiday diameter gets, the lower the AC corrosion likelihood.

	d=1mm	d=5mm	d=1cm	d=2cm	d=5cm
	J_{ch} in A/m^2				
Ui = 1V	50.92	10.18	5.08	2.54	1.01
Ui = 4V	203.69	40.71	20.34	10.15	4.04
Ui = 10V	509.21	101.78	50.84	25.38	10.11
Ui = 20V	1018.42	203.56	101.70	50.77	20.21

Table 3.2: J_{ch} for selected induced pipeline voltages, selected coating holiday diameters and ρ = 100 Ωm

	d=1mm	d=5mm	d=1cm	d=2cm	d=5cm
	J_{ch} in A/m^2				
Ui = 1V	5.09	1.02	0.51	0.25	0.10
Ui = 4V	20.37	4.07	2.03	1.02	0.40
Ui = 10V	50.92	10.18	5.08	2.54	1.01
Ui = 20V	101.84	20.36	10.17	5.08	2.02

Table 3.3: J_{ch} for selected induced pipeline voltages, selected coating holiday diameters and ρ = 1000 Ωm

When comparing tables 3.1 – 3.3 one can recognize that AC corrosion likelihood referring to the current density criterion (see also chapter 2.1.2) decreases with raising specific soil resistivity ρ.

These results coincide with long-term electrochemical experiments [24] of corrosion research institutions.

This effect can additionally be explained by the Pi-equivalent-circuit of an interfered pipeline and with Carson's and Pollaczek's infinite series. Mutual impedances and consequently induced pipeline voltages in direct axis get according to Carson [17] and Pollaczek higher with increasing soil resistivities [18]. Consequently voltage drops in shunt direction (see also figure 2.6) get proportionally lower.

Generally speaking AC corrosion likelihood decreases with raising soil resistivities, because the currents are more constraint to stay inside the metal.

Of course the impact of changing specific soil resistivities is in reality not as linear as shown in the tables above. The linearity in the mentioned tables comes from disregarding the nonlinear [19] polarisation resistance. The polarisation resistance bases on the pipeline potential jump (polarisation) in the case of corrosion. The nonlinear resistance can for most current densities not be calculated and has to be determined experimentally [21]. Knowing that there exist several empirical formulas [19], the polarisation resistance can be neglected in these cases.

Nevertheless the values are practicable reference values, if one thinks about uncertain variables like the prevailing specific soil resistivity, the seasonal changes of the specific soil resistivity or the geometry [20] of the coating holiday.

3.6 Conductive Interference through Coating Holidays

Conductive interference of coating holidays has to be considered in the vicinity of electrical power stations and pylons [14], precisely because the cumulated impact of inductive and conductive interference is relevant for AC corrosion. Mechanical destructions can damage pipeline coatings causing coating holidays. If they are damaged once, they are exposed to the risk of AC corrosion. Electric railways that lead their return currents partially through earth may bring some additional interfering voltages through coating holidays or earthing systems. Other interesting cases for conductive interference are pipelines in the vicinity of transposition poles as well as in the vicinity of unbalanced high-voltage transmission systems.

3.7 Summary

In this chapter coating holidays are assumed as circular plate earthing systems. The investigations in this chapter show that for higher specific soil resistivities (> 250 Ωm) that are typical in parts of Austria, higher induced voltages than the in [9] proposed 10 V are possible to remain nevertheless under the current density criterion for the AC corrosion likelihood. In these cases the voltage criterion and the current density criterion do not match. The voltage criterion is too general and inadequate; in the actual standard [9] there exists only a differentiation for specific soil resistivities less than 25 Ωm and bigger than 25 Ωm (see chapter 2.1.2). The current density criterion should in any case be kept because it is more precisely, less general and considers coating holiday dimensions, specific soil resistivities and induced voltages, whereas different coating holiday geometries are not considered.

4 Interference Voltage Mitigating Measures

This chapter describes the function of common pipeline interference voltage mitigating measures such as AC earthing systems, isolating joints, compensation conductors, increasing the distance between pipeline and interfering system and the optimisation of the phase conductor arrangement. The descriptions of these measures are based on measurements and simulations that are carried out with programs and tools developed within the scope of this PhD thesis.

4.1 Earthing of the Pipeline

Connecting the pipeline with low impedant earthing arrangements such as ground rods or horizontal earthing conductors represents an effective method to reduce induced pipeline interference voltages. For the cathodic corrosion protection it's necessary to connect the earthing arrangements with DC current blocking devices, as power capacitors or kirk-cells (see figure 4.1). With the help of the power capacitor or kirk-cell, cathodic corrosion protection DC currents can be prevented from draining off against remote earth [2].
In this connection the notion AC earthing is a common use [1].
The construction of earthing systems is an in Austria practicable option to reduce induced pipeline voltages. Earthing systems can be installed during or after construction of the pipeline if it occurs necessary. Effective earthing systems have to be very low impedant. This can be realized by expanded horizontal earthing conductors or vertical earthing rods. This can be very cost-intensive if one considers high soil resistivities of lime, brash or rock (500 Ωm ... 3000 Ωm). A significant analysis regarding the seasonal change of the specific soil resistivity is given in chapter 6.

The following figure 4.1 shows the principal impact of earthing systems on induced pipeline voltages, for a parallel interfering situation, in dependency of the location and the earthing resistance. The effects are hereby classified in

- No earthing
- One sided earthing
- Balanced earthing
  and
- Unbalanced earthing.

In the first subfigure the basic case, without a connected earthing system, is plotted in black. In the second subfigure the basic case is black dotted.

Only one earthing system at the beginning or the end of a parallel approach leads, assuming that the earthing system is sufficient low impedant to the full induced voltage at the end without earthing system. This one side earthing effect is shown in the second subfigure of figure 4.1.

Earthing systems with the same resistances at the beginning and the end of the pipeline lead to the same reduction of the pipeline interference voltage at both ends, without any increase. This effect is classified as balanced earthing effect and shown in the third subfigure of figure 4.1.

Earthing systems at the beginning and the end of a parallel approach with different resistivities lead to an increase of the pipeline interference voltage at the side with the higher earthing system resistance. This effect is named unbalanced earthing and shown in the fourth subfigure of figure 4.1.

In praxis increases of the pipeline interference voltage based on one sided earthing or unbalanced earthing effects should be avoided.

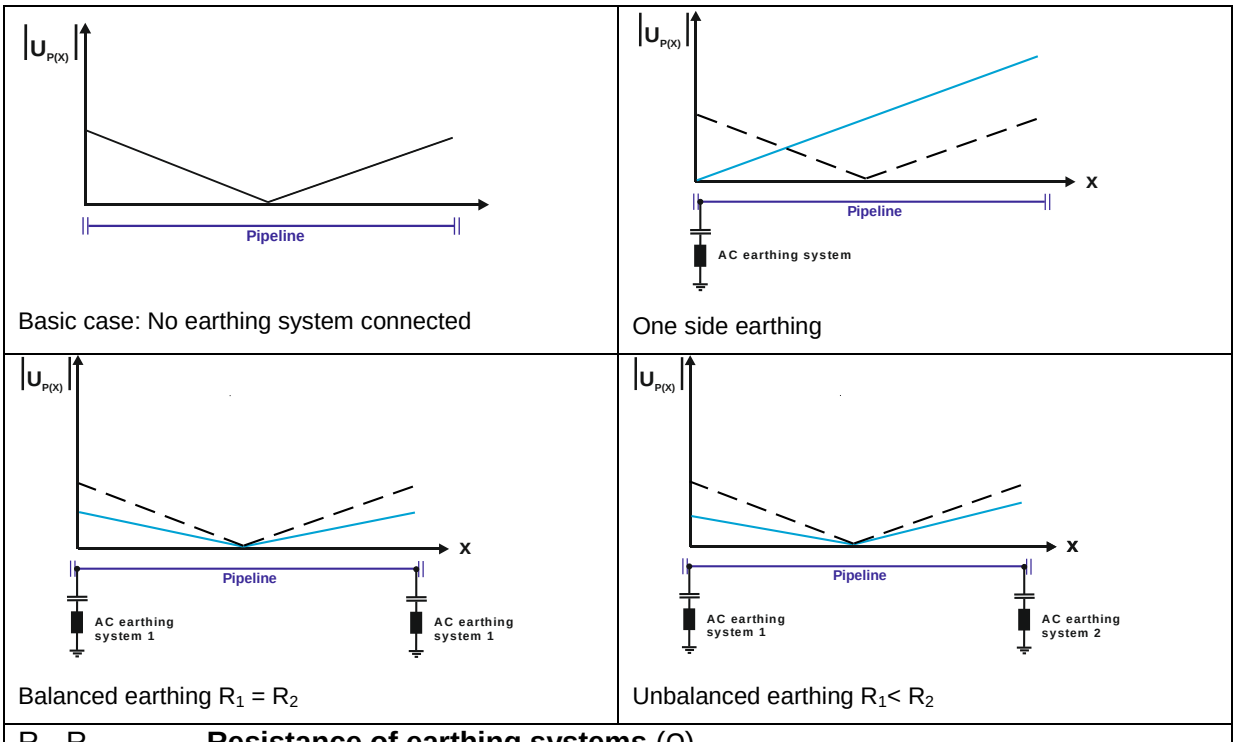

Figure 4.1: Principle impact of earthing systems to induced pipeline voltages

The figure 4.2 shows the approach between an in this example interfering railway system and an interfered pipeline for the first calculation example (see figure 4.3).

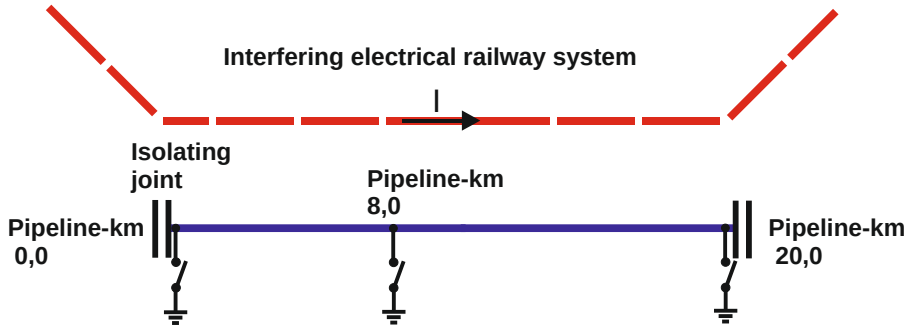

Figure 4.2: Approach between an interfered pipeline and electric railway, locations of earthing [2], modified

The basic case (no earthing system connected) in figure 4.3 is plotted in blue. The red plotted line demonstrates the potential raising effect if only one side of the pipeline is grounded. The maximum induced pipeline voltage is about 100 % higher than in the basic case without earthing systems. The best voltage reducing effect in this example can be achieved with low impedant (≤ 1 Ω) earthing at both ends of the pipeline (green line). This effect is caused by the low pipeline impedance derived in 2.2.3.

The position of the earthing systems has a real influence on the maximum induced pipeline voltage as it is shown in figure 4.3 by the black or the red line.

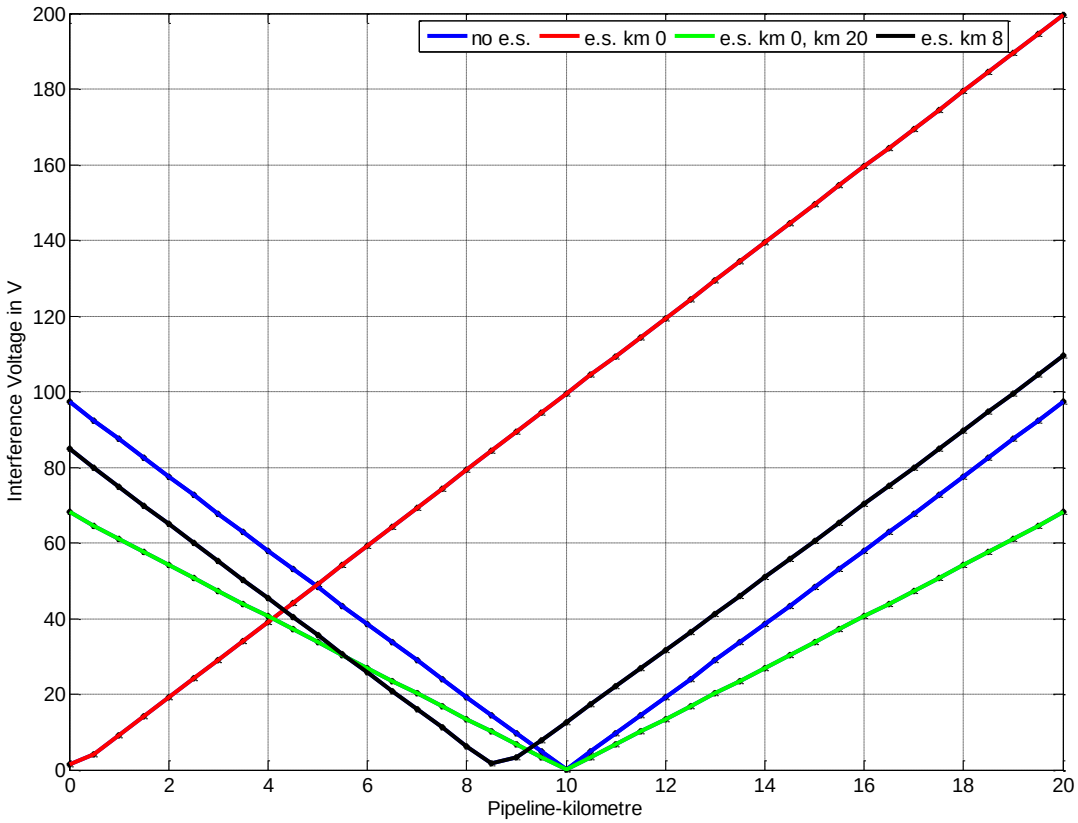

Figure 4.3: Principal pipeline voltage distribution along inductive interfered pipeline with different earthing locations [2]

The calculations in figure 4.3[2] show that earthing systems at inappropriate locations can raise the maximum induced pipeline voltage significantly [2]. In addition to the fact that they have to be very low impedant (< 1 Ω) to achieve significant results [4], [6]. Within the scope of chapter 8 algorithms for the optimum placement of earthing systems along interfered pipelines are described.

4.2 Installation of Isolating Joints

An isolating joint is a piece with an isolating inner layer, which is put between two pipeline parts. The isolating coupling interrupts the electrical continuity between the two pipeline pieces [9.]

The installation of isolating couplings can be an expensive and extensive measure (see also at the case studies in chapter 7). Isolating joints may cause problems regarding longevity. Originally they are installed for separating cathodic protection areas (see chapter 3.2), but they also have an impact on pipeline interference voltage distributions. It has to be taken into account that for every isolating joint an additional cathodic corrosion protection area with an additional rectifier has to be realised (see figure 3.3 and chapter 7.2).

The following figure 4.4 shows the principal impact of isolating joints to pipeline interference voltages, for a parallel interfering situation, in dependency of the location of the isolating joint.

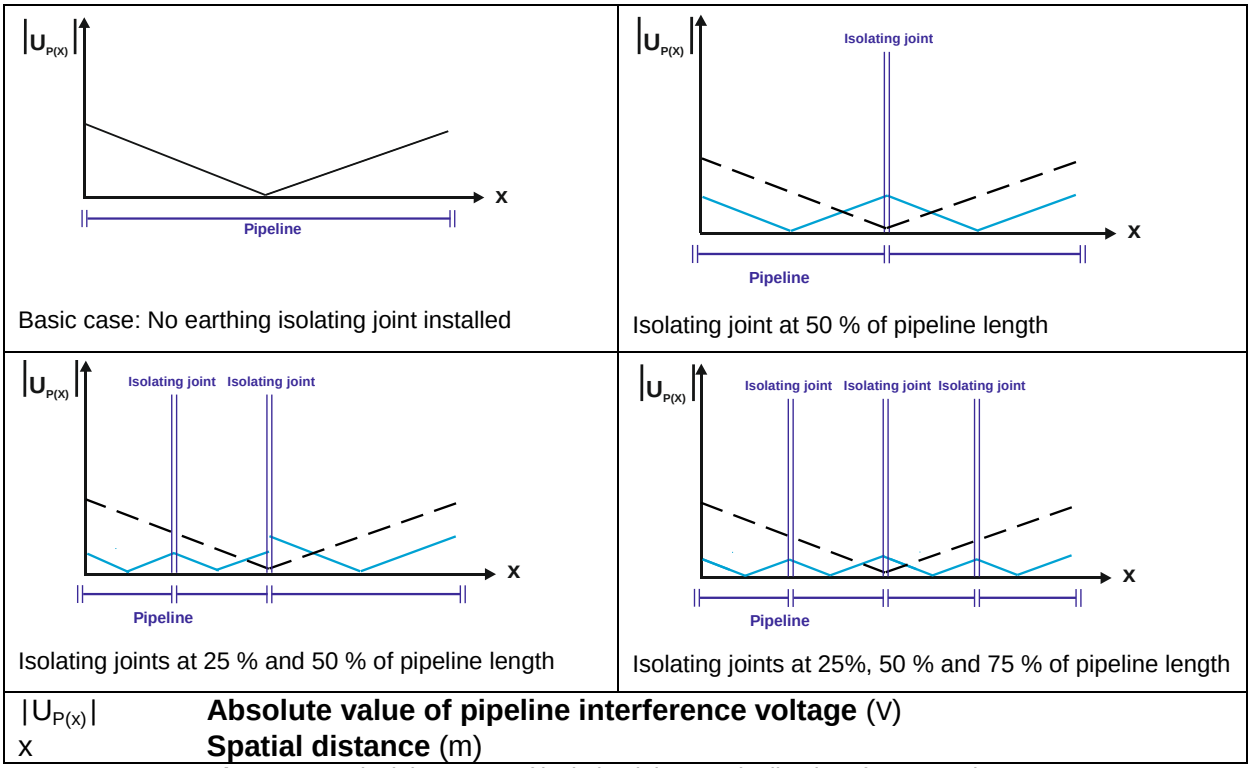

Figure 4.4: Principle Impact of isolating joints to pipeline interference voltages

[2]Detailed simulation parameters, see chapter 12.

In the first subfigure in figure 4.4 the basic case, without an installed isolating joint, is plotted in black. The second subfigure shows the basic case in dotted black, the effect of an isolating joint in the middle of the pipeline is shown in blue. For a parallel approach and a constant horizontal distance between pipeline and interfering system an isolating joint at the middle of the pipeline leads to a halving of the maximum pipeline interference voltage. This effect is shown in the second subfigure in figure 4.4.

Isolating joints at 25 % and 50 % of the pipeline lead in case of a parallel approach and a constant horizontal distance between the pipeline and the interfering system to a quartering of the maximum pipeline interference voltage between 0 % and 50 % of its length. Between 50 % and 100 % of the pipeline length the maximum interference voltage is halved. This effect is shown in the third subfigure of Figure 4.4.

Three balanced isolating joints at 25 %, 50 % and 75 % of the pipelines length lead to a quartering of the maximum pipeline interference voltage. This effect is shown in the fourth subplot of figure 4.4.

The figure 4.5 shows the approach between an in this example interfering railway system and an interfered pipeline for the second calculation example (figure 4.5).

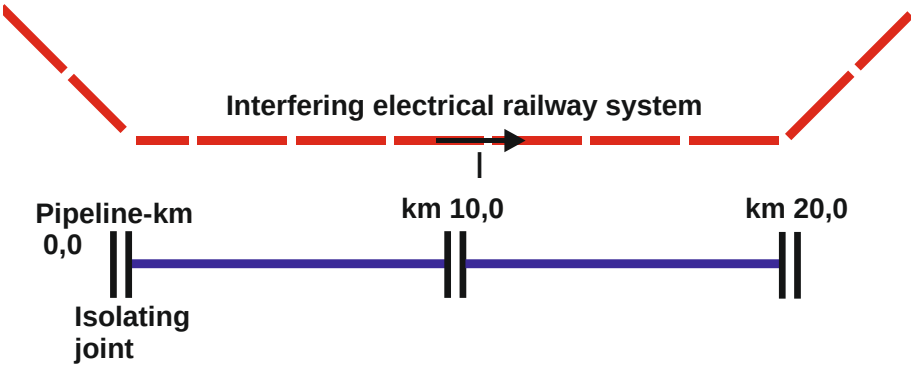

Figure 4.5: Approach between an interfered pipeline and electric railway, location of isolating joint [2]

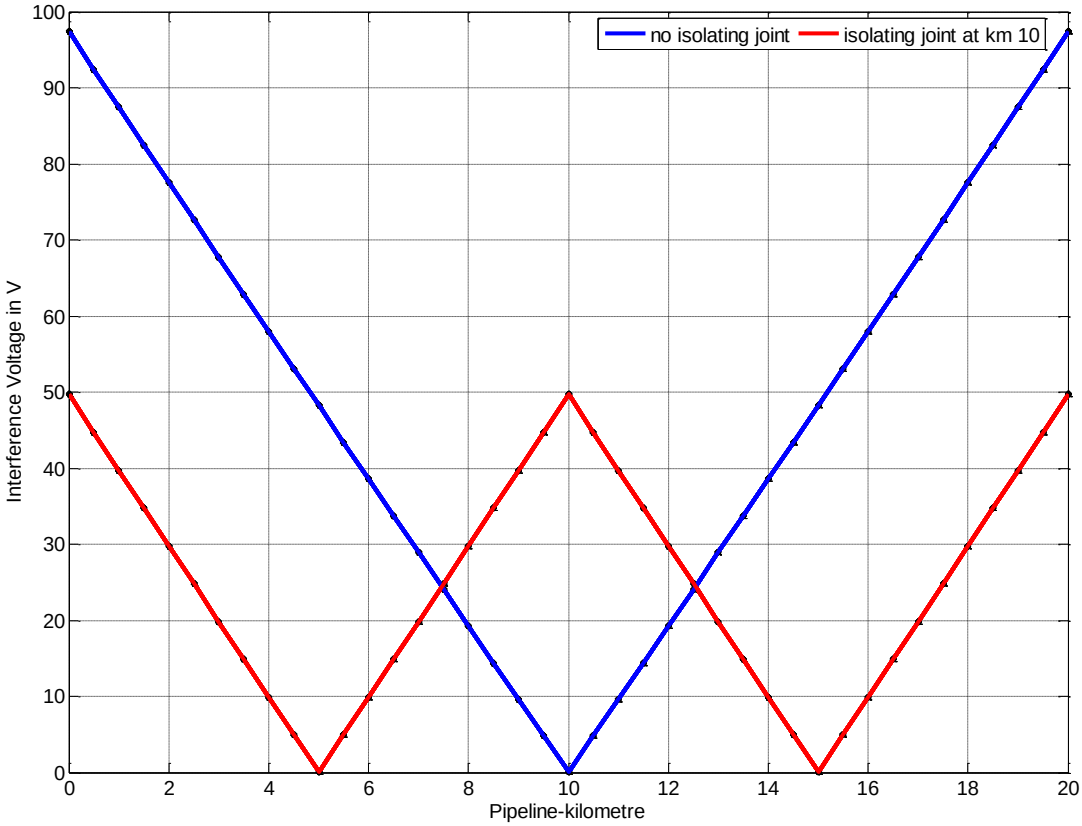

Figure 4.6: Absolute values of interference voltages along inductive interfered pipeline with and without an isolating joint [2]

The basic case (no isolating joint, approach between systems is shown in figure 4.5) in the previous figure 4.6 is plotted in blue. The induced pipeline voltage reaches about 98 V. The red line in figure 4.6 explains the use of an isolating joint at pipeline-kilometre 10. As it can be seen in figure 4.6, the pipeline voltage can be halved [2].

The following figure 4.7 shows the approach between the influenced pipeline and the railway for the third calculation example.

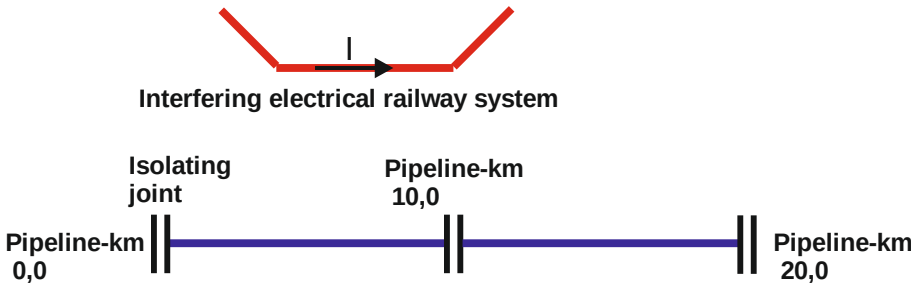

Figure 4.7: Approach between an interfered pipeline and electric railway, location of isolating joint [2]

The following figure 4.8 shows the induced pipeline voltage along the interfered pipeline for the approach in figure 4.7. The basic case (no isolating joint) is plotted blue. The case with an isolating joint at pipeline-kilometre 10 is shown in red. The maximal induced pipeline voltage without an isolating joint (plotted in blue) is in this case lower than the maximum

induced pipeline voltage with the option of an isolating joint at pipeline-kilometre 10 (plotted in red).

Another interesting effect, shown in figure 4.8, is the in 2.2.3 derived self-earthing effect [2].

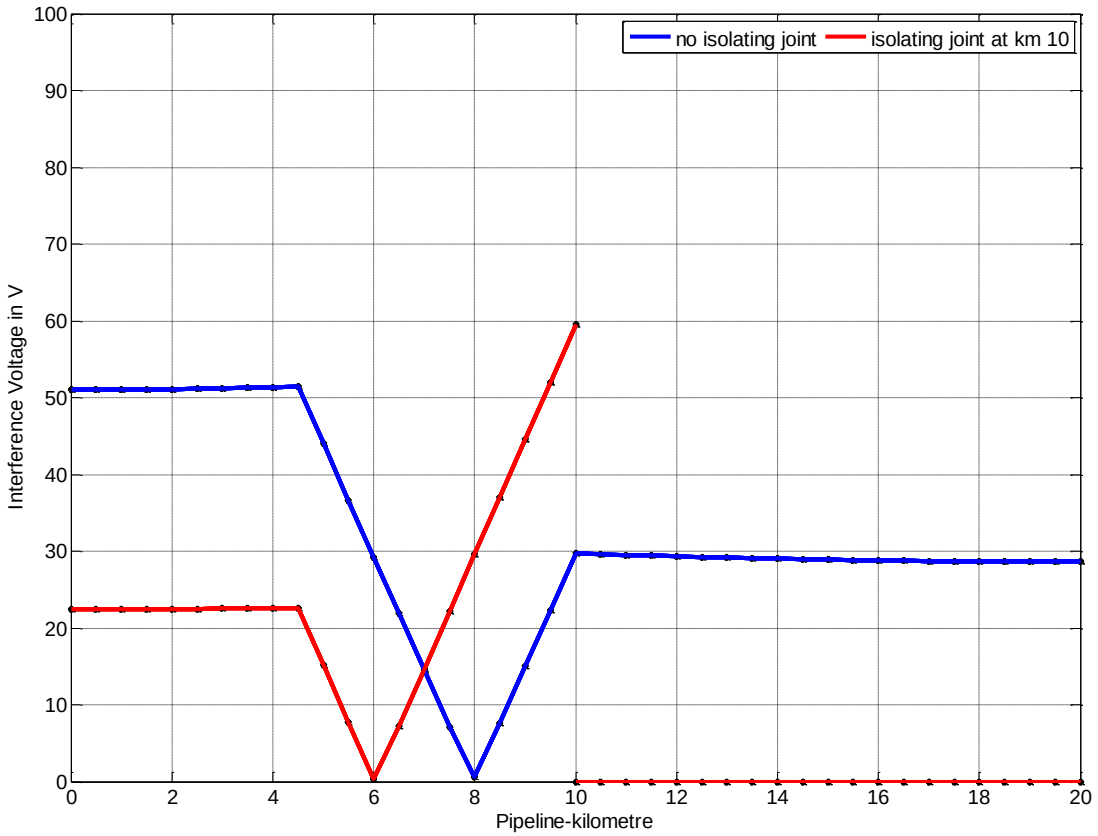

Figure 4.8: Induced voltage distribution along an inductive interfered pipeline with and without isolating joint [2]

The installation of isolating joints can already be realized during pipeline construction. The installation of an isolating joint at an already buried pipeline is very cost intensive. It makes sense to plan the isolating joints together with the pipeline operator during the planning phase. So the distribution of the cathodic corrosion protection areas can be adjusted with the interference situation. As the calculations in figure 4.8 show, an isolating joint at the wrong location can increase the maximum induced pipeline voltage. For this reason the interference situation and the design of the protection sections shall be considered in the planning process as equally important and be evaluated by experts [2].

4.3 Compensation Conductors

Generally speaking compensation conductors in earth have either to be buried barely or they have to be grounded with low impedances at both ends in order to enable the current flow. In order to avoid corrosion of bare compensation conductors in earth, tin coated copper can be used.

Established reduction factors of for example earth wires (approximately 0.7) or railway systems (approximately 0.15 – 0.5, depending on the number of rails and the distances to substations) are summarised in [10].

The in this thesis calculated reduction factors base on the series of Carson (see chapter 2.2.2), assuming the pipeline and compensation conductors as infinite long conductors with earth return. Therefore the computed values can be seen as the mitigation of the in the pipeline induced currents due to the existence of additional compensation conductors with earth return. As also mentioned in [35] these compensation conductors can be for example earth wires, cable sheaths, other metallic pipelines or horizontal earthing conductors.

Referring to [36] the advantages of bare buried compensation conductors are the mitigation of the pipeline interference voltage as well as the simultaneous existence of a horizontal earthing conductor which can be used for earthing the pipeline and the voltage grading effect which reduces touch voltages.

In the following subchapter 4.3.1 the calculation procedure is derived and described for a concrete example. In addition to that a simulation result for the influence of varying the horizontal distance between compensation conductor and pipeline on the pipeline reduction factor R_{FP} is shown and discussed.

In the following subchapter 4.3.2 the influence of the phase positions of an interfering high-voltage line is investigated.

In subchapter 4.3.3 the results of a concluded pipeline interference measurement are summarised and compared with the results of the computational simulation.

4.3.1 Calculation of the Pipeline Reduction Factor R_{FP}

The following figures 4.9 and 4.10 show schemes of interfering situations for explaining the calculation of the pipeline reduction factor R_{FP}.

For the calculation of the pipeline reduction factor, the pipeline current is important. Therefore the current has to be calculated as if there is no compensation conductor (see I_{P0}, figure 4.9). In a next step the pipeline current has to be calculated, taking the to be analysed compensation conductor into account (see I_{PC}, figure 4.10).

The pipeline reduction factor R_{FP} can be set up as:

$$R_{FP} = \left| \frac{\underline{I}_{PC}}{\underline{I}_{P0}} \right| \quad (41)$$

$\underline{I}_{PC}$ **Pipeline current** taking the to be analysed compensation conductor into account (A)

$\underline{I}_{P0}$ **Pipeline current** without taking the to be analysed compensation conductor into account (A)

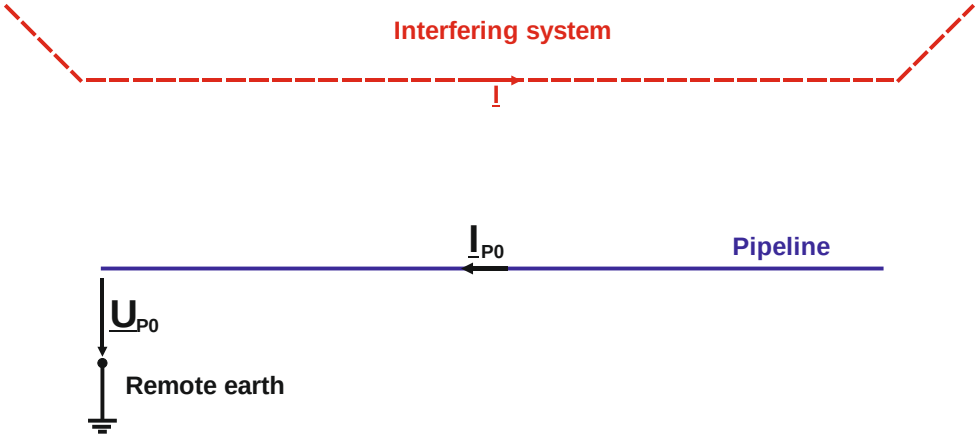

$\underline{I}$ ... Interfering current (A), $\underline{U}_{P0}$ … Pipeline interference voltage (V)

Figure 4.9: Scheme of an interfering situation between a pipeline and an interfering system

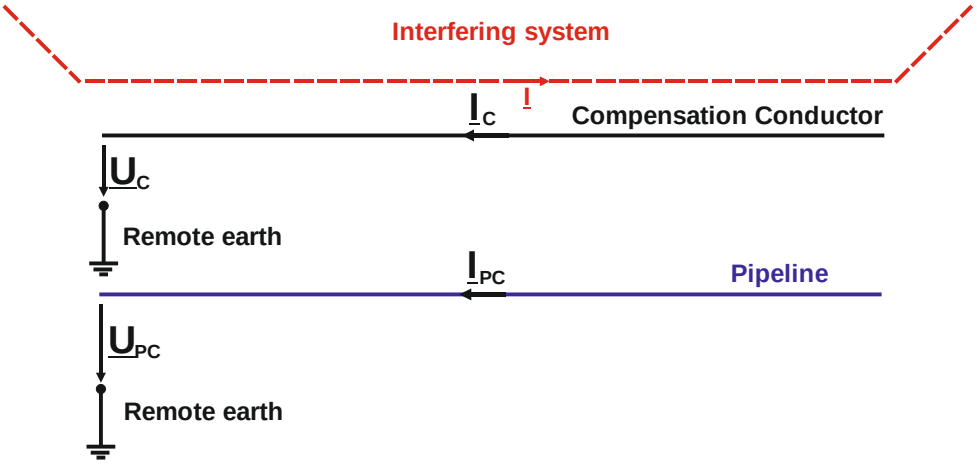

$\underline{I}_C$ … Induced compensation conductor current (A), $\underline{U}_{PC}$ … Induced compensation conductor voltage (V), $\underline{I}_{PC}$ … Induced pipeline current, $\underline{U}_{PC}$ … Pipeline interference voltage (V)

Figure 4.10: Scheme of an interfering situation between a pipeline, a compensation conductor and an interfering system

The following figure 4.11 shows the geometrical arrangements of an assumed one-circuit pylon with one earth wire, the in this example varying compensation conductor and the pipeline. For the simulation the crucial mutual impedances are based on simplifications of Carson's formulas, which can be found in [29].

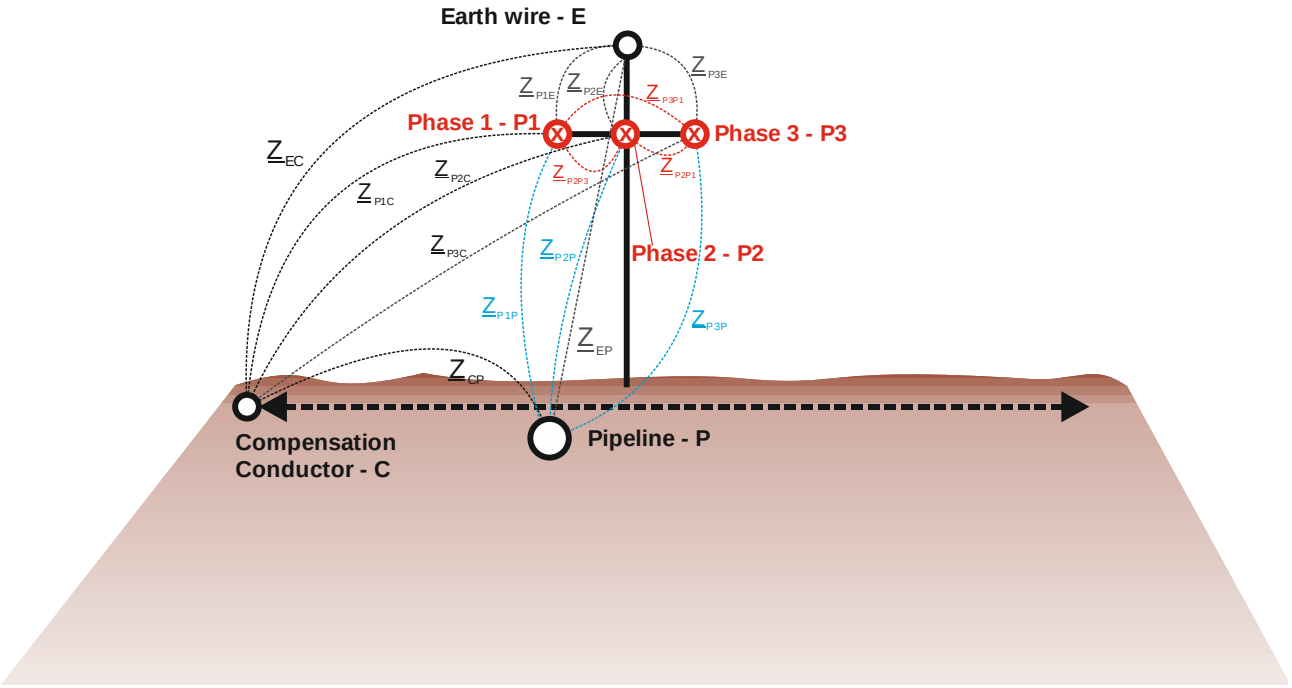

Figure 4.11: Mutual impedances between the phases of a one-circuit pylon, earth wire, horizontal movably compensation conductor and pipeline

The interfering phase currents $\underline{I}_1$, $\underline{I}_2$ and $\underline{I}_3$ are given. The currents along the earth wire $\underline{I}_E$, the compensation conductor $\underline{I}_C$ and the Pipeline $\underline{I}_P$ have to be calculated. The calculation procedure is principally described in [41].

The relation between mutual impedances[3], inducing currents, phase voltages and induced currents can be stated as:

$$\begin{bmatrix} \underline{U}_1 \\ \underline{U}_2 \\ \underline{U}_3 \\ 0 \\ 0 \\ 0 \end{bmatrix} = \begin{bmatrix} \underline{Z}_{P11} & \underline{Z}_{P12} & \underline{Z}_{P13} & \underline{Z}_{P1E} & \underline{Z}_{P1C} & \underline{Z}_{P1P} \\ \underline{Z}_{P21} & \underline{Z}_{P22} & \underline{Z}_{P23} & \underline{Z}_{P2E} & \underline{Z}_{P2C} & \underline{Z}_{P2P} \\ \underline{Z}_{P31} & \underline{Z}_{P32} & \underline{Z}_{P33} & \underline{Z}_{P3E} & \underline{Z}_{P3C} & \underline{Z}_{P3P} \\ \underline{Z}_{P1E} & \underline{Z}_{P2E} & \underline{Z}_{P3E} & \underline{Z}_{EE} & \underline{Z}_{EC} & \underline{Z}_{EP} \\ \underline{Z}_{P1C} & \underline{Z}_{P2C} & \underline{Z}_{P3C} & \underline{Z}_{EC} & \underline{Z}_{CC} & \underline{Z}_{CP} \\ \underline{Z}_{P1P} & \underline{Z}_{P2P} & \underline{Z}_{P3P} & \underline{Z}_{EP} & \underline{Z}_{CP} & \underline{Z}_{PP} \end{bmatrix} \cdot \begin{bmatrix} \underline{I}_1 \\ \underline{I}_2 \\ \underline{I}_3 \\ \underline{I}_E \\ \underline{I}_C \\ \underline{I}_P \end{bmatrix} \quad (42)$$

With the help of the areas marked green in the above equation (42), the following equation (43) can be set up in order to calculate the unknown currents $\underline{I}_E$, $\underline{I}_C$ and $\underline{I}_P$:

[3] The particular mutual impedances can be found in figure 4.9. $\underline{Z}_{P11}$, $\underline{Z}_{P22}$, $\underline{Z}_{P33}$, $\underline{Z}_{EE}$, $\underline{Z}_{CC}$ and $\underline{Z}_{PP}$ are the self-impedances of the particular conductors.

$$\begin{bmatrix} 0 \\ 0 \\ 0 \end{bmatrix} = \begin{bmatrix} \underline{Z}_{P1E} & \underline{Z}_{P2E} & \underline{Z}_{P3E} & \underline{Z}_{EE} & \underline{Z}_{EC} & \underline{Z}_{EP} \\ \underline{Z}_{P1C} & \underline{Z}_{P2C} & \underline{Z}_{P3C} & \underline{Z}_{EC} & \underline{Z}_{CC} & \underline{Z}_{CP} \\ \underline{Z}_{P1P} & \underline{Z}_{P2P} & \underline{Z}_{P3P} & \underline{Z}_{EP} & \underline{Z}_{CP} & \underline{Z}_{PP} \end{bmatrix} \cdot \begin{bmatrix} \underline{I}_1 \\ \underline{I}_2 \\ \underline{I}_3 \\ \underline{I}_E \\ \underline{I}_C \\ \underline{I}_P \end{bmatrix} \quad (43)$$

The next algebraic transformations offer equations (44) and (45).

$$\begin{bmatrix} 0 \\ 0 \\ 0 \end{bmatrix} = \begin{bmatrix} \underline{Z}_{P1E} & \underline{Z}_{P2E} & \underline{Z}_{P3E} \\ \underline{Z}_{P1C} & \underline{Z}_{P2C} & \underline{Z}_{P3C} \\ \underline{Z}_{P1P} & \underline{Z}_{P2P} & \underline{Z}_{P3P} \end{bmatrix} \cdot \begin{bmatrix} \underline{I}_1 \\ \underline{I}_2 \\ \underline{I}_3 \end{bmatrix} + \begin{bmatrix} \underline{Z}_{EE} & \underline{Z}_{EC} & \underline{Z}_{EP} \\ \underline{Z}_{EC} & \underline{Z}_{CC} & \underline{Z}_{CP} \\ \underline{Z}_{EP} & \underline{Z}_{CP} & \underline{Z}_{PP} \end{bmatrix} \cdot \begin{bmatrix} \underline{I}_E \\ \underline{I}_C \\ \underline{I}_P \end{bmatrix} \quad (44)$$

$$\begin{bmatrix} \underline{I}_E \\ \underline{I}_C \\ \underline{I}_P \end{bmatrix} = - \begin{bmatrix} \underline{Z}_{EE} & \underline{Z}_{EC} & \underline{Z}_{EP} \\ \underline{Z}_{EC} & \underline{Z}_{CC} & \underline{Z}_{CP} \\ \underline{Z}_{EP} & \underline{Z}_{CP} & \underline{Z}_{PP} \end{bmatrix}^{-1} \cdot \begin{bmatrix} \underline{Z}_{P1E} & \underline{Z}_{P2E} & \underline{Z}_{P3E} \\ \underline{Z}_{P1C} & \underline{Z}_{P2C} & \underline{Z}_{P3C} \\ \underline{Z}_{P1P} & \underline{Z}_{P2P} & \underline{Z}_{P3P} \end{bmatrix} \cdot \begin{bmatrix} \underline{I}_1 \\ \underline{I}_2 \\ \underline{I}_3 \end{bmatrix} \quad (45)$$

Using the law of Sarrus for symmetrical matrices with more or equal than 3 line- and column elements the following equation (46) can be set up:

$$\begin{bmatrix} \underline{I}_E \\ \underline{I}_C \\ \underline{I}_P \end{bmatrix} = \frac{- \begin{bmatrix} \underline{Z}_{EE} \cdot \underline{Z}_{PP} - \underline{Z}_{CP}^2 & \underline{Z}_{EP} \cdot \underline{Z}_{CP} - \underline{Z}_{EC} \cdot \underline{Z}_{PP} & \underline{Z}_{EC} \cdot \underline{Z}_{CP} - \underline{Z}_{EP} \cdot \underline{Z}_{CC} \\ \underline{Z}_{CP} \cdot \underline{Z}_{EP} - \underline{Z}_{EC} \cdot \underline{Z}_{PP} & \underline{Z}_{EE} \cdot \underline{Z}_{PP} - \underline{Z}_{EP}^2 & \underline{Z}_{EP} \cdot \underline{Z}_{EC} - \underline{Z}_{EE} \cdot \underline{Z}_{CP} \\ \underline{Z}_{EC} \cdot \underline{Z}_{CP} - \underline{Z}_{PP} \cdot \underline{Z}_{EP} & \underline{Z}_{EC} \cdot \underline{Z}_{EP} - \underline{Z}_{EE} \cdot \underline{Z}_{CP} & \underline{Z}_{EE} \cdot \underline{Z}_{CC} - \underline{Z}_{EC}^2 \end{bmatrix}}{\underline{Z}_{EE} \cdot \underline{Z}_{CC} \cdot \underline{Z}_{PP} + \underline{Z}_{EC} \cdot \underline{Z}_{CP} \cdot \underline{Z}_{EP} + \underline{Z}_{EP} \cdot \underline{Z}_{EC} \cdot \underline{Z}_{CP} - \underline{Z}_{EP}^2 \cdot \underline{Z}_{CC} - \underline{Z}_{CP}^2 \cdot \underline{Z}_{EE} - \underline{Z}_{PP} \cdot \underline{Z}_{EC}^2} \cdot \begin{bmatrix} \underline{Z}_{P1E} & \underline{Z}_{P2E} & \underline{Z}_{P3E} \\ \underline{Z}_{P1C} & \underline{Z}_{P2C} & \underline{Z}_{P3C} \\ \underline{Z}_{P1P} & \underline{Z}_{P2P} & \underline{Z}_{P3P} \end{bmatrix} \cdot \begin{bmatrix} \underline{I}_1 \\ \underline{I}_2 \\ \underline{I}_3 \end{bmatrix} \quad (46)$$

The unknown currents I_E, $\underline{I}_C$ and $\underline{I}_P$ are calculated with the following equations (47), (48) and (49).

$$\underline{I}_E = \frac{- \{[(\underline{I}_1 \cdot \underline{Z}_{P1E} + \underline{I}_2 \cdot \underline{Z}_{P2E} + \underline{I}_3 \cdot \underline{Z}_{P3E})] \cdot [(\underline{Z}_{EE} \cdot \underline{Z}_{PP} - \underline{Z}_{CP}^2) + (\underline{Z}_{EP} \cdot \underline{Z}_{CP} - \underline{Z}_{EC} \cdot \underline{Z}_{PP}) + (\underline{Z}_{EC} \cdot \underline{Z}_{CP} - \underline{Z}_{EP} \cdot \underline{Z}_{CC})]\}}{\underline{Z}_{EE} \cdot \underline{Z}_{CC} \cdot \underline{Z}_{PP} + \underline{Z}_{EC} \cdot \underline{Z}_{CP} \cdot \underline{Z}_{EP} + \underline{Z}_{EP} \cdot \underline{Z}_{EC} \cdot \underline{Z}_{CP} - \underline{Z}_{EP}^2 \cdot \underline{Z}_{CC} - \underline{Z}_{CP}^2 \cdot \underline{Z}_{EE} - \underline{Z}_{PP} \cdot \underline{Z}_{EC}^2} \quad (47)$$

$$\underline{I}_C = \frac{- \{[(\underline{I}_1 \cdot \underline{Z}_{P1C} + \underline{I}_2 \cdot \underline{Z}_{P2C} + \underline{I}_3 \cdot \underline{Z}_{P3C})] \cdot [(\underline{Z}_{CP} \cdot \underline{Z}_{EP} - \underline{Z}_{EC} \cdot \underline{Z}_{PP}) + (\underline{Z}_{EE} \cdot \underline{Z}_{PP} - \underline{Z}_{EP}^2) + (\underline{Z}_{EP} \cdot \underline{Z}_{EC} - \underline{Z}_{EE} \cdot \underline{Z}_{CP})]\}}{\underline{Z}_{EE} \cdot \underline{Z}_{CC} \cdot \underline{Z}_{PP} + \underline{Z}_{EC} \cdot \underline{Z}_{CP} \cdot \underline{Z}_{EP} + \underline{Z}_{EP} \cdot \underline{Z}_{EC} \cdot \underline{Z}_{CP} - \underline{Z}_{EP}^2 \cdot \underline{Z}_{CC} - \underline{Z}_{CP}^2 \cdot \underline{Z}_{EE} - \underline{Z}_{PP} \cdot \underline{Z}_{EC}^2} \quad (48)$$

$$\underline{I}_P = \frac{-\{[(\underline{I}_1 \cdot \underline{Z}_{P1P} + \underline{I}_2 \cdot \underline{Z}_{P2P} + \underline{I}_3 \cdot \underline{Z}_{P3P})] \cdot [(\underline{Z}_{EC} \cdot \underline{Z}_{CP} - \underline{Z}_{PP} \cdot \underline{Z}_{EP}) + (\underline{Z}_{EC} \cdot \underline{Z}_{EP} - \underline{Z}_{EE} \cdot \underline{Z}_{CP}) + (\underline{Z}_{EE} \cdot \underline{Z}_{CC} - \underline{Z}_{EC}^{\,2})]\}}{\underline{Z}_{EE} \cdot \underline{Z}_{CC} \cdot \underline{Z}_{PP} + \underline{Z}_{EC} \cdot \underline{Z}_{CP} \cdot \underline{Z}_{EP} + \underline{Z}_{EP} \cdot \underline{Z}_{EC} \cdot \underline{Z}_{CP} - \underline{Z}_{EP}^{\,2} \cdot \underline{Z}_{CC} - \underline{Z}_{CP}^{\,2} \cdot \underline{Z}_{EE} - \underline{Z}_{PP} \cdot \underline{Z}_{EC}^{\,2}} \quad (49)$$

Based on the mentioned equations (42) – (49) the pipeline reduction factor R_{FP} can be defined for the in figure 4.11 introduced conductor arrangement. For calculating the pipeline current as if there is no compensation conductor, the elements of the 4th line and 4th row of the in equation (42) shown impedance matrix have to be eliminated.

Based on formula (41), the pipeline reduction factor R_{FP} for the example introduced in figure 4.11 can be set up as:

$$R_{FP} = \frac{\dfrac{-\{[(\underline{I}_1 \cdot \underline{Z}_{P1P} + \underline{I}_2 \cdot \underline{Z}_{P2P} + \underline{I}_3 \cdot \underline{Z}_{P3P})] \cdot [(\underline{Z}_{EC} \cdot \underline{Z}_{CP} - \underline{Z}_{CC} \cdot \underline{Z}_{EP}) + (\underline{Z}_{EC} \cdot \underline{Z}_{EP} - \underline{Z}_{EE} \cdot \underline{Z}_{CP}) + (\underline{Z}_{EE} \cdot \underline{Z}_{CC} - \underline{Z}_{EC}^{\,2})]\}}{\underline{Z}_{EE} \cdot \underline{Z}_{CC} \cdot \underline{Z}_{PP} + \underline{Z}_{EC} \cdot \underline{Z}_{CP} \cdot \underline{Z}_{EP} + \underline{Z}_{EP} \cdot \underline{Z}_{EC} \cdot \underline{Z}_{CP} - \underline{Z}_{EP}^{\,2} \cdot \underline{Z}_{CC} - \underline{Z}_{CP}^{\,2} \cdot \underline{Z}_{EE} - \underline{Z}_{PP} \cdot \underline{Z}_{EC}^{\,2}}}{\dfrac{-\{[(\underline{I}_1 \cdot \underline{Z}_{P1P} + \underline{I}_2 \cdot \underline{Z}_{P2P} + \underline{I}_3 \cdot \underline{Z}_{P3P}) \cdot (-\underline{Z}_{EP})] + [(\underline{I}_1 \cdot \underline{Z}_{P1P} + \underline{I}_2 \cdot \underline{Z}_{P2P} + \underline{I}_3 \cdot \underline{Z}_{P3P}) \cdot (-\underline{Z}_{EE})]\}}{\underline{Z}_{EE} \cdot \underline{Z}_{PP} - \underline{Z}_{EP}^{\,2}}} \quad (50)$$

The calculation procedures derived in this subchapter show that it gets complex very quickly, if one takes more phase- or compensation conductors than in the introduced example into account, which underlines the benefit of a Matlab® based tool with matrix algebra.

As formula (50) shows, the impact of the earth wire is taken into account for the calculation of the pipeline reduction factor, because also the passive conductors influence each other. Consequently the following figures 4.12 – 4.14 demonstrate the shared influence of a fixed earth wire and a varying compensation conductor.

The following figure 4.12 shows the pipeline reduction factor R_{FP} for the in figure 4.9 shown one-circuit pylon and varying horizontal distances between compensation conductor and pipeline.

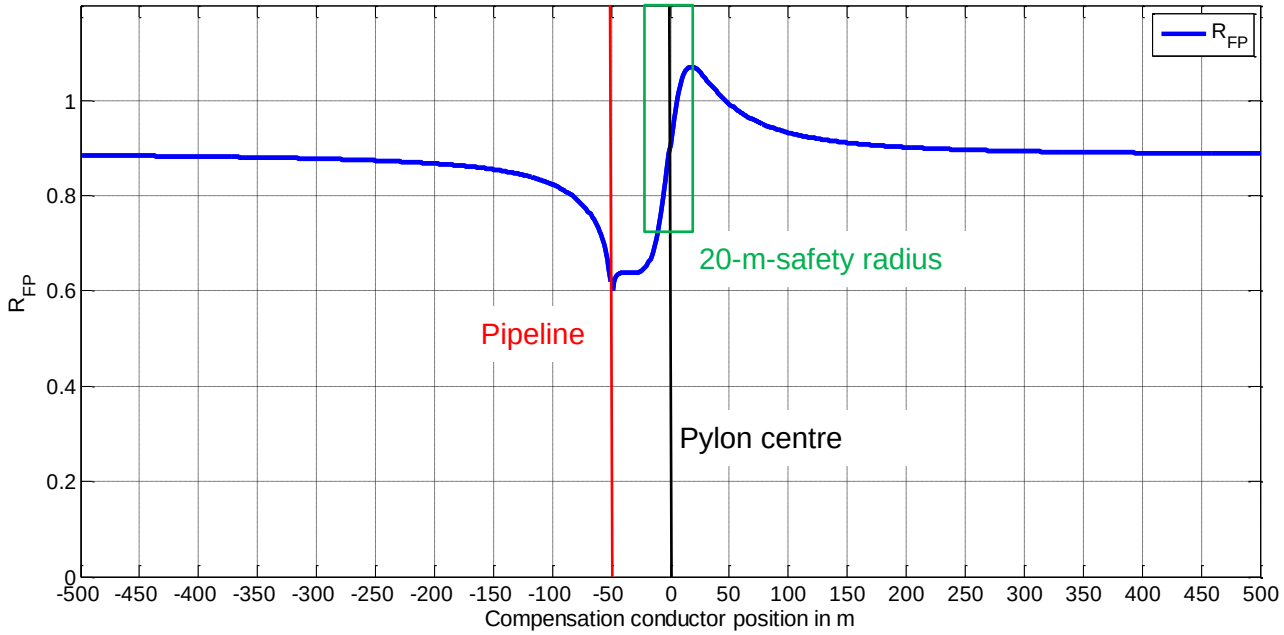

Figure 4.12: Pipeline reduction factor R_{FP} for varying horizontal distance between compensation conductor and pipeline

The figure 4.12 shows the pipeline reduction factor R_{FP} for moving horizontal locations of the compensation conductor. The pipeline is located 50 m on the left side of the overhead line and buried in a depth of 1 m. The compensation conductor is buried at the same depth. A demonstrably positive effect is evident for a compensation conductor position between - 70 m and -30 m (related to the pylon centre). Between -20 m and 20 m the compensation conductor is inside the 20-m-safety radius which is in Austria required [7] between 110 kV pylons and pipelines. In this area conductive interferences between pylon earthing system and compensation conductor is very likely. Therefore this green marked area should be avoided as position of the compensation conductor. In the close area to the best result for the pipeline reduction factor R_{FP} can be achieved. Consequently the optimum position of the compensation conductor is between -52 m and -47 m (related to the pylon centre). The main result of this simulation is that compensation conductors should be located very close to the pipeline. In order to investigate the optimum burying depth of a compensation conductor additional simulations are carried out and shown in figure 4.13.

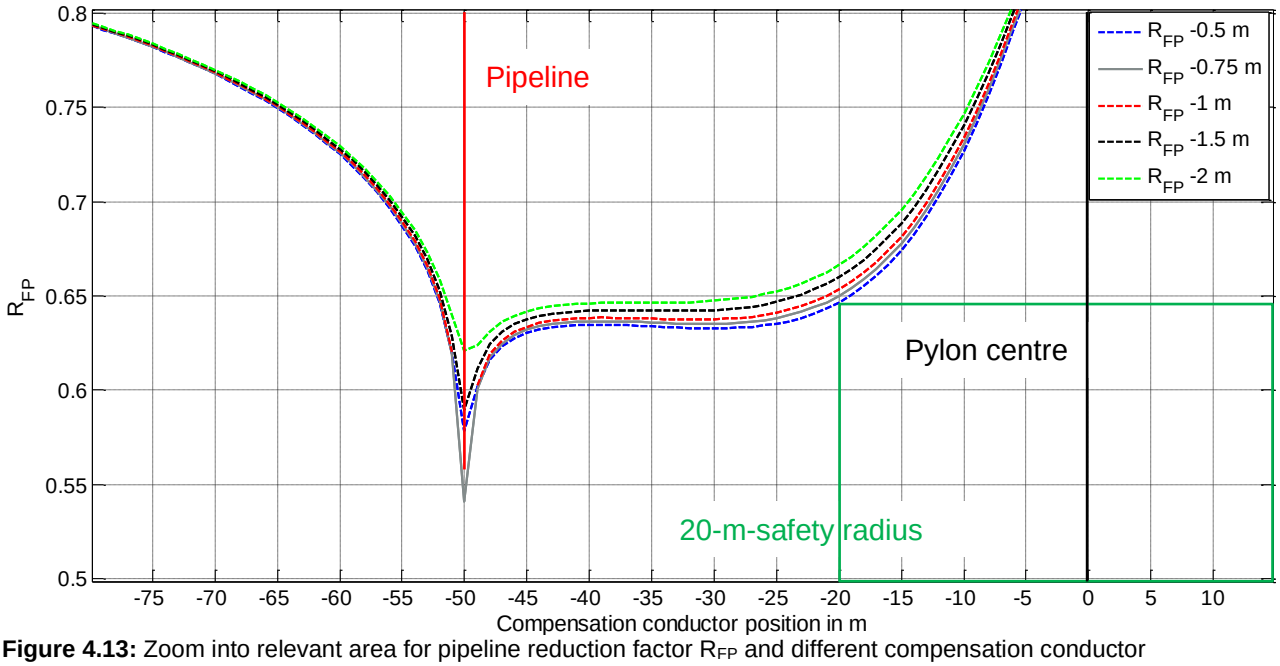

Figure 4.13: Zoom into relevant area for pipeline reduction factor R_{FP} and different compensation conductor burying depths

The figure 4.13 shows the pipeline reduction factor R_{FP} for the introduced example and different compensation conductor installation depths. The pipeline is buried at a depth of 1 m, the compensation conductor is buried between depths of 0.5 m and 2 m. The best result can be achieved by burying the compensation conductor 0.25 m directly above the pipeline. This result stands similar for putting the compensation conductor 0.25 m beside the pipeline.

The figure 4.14 shows the pipeline reduction factor R_{FP} for varying pipeline positions and varying compensation conductor positions. The pipeline is located between -450 m and 450 m from the overhead line and buried in a depth of 1 m. The compensation conductor is buried at the same depth. The deviation between the varying pipeline positions having the same distance to the overhead line but lying on the opposite side of the high-voltage line can be explained by the influence of the phase conductor arrangements (see also 4.3.2). It is evident, that the phase conductor arrangements have the biggest influence if the compensation conductor is close to the overhead line. If the compensation conductor is in the vicinity of the pipeline, the influence of the phase positions is very low.

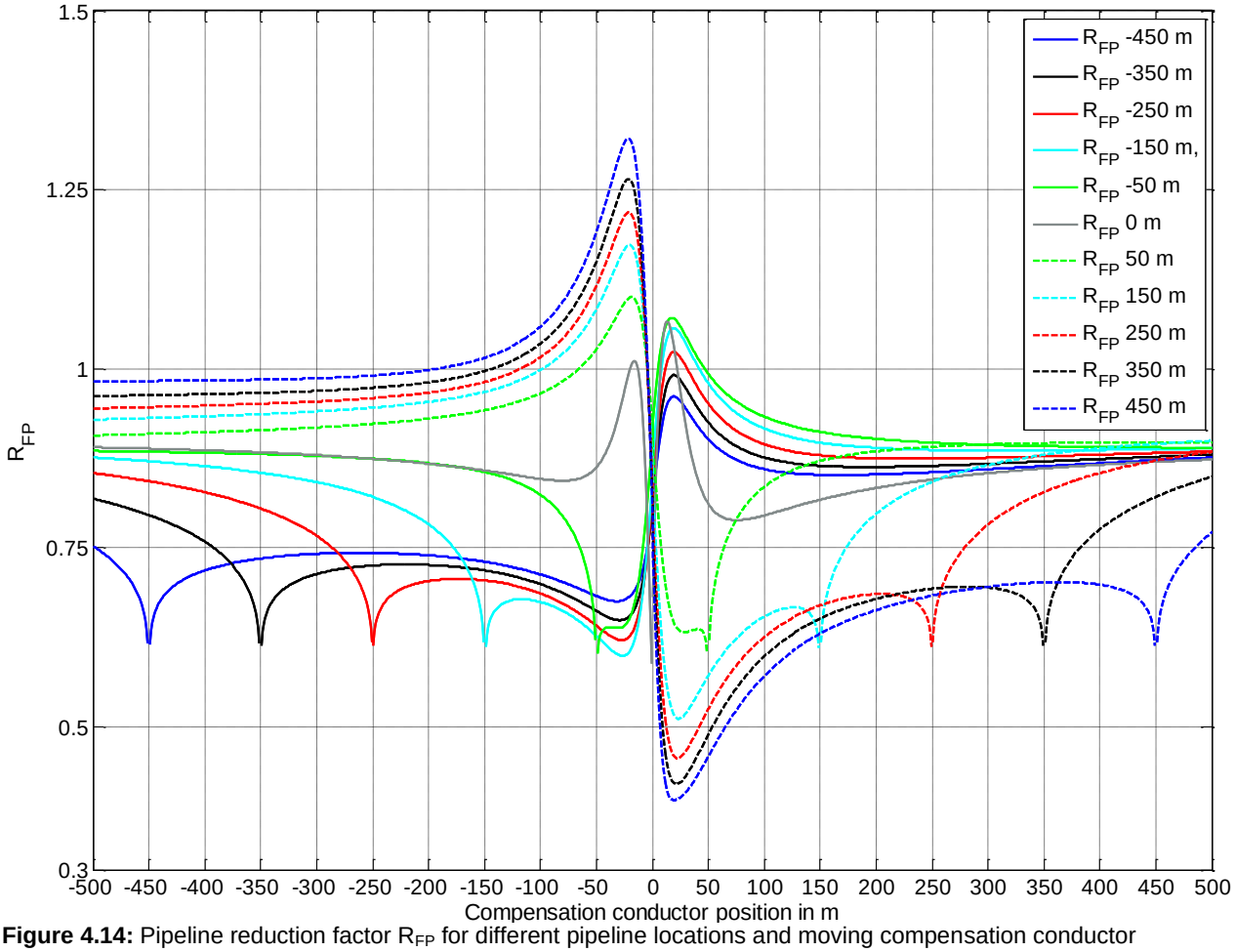

Figure 4.14: Pipeline reduction factor R_{FP} for different pipeline locations and moving compensation conductor

There exists a local dependency of the pipeline reduction factor R_{FP} in relation to the distance between pipeline and compensation conductor. In cases where the compensation conductor is close to the pipeline, the pipeline position plays a minor role. In cases where the pipeline is closer to the high-voltage line, a comparably better effect can be achieved by positioning the compensation conductor close to the overhead line.

Generally speaking, there are two possibilities of placing the compensation conductor either close to the pipeline or close to the overhead line whereas the 20-m-safety radius has to be taken into account. Effects based on the phase conductor arrangement may worsen the situation. Consequently one is on the safe side by burying the compensation conductor close to the pipeline.

The simulations for the pipeline system show, that a the situation depends on a lot of parameters as there are for example the specific soil resistivities, the number of influencing conductors, the frequency, the conductor self-resistances per unit length, the phase positions or the geometry. All significant parameters have to be separately evaluated for each case.

4.3.2 Influence of Phase Conductor Arrangements

The influence of different phase conductor arrangements is investigated for the in figure 4.15 introduced overhead-pylon. For a single circuit-system, the following phase conductor arrangements can be defined:

- Phase position 1: Phase 1: 0°, Phase 2: 120°, Phase 3: 240°
- Phase position 2: Phase 1: 0°, Phase 2: 240°, Phase 3: 120°
- Phase position 3: Phase 1: 240°, Phase 2: 120°, Phase 3: 0°
- Phase position 4: Phase 1: 240°, Phase 2: 0°, Phase 3: 120°
- Phase position 5: Phase 1: 120°, Phase 2: 0°, Phase 3: 240°
- Phase position 6: Phase 1: 120°, Phase 2: 240°, Phase 3: 0°

In the table 4.1 the results for a typical arrangement of 3 phase wires, an earth wire and a pipeline (see also figure 4.15) are summarised.

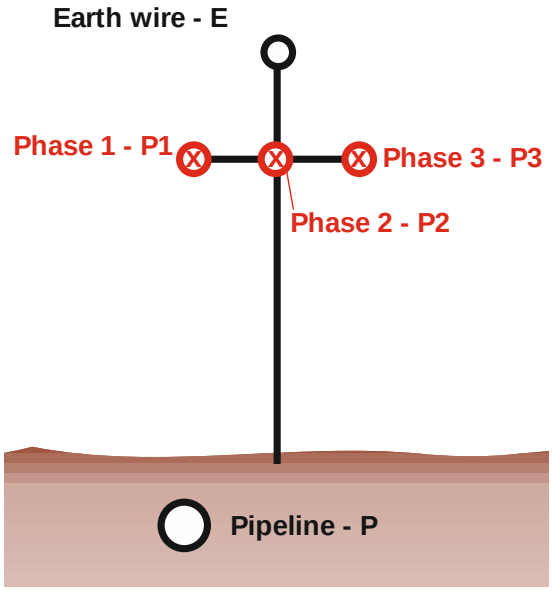

Figure 4.15: Conductor- and pipeline arrangement for the first investigated case summarised in table 4.1

	Absolute value of $\underline{I}_E$	Phase angle of $\underline{I}_E$	Absolute value of $\underline{I}_P$	Phase angle of $\underline{I}_P$
Phase position 1	Value E1	Value EI	Value P1	Value PI
Phase position 2	Value E2	Value EII	Value P2	Value PII
Phase position 3	Value E2	Value EIII	Value P2	Value PIII
Phase position 4	Value E1	Value EIV	Value P1	Value PIV
Phase position 5	Value E2	Value EV	Value P2	Value PV
Phase position 6	Value E1	Value EVI	Value P1	Value PVI

Table 4.1: Influence of the phase positions for an arrangement with 3 phase wires, 1 pipeline and 1 earth wire

The general results in table 4.1 show that the investigated phase positions lead for a configuration with three horizontal phase wires, one earth wire and one pipeline to two possible results regarding the absolute values of the currents in the earth wire $\underline{I}_E$ and in the pipeline $\underline{I}_P$. Two obvious classes develop (marked in yellow and green). Phase positions 1, 4 and 6 lead to the same absolute values as the phase positions 2, 3 and 5.

This effect can be explained by the two passive conductors (earth wire and pipeline) additionally influencing each other. The phase angles of the earth wire current $\underline{I}_E$ and the pipeline current $\underline{I}_P$ are different for each investigated type of phase position.

In the table 4.2 the results for a typical arrangement of 3 phase wires and a pipeline (see figure 4.16) are summarised.

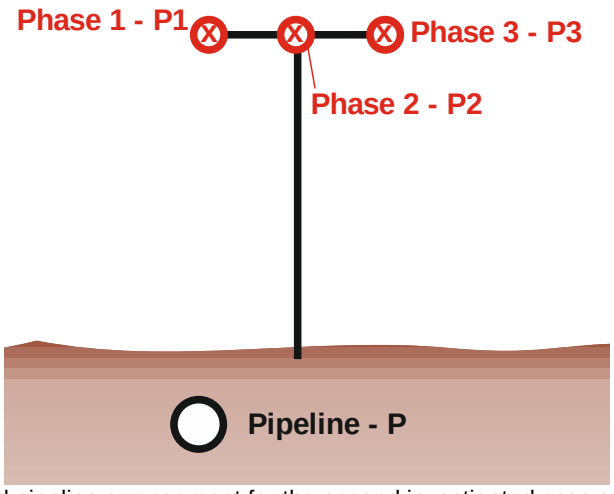

Figure 4.16: Conductor- and pipeline arrangement for the second investigated case summarised in table 4.2

	Absolute value of $\underline{I}_P$	Phase angle of $\underline{I}_P$
Phase position 1	Value P3	Value PVII
Phase position 2	Value P3	Value PVII
Phase position 3	Value P3	Value PVIII
Phase position 4	Value P3	Value PIX
Phase position 5	Value P3	Value PX
Phase position 6	Value P3	Value PXI

Table 4.2: Influence of the phase positions for an arrangement with 3 phase wires and 1 pipeline

The general results summarised in table 4.2 show that for the investigated arrangement of 3 phase wires and one pipeline, the pipeline currents $\underline{I}_P$ are independent from the phase position. In this case no obvious classes develop.

In the table 4.3 the results for a typical arrangement of 3 phase wires and an earth wire (see figure 4.17) are summarised. The difference to the previous simulation is that the mutual impedances between phase 1 and earth wire (figure 4.11 $\underline{Z}_{P1E}$ and Phase 3 and earth wire $\underline{Z}_{P1E}$) are identical.

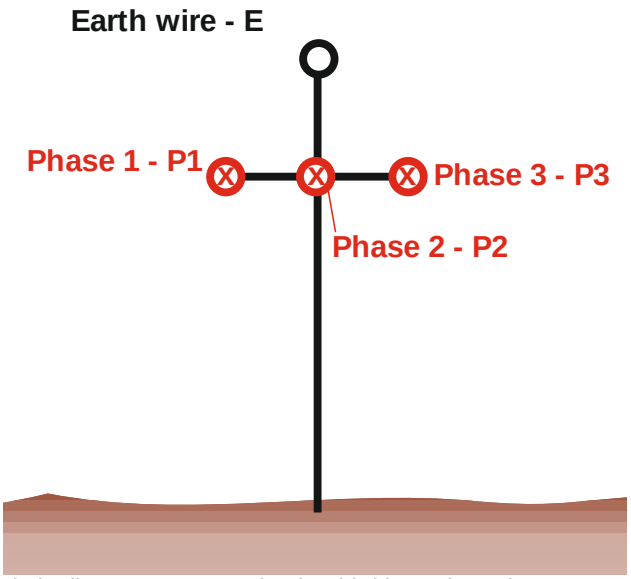

Figure 4.17: Conductor- and pipeline arrangement for the third investigated case summarised in table 4.3

	Absolute value of $\underline{I}_E$	Phase angle of $\underline{I}_E$
Phase position 1	Value E3	Value EVII
Phase position 2	Value E3	Value EVIII
Phase position 3	Value E3	Value EVII
Phase position 4	Value E3	Value EIX
Phase position 5	Value E3	Value EIX
Phase position 6	Value E3	Value EVIII

Table 4.3: Influence of the phase positions for an arrangement with 3 phase wires and 1 earth wire

The general results summarised in table 4.3 show that for the investigated arrangement of 3 phase wires and one Pipeline, the earth wire currents $\underline{I}_E$ are independent from the phase position. In this case no obvious classes develop. The phase angles of $\underline{I}_E$ however show a dependency of the phase positions. Therefore three obvious groups develop. Phase positions 1 and 3 lead to the same phase angles as well as the phase positions 2 and 6 and the phase positions 4 and 5.

The results of this investigation show that pipeline currents and accordingly pipeline interference voltages depend on phase positions of overhead lines, if there are two or more passive conductors.

4.3.3 Simulation and Measurement

The calculated pipeline reduction factors that base on Carson's formulas give good indications about the optimal compensation conductor position. If the compensation conductor is not buried barely it has to be grounded at both ends with low impedances. This is not investigated in the simulations. For calculating the impact of isolated compensation conductors that are directly connected to both ends of the pipeline other calculation methods have to be taken into account. An iterative network considering pipeline impedances (see figure 2.5) can for example be set up and solved. If the compensation conductor is already buried measurements can give additional information about the impact of the compensation conductor for different circuits, well knowing that the effective impact depends on multiple parameters like the specific soil resistivity or other metallic installations (earth wires of other interfering systems, horizontal earthing conductors of transformer stations) in the interfering area. Therefore measurements [37] of the pipeline interference voltages considering the impact of an existing compensation conductor took place. The principal arrangement of the investigated case can be found in the figure 4.18. The distance between the pipeline and the compensation conductor is approximately 30 cm. In the investigated case, the railway system is only equipped with contact- , messenger wire and rails.

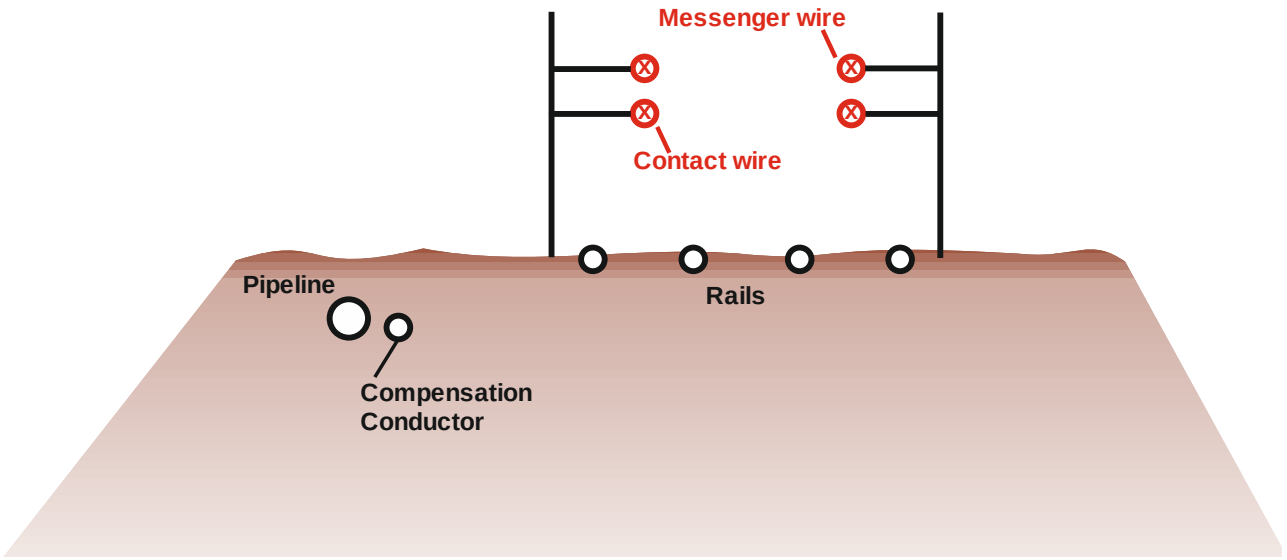

Figure 4.18: Principal conductor arrangement of the investigated case

The rail reduction factor R_{FR} can be calculated with the introduced procedure in chapter 4.3.1. Assuming that there is no functional compensation conductor, the calculation of rail the rail reduction factor amounts to 0.32.

The pipeline reduction factor R_{FP} is, under the assumption that no rails exist, 0.62. The product of both reduction factors leads to in the classical approach to an overall reduction

factor of approximately 0.20. Well knowing that passive conductors have a coupling influence to each other the overall reduction factor is calculated for an interfered arrangement with pipeline and compensation conductor and amounts to 0.22.

The figure 4.19 shows a scheme of the approach between the interfered pipeline and the interfering railway system.

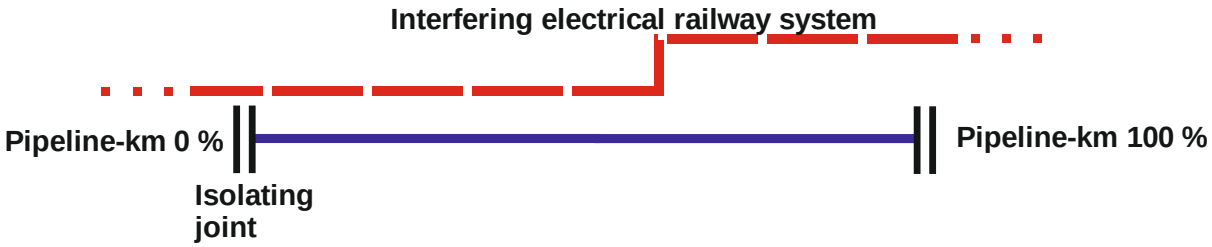

Figure 4.19: Approach between the interfered pipeline and interfering railway system in the investigated case

In the figure 4.20 possible switching possibilities of the compensation conductor are shown.

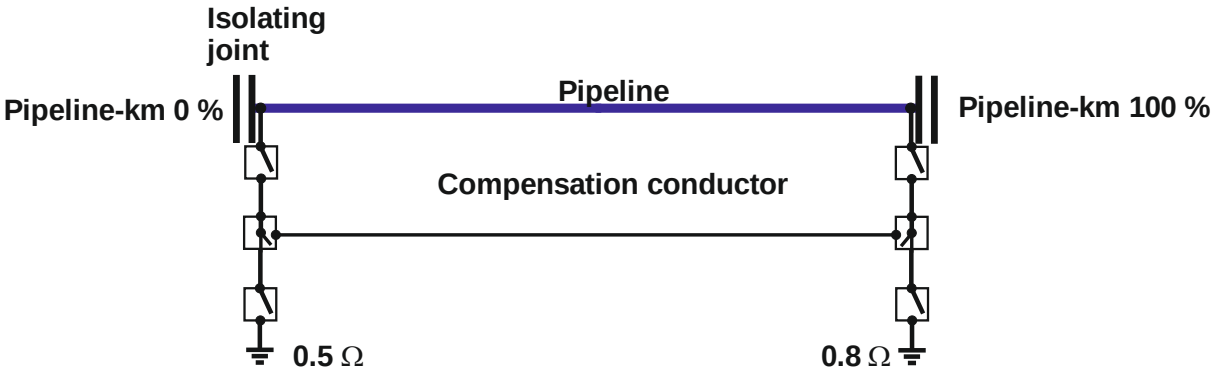

Figure 4.20: Pipeline and compensation conductor, switching possibilities

Within the context of this PhD thesis the following switching scenarios S1 - S7 are defined for the measurement in order to demonstrate the effect of the compensation conductor.

- S1: The pipeline connected with compensation conductor at both ends and both earthing systems.
- S2: The pipeline is connected with compensation conductor at one end and with both earthing systems.
- S3: The pipeline is connected with both earthing systems. The compensation conductor lies isolated in earth.
- S4: The pipeline is not connected to earthing systems. The compensation conductor is connected to the earthing systems at both ends.

- S5: The pipeline is not directly connected to any earthing system. The compensation conductor is connected to the pipeline at one end. At the other end the compensation conductor is connected to an earthing system.
- S6: The pipeline is connected with compensation conductor at both ends. No connection to earthing systems.
- S7: The compensation conductor is connected to the pipeline at one end. No connection to earthing systems.
- S8: The pipeline and the compensation conductor are not connected with each other and not connected to earthing systems.

With the help of the at the beginning of this chapter introduced method, based on Carson's formulas it is possible to calculate the impact of switching scenario 4– Pipeline not connected to earthing system, compensation conductor is grounded at both ends. The calculation of the pipeline reduction factor R_{FP} is carried out within this thesis. The simulation of this switching scenario (R_{FP} 0.62) coincides with the measurement (R_{FP}=0.59).

The measurements showed that the best effect can be achieved with switching scenario 6 – pipeline connected with the compensation conductor at both ends without a connection to the earthing systems. This effect can be explained by the compensation of the currents along the pipeline by the return currents in the reduction conductor based on the small distance of approximately 30 cm between the pipeline and the compensation conductor.

Based on the measurements the best pipeline interference voltage mitigating effects can be achieved by

- Earthing the pipeline at both ends (S3).
- Earthing the compensation conductor at both ends (S4).
- Connecting the compensation conductor with the pipeline at both ends (S6).

In order to get sufficient compensation currents, simulations show that the self-resistance of the compensation conductor (see R_i, formula (14)) should be less or equal than the self-resistance of the pipeline. For the simulation of the impact of switching scenario 4, the earthing systems where not considered. It is apparent that the compensation conductor can be a preferable variant under certain circumstances, if there is for example a full and constant parallel approach over some kilometres where very high specific soil resistivities (> 250 Ωm) prevail and low impedant earthing systems are not possible.

During the measurement carried out, the pipeline interference voltage against remote earth was measured at 6 measuring points along the pipeline. The interfering railway system was

fed from one substation. The interfering currents were measured directly in the substation. The measurements as well as the simulation in figure 4.21 are extrapolated to a given current feeding current of 1000 A from the substation. The measurement and the simulation base on a switching scenario without a functional compensation conductor. Therefore the railway reduction factor of R_{FR}= 0.32 is considered for the simulation. The following figure 4.21 shows the comparison between measurement and simulation of the introduced case and switching scenario 8. In the investigated case the compensation conductor is an isolated copper conductor with a cross section of 50 mm^2. Due to the fact of an isolated conductor and consequently no current flow, the compensation conductor in scenario 8 has no influence on the pipeline interference voltage.

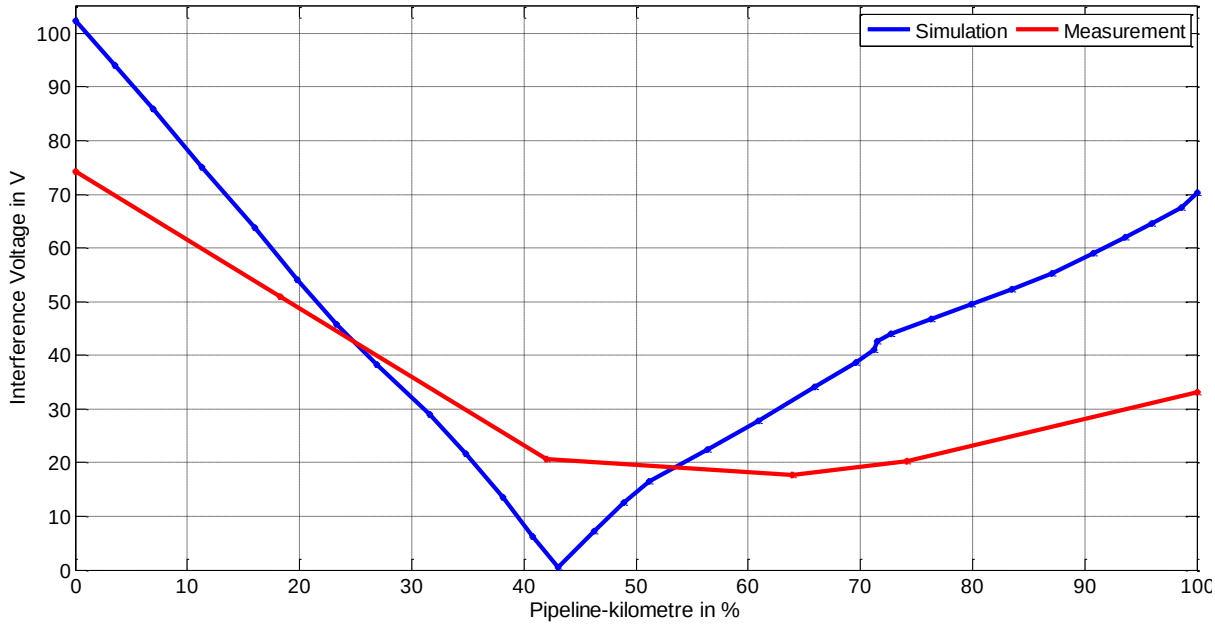

Figure 4.21: Comparison between measurement and simulation for the investigated case

As figure 4.21 shows, the simulation gives higher values than the measurement. A difference between the simulation and the measurement is that from the middle the measured curve doesn't rise with the same gradient as the simulated curve. This can be explained by the fact that for the simulation a constant current is assumed over the whole interfering section. In reality in case of one side infeed the current decreases over the length of the contact wire, because different vehicle positions have to be considered (see also figure 5.1).

The existence of other conductive material in earth, for example horizontal earthing conductors of transformer stations or two additional inoperative rails along some parts of the railway section is known but not part of the simulation model. Some older publications, for example [35] mention a civilisation (reduction) factor in order to regard these circumstances.

As it can be seen in the comparison it could be meaningful to reintroduce the civilisation (reduction factor) especially in urbanised areas with global earthing systems.

The calculation of mutual impedances was performed for a in this region conservative value of the specific soil resistivity of 100 Ωm. According to the in chapter 2.2.2 introduced formulas, the mutual impedances and consequently induced voltages in longitudinal direction raise with raising specific soil resistivity.

Another argument for explaining the differences between measurement and simulation is the fact that it was due to the topological conditions not always possible to place the measuring conductor electrode at a sufficient high distance from the pipeline to find remote earth, consequently the measured voltages would not correspond to the pipeline interference voltages.

4.4 Increasing of the Distance between Pipeline and Interfering System

An alternative to the above mentioned measures is the spatial separation of influencing and influenced system. The following example in figure 4.22 shows clearly that for keeping the pipeline voltages under the 10 V AC corrosion risk criterion, it is necessary to consider a protective distance between pipeline and influencing system [4].

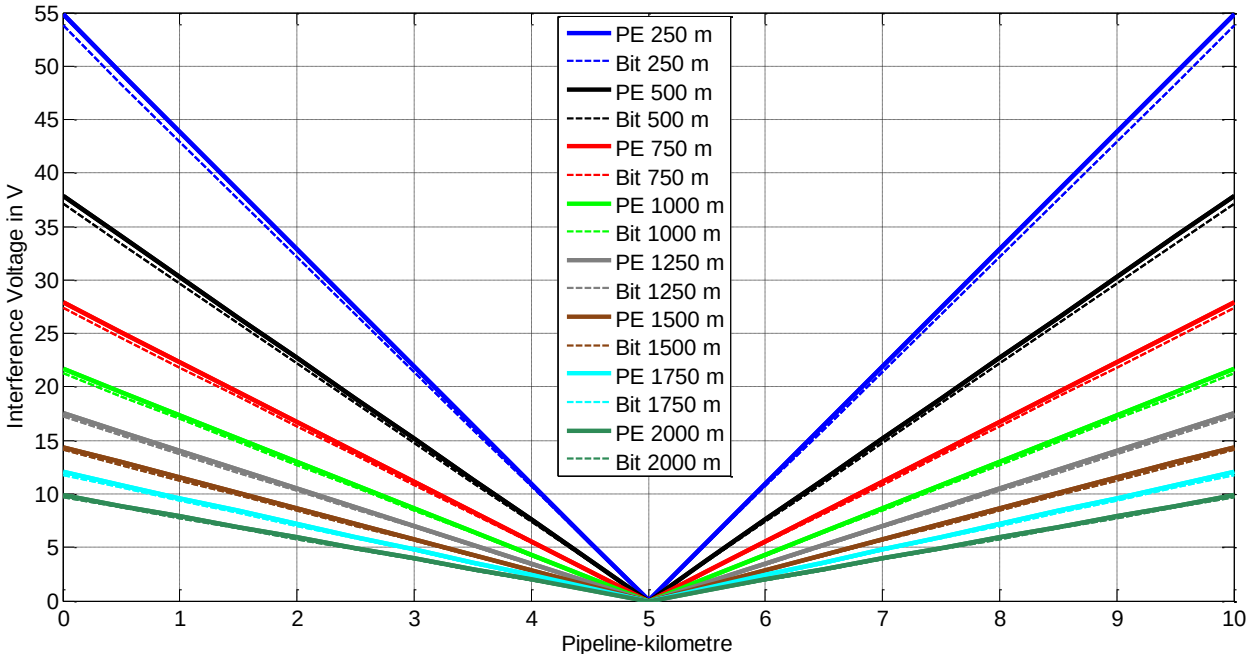

Figure 4.22: Pipeline interference voltage as a function of the horizontal distance [4], modified

The smaller induced voltage distribution in Bitumen isolated pipelines compared to PE isolated pipelines with the same system distance is evident in figure 4.20.

Thus results for a 10-km-long parallel course, with a homopolar influencing current (in the figure 4.22: 1000 A traction current), as it might be caused by electric railway equipment, to distances of approximately 2000 m, in order to keep the pipeline voltage under the requested 10 V-limit.

Additional Results as for example for a 1000-m-long parallel course can be derived from formula (23) which amount to a necessary horizontal distance of 200 m to keep the pipeline voltage under the 10 V-limit. Such easy developable distances should be taken as far as possible into consideration during spatial planning processes [6].

4.5 Other Measures

The optimisation of the phase conductor arrangement of high-voltage-overhead lines can reduce induced pipeline voltages. In the previous chapter 4.3.2 of this thesis, the effect of different phase conductor arrangements of a single circuit-system is already demonstrated.

Former investigations [12] of the Institute of Electrical Power Systems of Graz University of Technology show a significant effect of the phase positions on the magnetic field in the vicinity as well as in the far area of high-voltage lines. In [38] the impact of the phase conductor arrangements of a three-level pylon („Tonne") on the induced interference voltages of a parallel 10-km-long pipeline in a horizontal distance of 250 m buried pipeline is investigated. The figure 4.23 shows the investigated phase conductor arrangements.

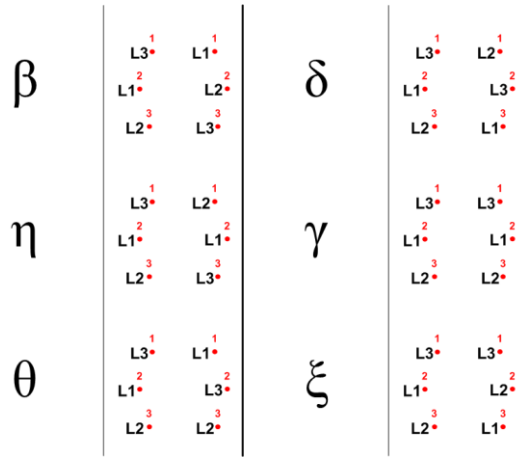

Figure 4.23: Investigated phase conductor arrangements [38], modified

In figure 4.24 the pipeline interference voltages for the in figure 4.23 introduced phase positions are shown.

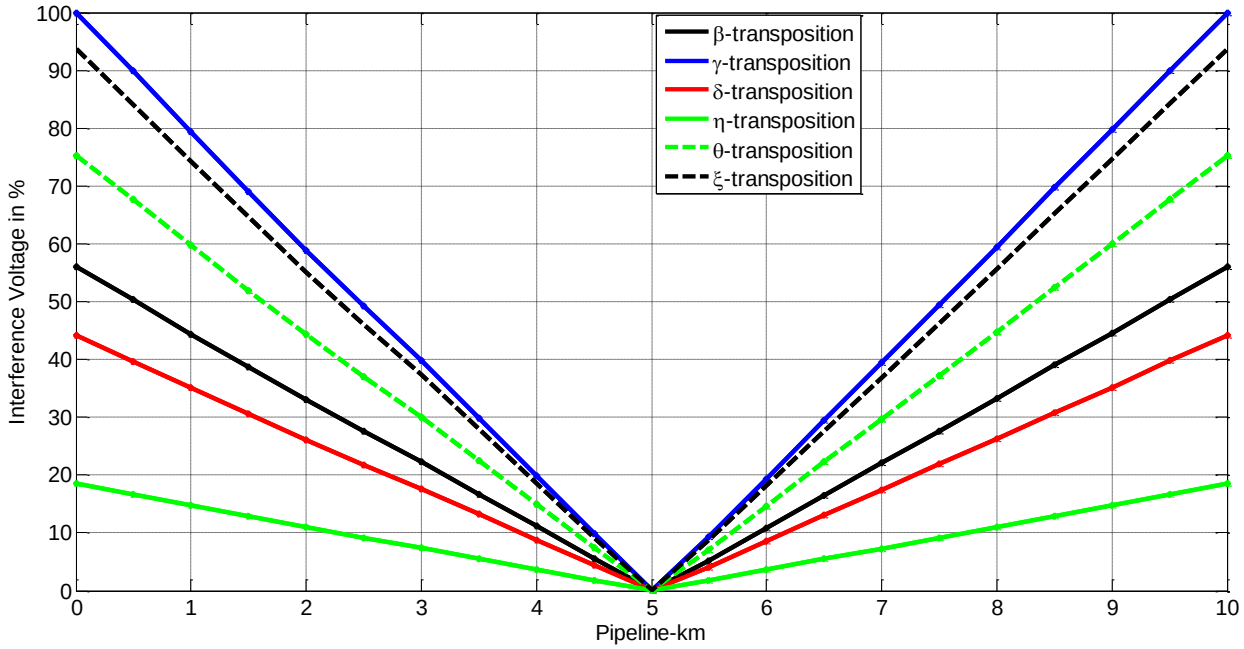

Figure 4.24: Pipeline interference voltage for different phase positions [38], modified

The pipeline interference voltages in figure 4.24 are rated to the maximum (γ-transposition) and shown in per cent. It is evident that there is a factor of 5-6 between best-case (symmetrical η-transposition) and the worst-case (γ-transposition). In summary it can be said that the optimisation of the phase positions is a supplement to the introduced measures like AC earthing systems, isolating joints or compensation conductors especially for shorter pipelines of some ten kilometres, if the phase positions do not change along the interfered pipeline section. Nevertheless, the scope of this thesis is focused on the measures AC earthing systems, isolating joints and compensation conductors.

Partial and full active compensation of induced pipeline voltages are effective, but expensive measures. In the case of short parallel courses between pipeline and interfering system, the methods are too cost-intensive. In the case of long parallel courses the required electric power of the active compensation system might be very high [1]. Until today this measure hasn't been applied in Austria.

4.6 Summary

The multiple possibilities to reduce pipeline interference voltages are demonstrated in this chapter with the help of simulations and measurements. The analyses of the impact of varying distances between pipeline, interfering system and compensation conductor on the pipeline reduction factor R_{FP} shows a dependency on the distance. Therefore established constant reduction factors should in future be mentioned with a corresponding distance.

Well knowing that the focused interference voltage mitigating measures AC earthing systems, isolating joints and compensation conductors relate to specific costs, the preferred fields of application of these measures are illustrated with the help of a representative case study in chapter 7.

5 Interfering Systems

In this chapter the procedures for calculating pipeline interference voltages due to the influence of electric railways and high-voltage transmission lines are described. The impacts of electric railways and 400 kV overhead lines on maximum pipeline interference voltages are compared with each other.

5.1 Electric Railways

The electrical railway traction vehicles can be seen as moving electrical loads along the railway feeding section (see also figure 5.1). Railway traction vehicles can be fed by one side only (one substation) or two sides (two substations).To calculate all possible pipeline interference voltages along the pipeline all possible inducing current situations have to be considered, which means all possible positions of the locomotives for both- or one side infeed [2]. In practice both side infeed is preferred to one side infeed regarding reliability as well as overhead line losses. The following figure 5.1 shows a scheme of a one side fed railway section, the locomotive positions for the highest time-table load and the current sharing of operating- and back currents.

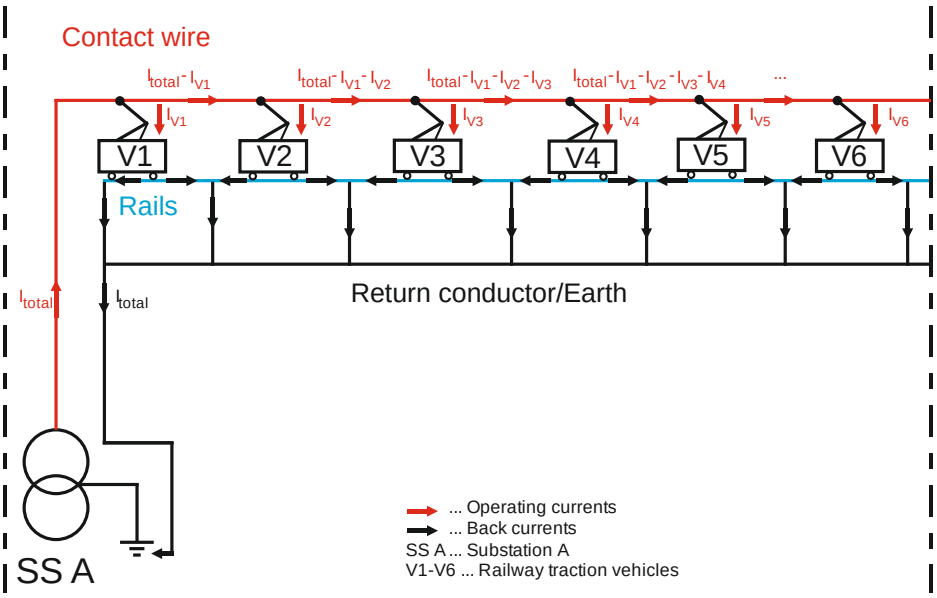

Figure 5.1: Positions of Railway traction vehicles for highest time-table load, scheme for operating- and back currents [27], [28], modified

If the operation current at the end of a feeding section is too small to supply the relevant traction vehicles another feeding section has to provide the infeed. Another criterion for the implementation of feeding sections is the admissible voltage range which is for Austria defined in ÖVE/ÖNORM EN 15163 [45] and amounts to ± 20 % from the nominal voltage (15 kV).

5.1.1 Normal Operation

The first subplot of the following figure 5.2 shows a typical traction-current diagram. The development of such traction diagrams is defined in the German standard DIN VDE 0228 – part 3 [27]. These diagrams are usually prepared by the operational management of the railway system. The traction-current diagrams in figure 5.2 and 5.3 base on the simplified diagram in the standard.

These traction-current diagrams depend on multiple parameters [28], as for example:

- Numbers of rails
- Type of railway traction vehicle (interurban train, freight train etc.)
- Single traction or multiple traction
- Traction time-table
- Simultaneous acceleration processes
- Technical equipment of substations (transformers)
- Specification and material of feeding lines

So the traction-current diagrams give information what kind of currents (amplitude and direction) can be generally expected along the railway section.

In the second subplot of the above figure 5.2 the influence of a typical one side fed railway section on a pipeline is shown. The blue plotted line - U_{max} shows the theoretical worst-case assumption, which means the maximum current along the whole pipeline. Well knowing that this assumption appears only under special conditions. If considering the locomotive positions for the highest time-table load (see figure 5.1) and accordingly the possible currents flowing from substation 1 (see 1st subplot in figure 5.2), one can recognize that the maximum induced pipeline interference voltage is in the range of about 75 % of the theoretical worst-case. The orange plotted envelope curve demonstrates the operational worst-case.

In the second subplot of the following figure 5.3 the influence of a typical both side fed railway section on a pipeline is shown. The blue plotted line - U_{max} shows again theoretical worst-case assumption, which means the maximum current along the whole pipeline. If considering the locomotive positions and the accordingly maximum current composed of two partial currents from both sides (substation 1 and 2), one can recognize that the maximum induced pipeline interference voltage is in the range of about 40 % of the theoretical worst-case [2]. The orange plotted envelope curve demonstrates again the operational worst-case.

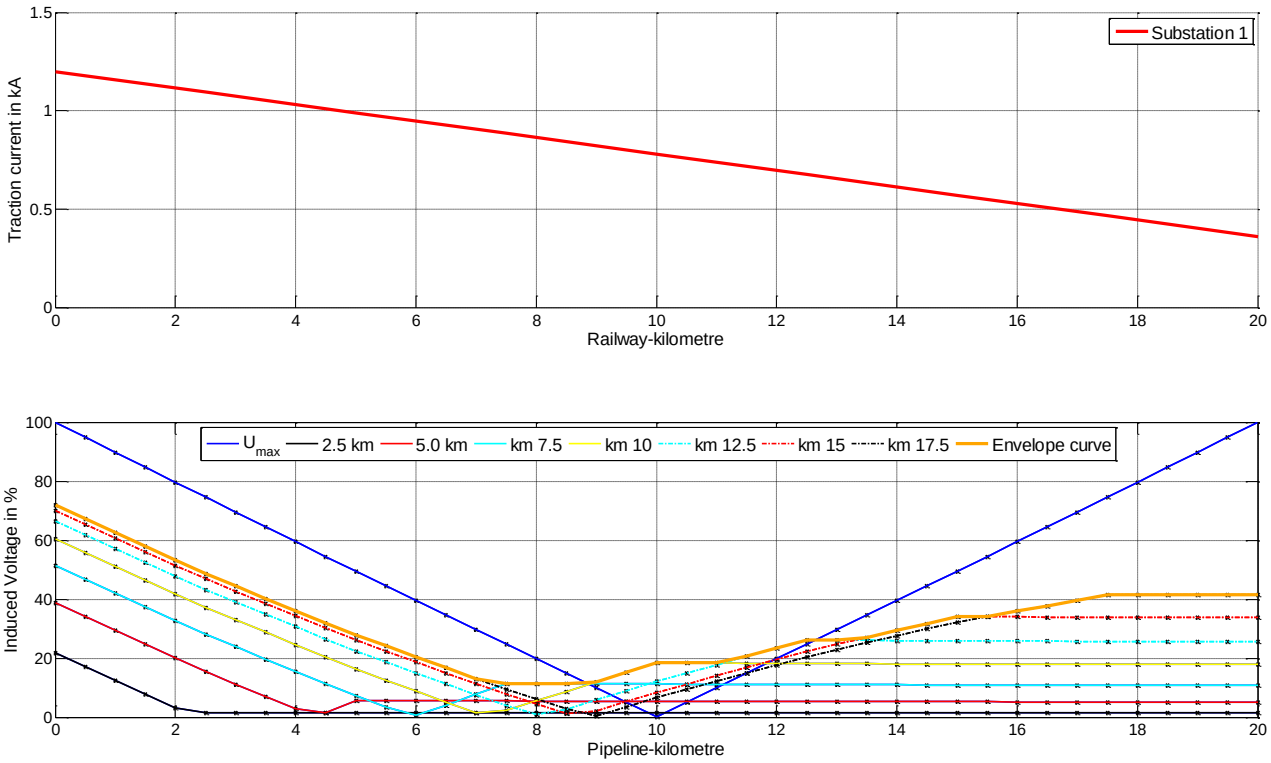

Figure 5.2: Typical traction current diagram referring to [27] for one side infeed and induced pipe voltages for moving locomotive positions, 20-km paralell approach

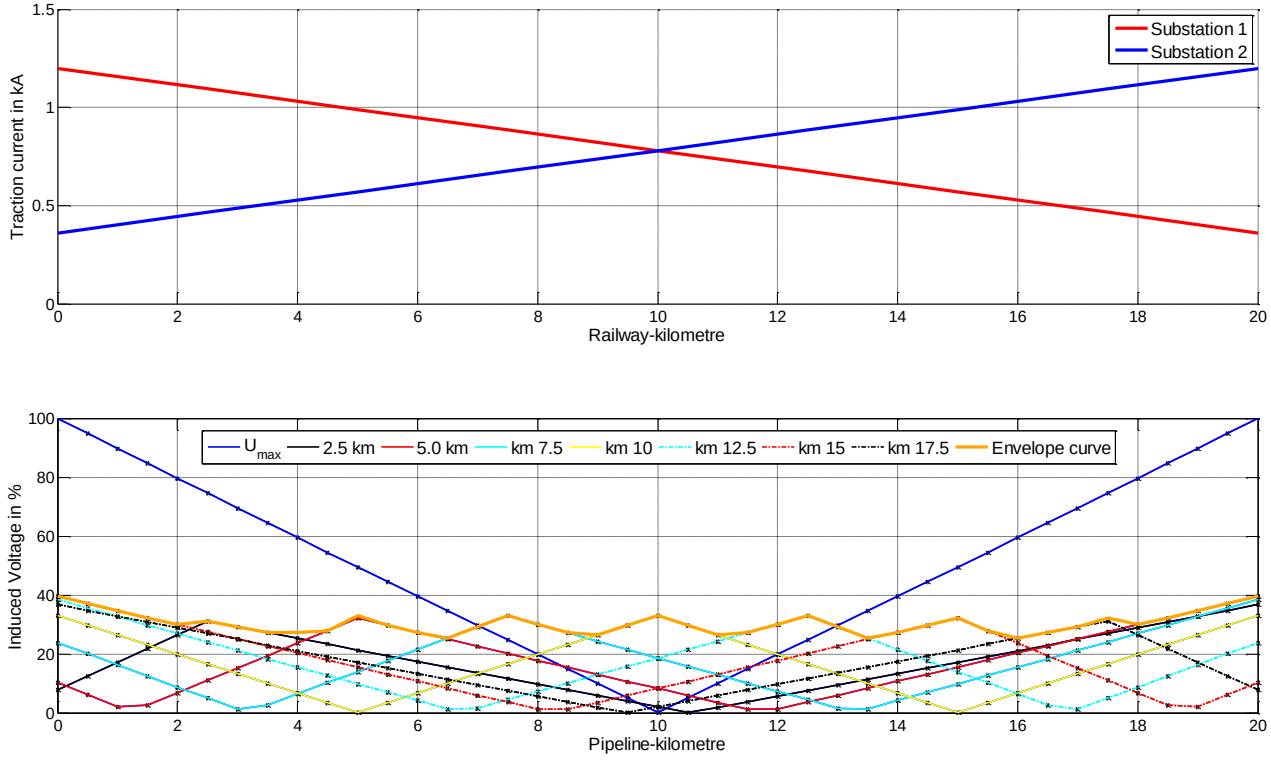

Figure 5.3: Typical traction current diagram referring to [27] for both side infeed and induced pipe voltages for moving locomotive positions, 20-km parallel approach

The analysis of pipeline interference voltage distributions for one side infeed, double side infeed and the maximum current over the whole section show some differences:

- Taking the maximum current over the whole section demonstrates the theoretical worst-case. This current- and load flow situation should be taken into account for evaluating the risk of hazard. For evaluating the risk of hazard the peaks of the pipeline interference voltage are interesting. The maximum values of the operational worst-case are depending on infeed and load flow scenarios in the range of 40 % to 75 % (see orange envelope curves in figures 5.2 and 5.3) of the theoretical worst-case.

- As the shown examples in the figures 5.2 and 5.3 show, the consideration of load-flow situations leads to different results than the assumption of the maximum current over the whole section. Therefore they are not suitable for evaluating the risk of hazard. The orange lines in figures 5.2 and 5.3 show the envelope curve and mark the operational worst-case. In the middle section of the pipeline higher results for the pipeline interference voltages are to be expected as with the method in which a constant current is assumed over the whole section. The distribution of the pipeline interference voltages along the pipeline is useful to evaluate the AC corrosion risk along the pipeline.

5.1.2 Short-Circuit Situation

Analogous to the calculation for normal operation mode the calculations for short-circuit cases base on the short-circuit diagram. These diagrams are usually prepared by the operational management of the railway line. The following parameters can be seen as determinant for short-circuit diagrams:

- Numbers of rails
- Technical equipment of substations (transformers)
- Specification and material of feeding lines

The short-circuit diagram is based on a diagram shown in the standard [27].The curves plotted in blue and in red show the values of the short-circuit currents flowing from each substation along the whole railway infeed section. The black curve is the cumulated short-circuit curve from both substations. With the help of theses curves, the pipeline interference voltage along an inductive interfered pipeline can be calculated. Generally speaking for both side infeed sections the maximum induced pipeline interference voltages usually result from faults at the ends of the approach between railways and pipelines (figure 5.4). Well knowing that this strongly depends on the approach between pipeline and railway, the method of moving fault location is appropriate to cover the worst-case.

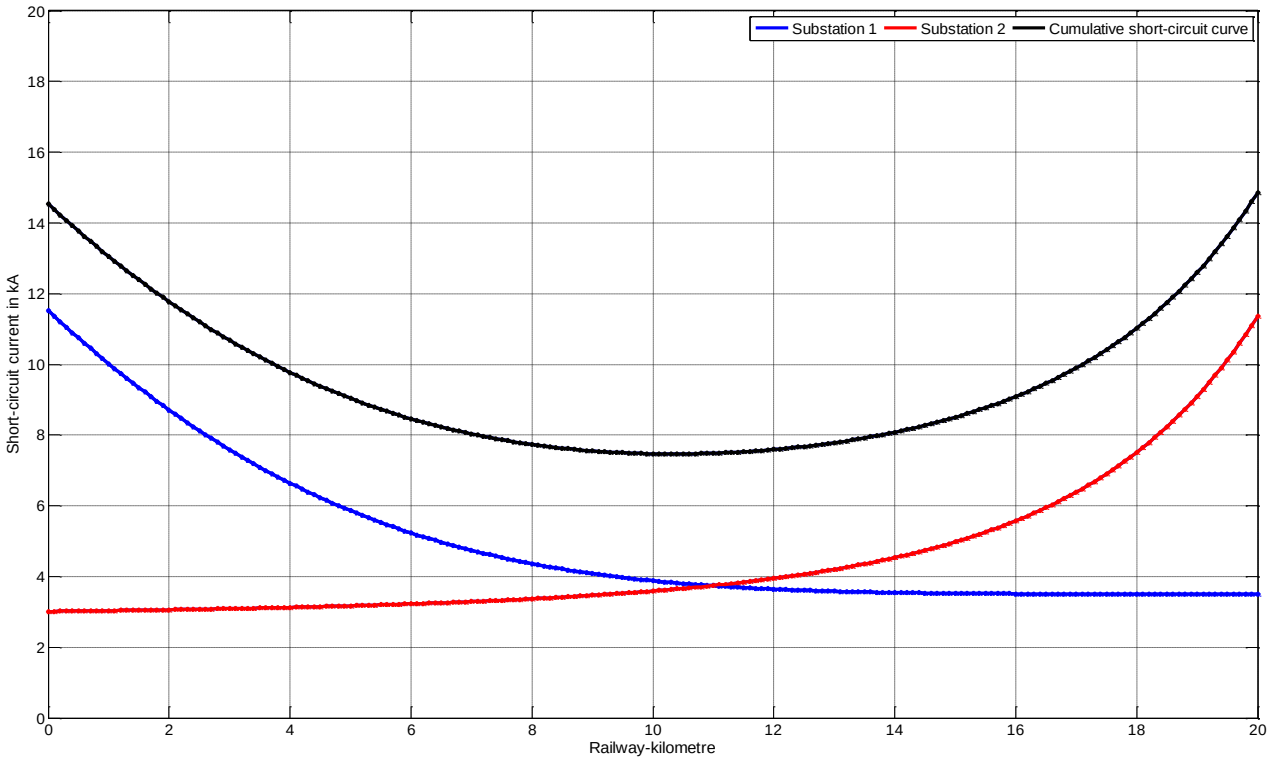

Figure 5.4: Typical short-circuit current diagram for a both side infeed section

The next figure shows the approach between two interfering railway systems and an interfered pipeline. The example is derived from praxis in order to show the methodology which is already indicated but not explicitly described in [35]. In this example three isolating joints are installed along the pipeline. The faults F1 to F4 are assumed at the beginnings and the ends of the approaches between the two railway systems and the pipeline.

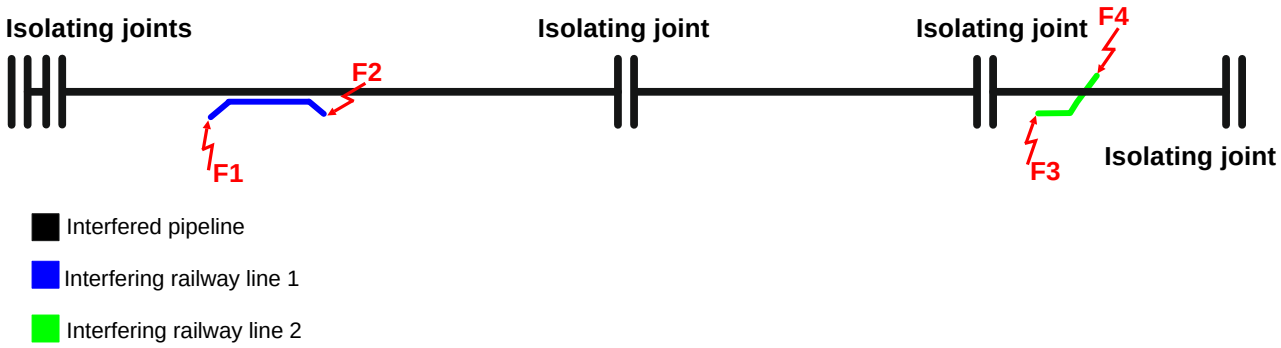

Figure 5.5: Scheme of the approach between interfered pipeline with isolating joints and electric railways, indicating the fault locations F1-F4

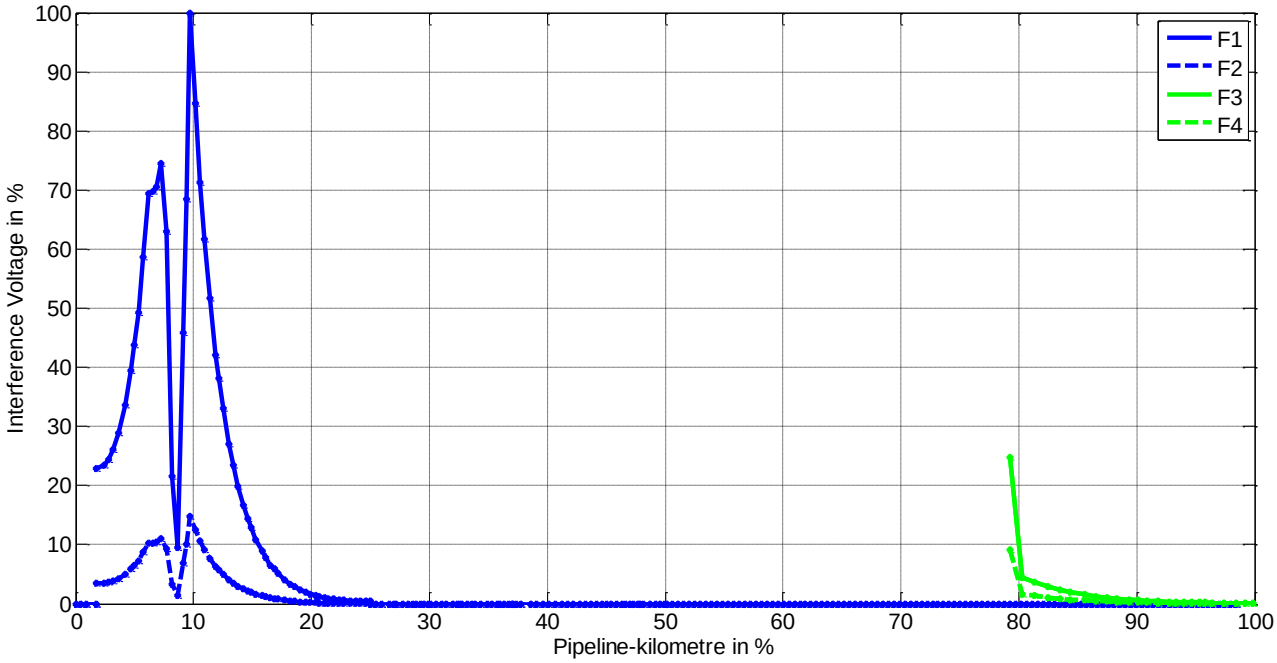

Figure 5.6: Induced pipeline interference voltage for moving fault locations F1-F4

5.2 High-Voltage Transmission Lines

A relevant influence from high-voltage lines to pipelines is given by the voltage levels of 110 kV and above. Based on the Austrian standards regarding touch voltages [7], 110 kV overhead lines can be neglected. This arises in case of normal operation from lower operation currents, compared with 220/400kV lines. In short-circuit cases 110 kV lines can be neglected due to the fact of the in Austria common earth-fault extinction. Additionally it has to be mentioned that regarding to actual Austrian standards [7], double-faults have not to be taken into account. Above all 110 kV lines are nevertheless interesting for evaluating the risk of AC corrosion.
The higher the voltage level of a high-voltage overhead line, the higher the possibilities of energy transport over the line. Consequently there exist more and longer parallel courses between interfered pipelines and 220/400 kV overhead lines than to 110 kV overhead lines.

5.2.1 Normal Operation Mode

From an ordinary point of view an overhead line is a connection between substations. For modelling a high voltage line (or cable), the same pi-circuit as for a pipeline (see chapter 2.2.4) can be used. Small losses in shunt-direction (for example corona losses, currents over operating capacity) are neglected for pipeline-interference investigations. Therefore the for AC corrosion- or touch voltages relevant currents are constantly assumed along the whole pipeline. The principal pipeline interference voltage distribution for a parallel approach can for example be seen in figure 5.1 (2^{nd} subplot, blue line). Based on worst-case-considerations the load flows, for example for double-circuit-pylons, are assumed in the same direction.

5.2.2 Short-Circuit Case

Short-circuit diagrams for high-voltage lines exist similar to electric railways. Usually these diagrams are prepared by the operational management of the high-voltage line operator. These short-circuit diagrams depend on the following parameters:

- Scale of intermeshing
- Technical equipment of substations (transformers)
- Specification and material of feeding lines
- Neutral point treatment

For high-voltage lines there usually exist short-circuit components from both substations since the so called weak infeed situations are usually rare. Based on the meshed operation of high voltage lines, in short-circuit cases, additional currents along neighbouring lines can occur (see figure 5.7). The influence of these currents along neighbouring lines is taken into

account for accurate pipeline interference investigations. The fault currents flowing to the fault location are considered mathematically correct (current direction).

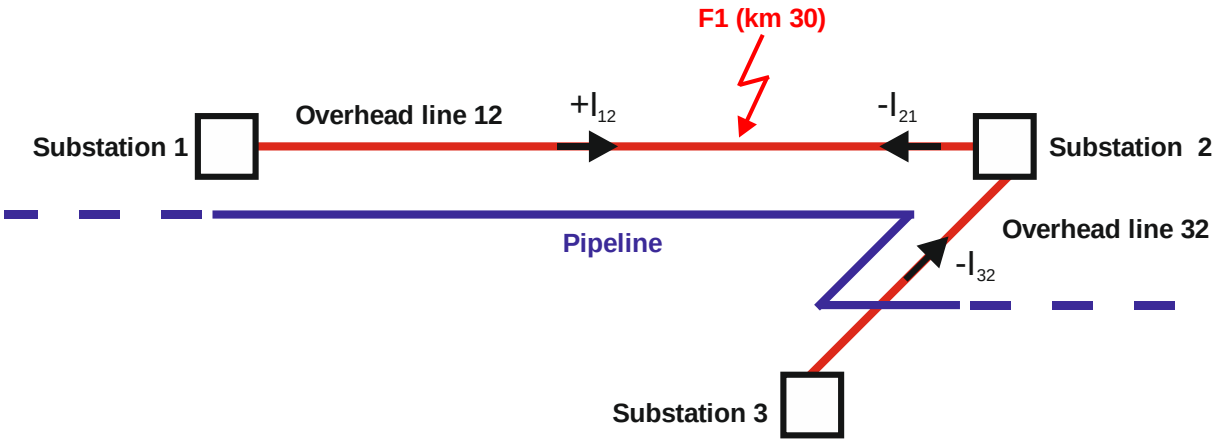

Figure 5.7: Interfering currents in short-circuit case F1, currents flowing from 3 substations

As it can be seen in figure 5.7, the pipeline is interfered by fault currents, with different algebraic signs, flowing from the substations 1, 2 and 3.

The following figure 5.8 shows a typical short-circuit current diagram of a high-voltage line, including a neighbouring curve. With the help of these short-circuit diagrams the interfering currents for every fault along the interfering high-voltage line can be determined.

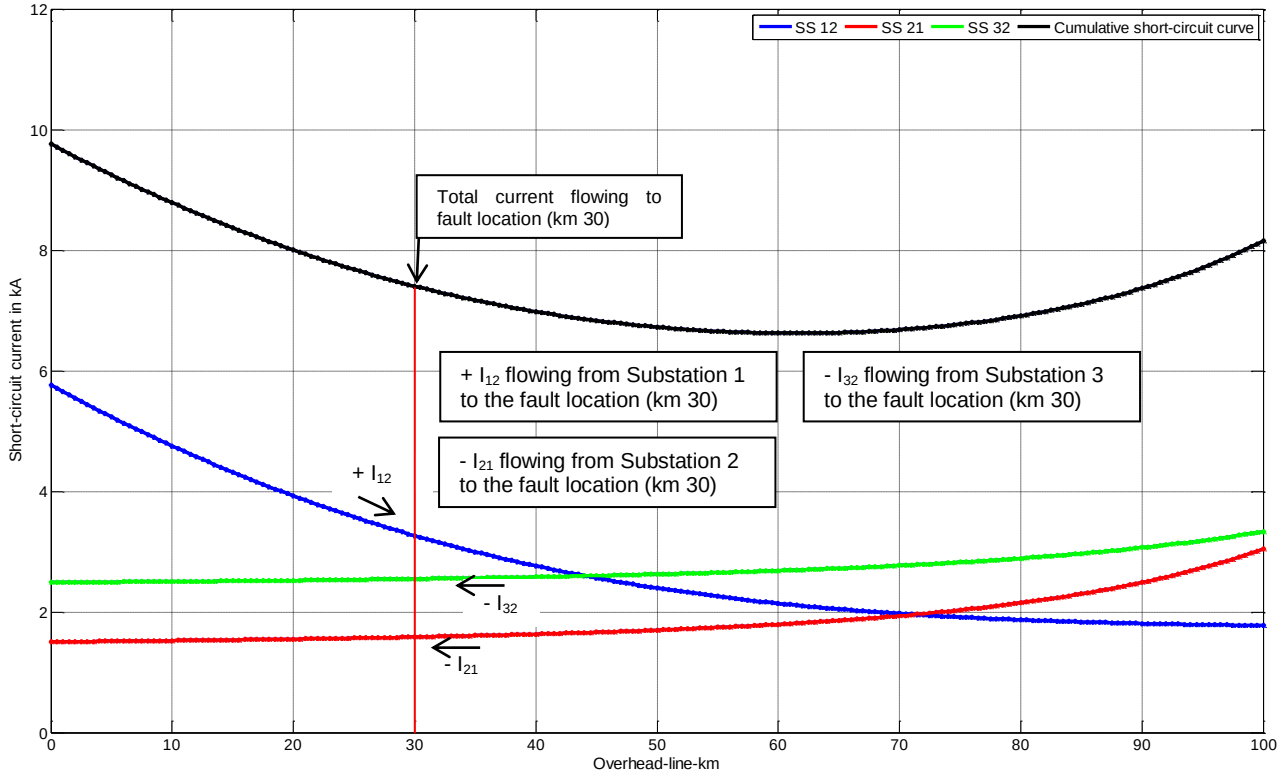

Figure 5.8: Typical short-circuit current diagram for a high-voltage line including neighbouring curve

The next figure 5.9 shows the approach between in this example four interfering high-voltage lines and an interfered pipeline. The example is derived from a practical example in order to show the methodology which is already indicated but not explicitly described in [35]. In this

example three isolating joints are installed along the pipeline. The faults F1 to F11 are assumed at the approaches between the two railway systems and the pipeline.

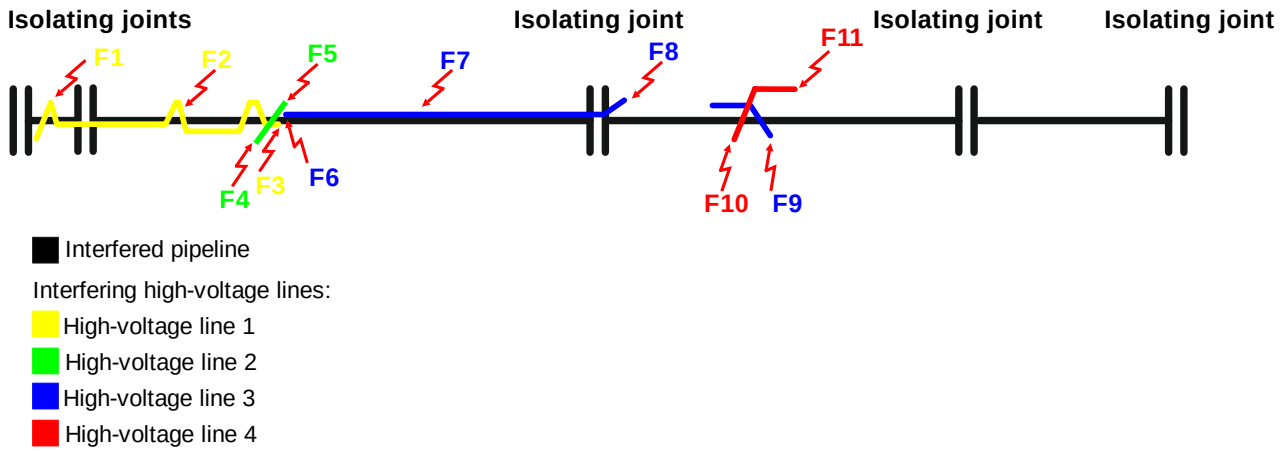

Figure 5.9: Scheme of the approach between interfered pipeline with isolating joints and 4 high-voltage lines, fault locations F1-F11

In this example meshed structures, appear as exemplarily shown in figures 5.7 and 5.8. High-voltage line 1 (yellow) goes from Substation 1 (SS1) to Substation 2 (SS2). High-voltage line 2 (green) goes from Substation 1 (SS1) to Substation 3 (SS3). High-voltage line 3 (blue) goes from Substation 4 (SS4) to Substation 1 (SS1) and high-voltage line 4 (red) goes from Substation 4 (SS4) to Substation 4 (SS5). High-voltage lines 3 and 4 have different voltage levels than the other high voltage lines (400 kV and accordingly 220 kV). The following table 5.1 shows the composition of the fault currents, for the fault locations F1-F11 in %. The percentage of the fault current components is noted with algebraic signs standing for the directions relatively to the pipeline location.

Fault	High-voltage line	Fault-location Pipeline-km (%)	Fault current distribution		
			Main curves Fault currents in %		Neighbouring curve
F1	High-voltage line 1	5 %	+ 81 % SS1	- 10 % SS2	- 9 % SS3
F2	High-voltage line 1	12 %	+ 66 % SS1	- 26 % SS2	- 8 % SS3
F3	High-voltage line 1	22 %	0 %	- 63 % SS2	- 37 % SS3
F4	High-voltage line 2	21 %	+ 87 % SS1	0 %	- 13 % SS2
F5	High-voltage line 2	22 %	0 %	- 51 % SS3	- 49 % SS2
F6	High-voltage line 3	22 %	+ 61 % SS4	0 %	- 39 % SS5
F7	High-voltage line 3	38 %	+ 46 % SS4	- 24 % SS1	- 30 % SS5
F8	High-voltage line 3	51 %	+ 48 % SS4	- 21 % SS1	- 31 % SS5
F9	High-voltage line 3	63 %	0 %	- 33 % SS1	- 67 % SS5
F10	High-voltage line 4	62 %	+ 71 % SS4	0 %	- 29 % SS1
F11	High-voltage line 4	64 %	0 %	- 81 % SS5	- 19 % SS1

Table 5.1: Composition of the fault currents F1-F11 including mathematical directions relatively to the pipeline

A fault current of 0 % from one side occurs if the fault is assumed at the beginning or the end of an approach area between pipeline and interfering high-voltage line.

The following figure 5.10 shows the simulation result for the pipeline interference voltages for the above mentioned conditions and the moving fault locations F1 to F11. With the help of this method a widespread view of possibly pipeline interference voltages in short-circuit cases is possible.

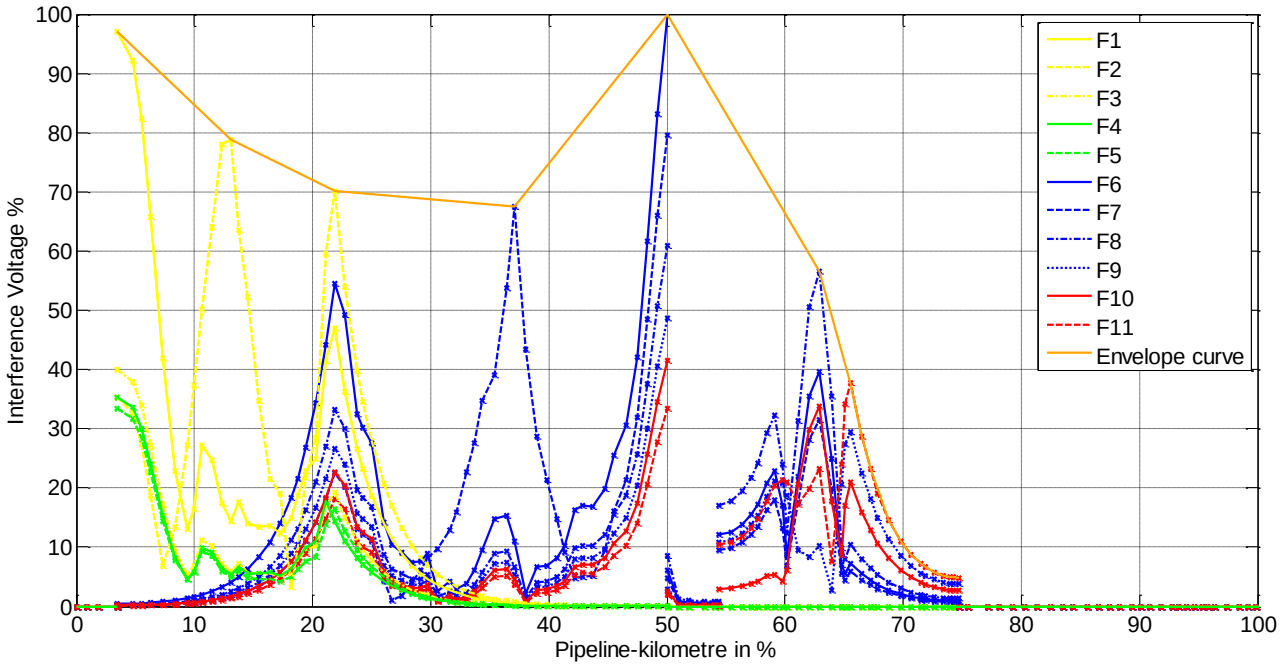

Figure 5.10: Induced pipeline interference voltage for moving fault locations F1-F11

Because only selected fault locations (F1-F11) are calculated, the orange envelope curve visualizes the in worst-case to be expected pipeline interference voltages along the entire pipeline.

5.3 Comparison between Interfering Systems

5.3.1 Thermal Currents and Risk of Hazard

In the following figures 5.11 and 5.12 the influence of the two introduced interfering systems is exemplary investigated for thermal currents. Basis for the calculation is a 10-km parallel course between pipeline and interfering systems. The horizontal distance between the systems is varied between 50 m and 2000 m. The influence of a double-track high-power railway line and a 400 kV overhead line are compared with each other. The for the simulation used thermal currents base on exemplary practicable values of the Austrian operators. The thermal current for the railway line is varied between 2500 A and 1500 A in 10 A steps in order to create an envelope curve. Base is the thermal limit of common contact wires. Well knowing that there exist several current limiting elements like transformers and contact wires in the railway system. In addition to that thermal currents also strongly depend on wind speed and temperature.

The base for the 400 kV overhead line is an in Austria common 3-level pylon with 3 sub-conductors and 2 circuits. Well knowing that due to penetration depth and field-effects 3 sub-conductors cannot transport the triple thermal limit current of one conductor, the thermal current of one system of 3 sub-conductors is varied between 2100 A and 3600 A in steps of 10 A in order the create an envelope curve.

Thermal currents are as already mentioned used for evaluating the maximum occurring possible touch voltages. Therefore the following simulations in figure 5.11 are based on the thermal currents in order to compare the impacts on the risk of hazard.

The simulations reflect worst-case assumptions and cannot be compared with normal operation modes. The highest currents of an electric traction vehicle are for instance needed during acceleration processes or for going uphill. In motion the losses have to be covered.

The following figure 5.10 shows the comparison between the influences of the introduced 400 kV overhead line and the railway system on maximum induced pipeline interference voltages, considering the above mentioned currents and horizontal distances. As it can be seen in figure 5.8 the electric railway has compared with the 400 kV overhead line a dominant influence on the maximum pipeline interference voltage. In the vicinity area up to approximately 70 m the 400 kV overhead line has for some currents a bigger impact than the electric railway. According to the Austrian standards [7] because of possible conductive interference, there should be a 30-m-safety radius between the pipeline and the centre of 400 kV pylons. Consequently the simulation results for the vicinity area show a borderline-case and are due to the safety radius not significantly practicable. The results show clearly that there exists an influence up to a horizontal distance of 2000 m.

Figure 5.11 also shows that the influence of 400 kV overhead lines decreases more rapidly with increasing horizontal distance than the influence of the electric railway. In addition, it can be seen that the influence of the electric railway is because of for the magnetic field disadvantageous conductor arrangement dominant over the whole investigated section.

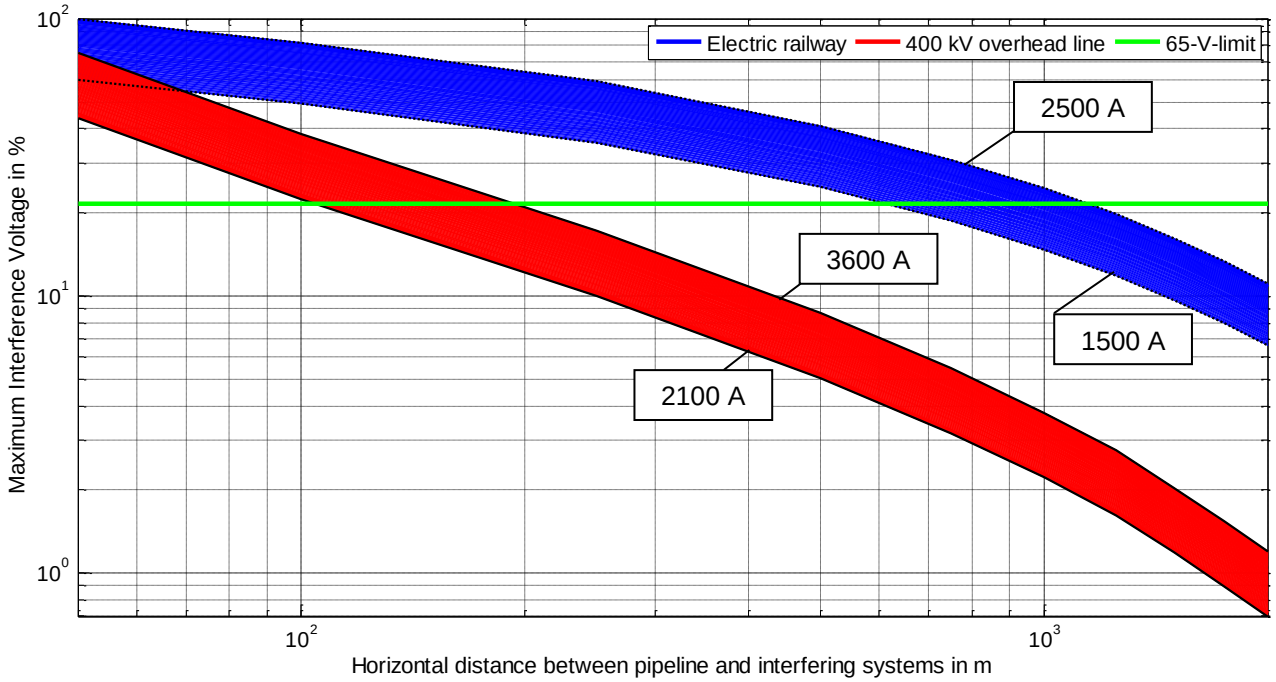

Figure 5.11: Comparison of the Influence of an electric railway system and a 400 kV overhead line for exemplary, practicable thermal currents, thermal currents over whole interfering section

5.3.2 Practicable values for steady currents and AC corrosion likelihood

Basis for the calculation is again a 10-km parallel course between pipeline and interfering systems. The horizontal distance between the systems is varied again between 50 m and 2000 m. Regarding AC corrosion likelihood short-term peaks can be neglected [25]. The AC corrosion likelihood is evaluated by currents that last for a certain duration in order to start electrochemical processes for instance by a 95 %-quantile of the current load duration curve. Based on load flow- and train run simulations these values in Austria can be obtained from the railway operator. Therefore practicable values between 250 A and 500 A are taken for the simulation in the following figure 5.12.

A rule of thumb says that high-voltage lines are maximal aimed to be operated with the (n-1)-current which is defined between 60 % and 70 % of the thermal current. Therefore the following simulation bases on practicable values of 1200 A up to 1600 A (approximately 35% and 45 % of the thermal rated current), which can cover the 95 %-quantile of the current load duration curve.

The following figure 5.12 shows the simulation results for the maximum pipeline interference voltages for the mentioned currents and horizontal distances. It is evident that the 400 kV overhead line has a bigger influence in the vicinity area up to approximately 100 m, caused by the higher currents. With horizontal distances above 100 m the disadvantageous (conductor-) geometry of the railway system becomes more important and leads to higher pipeline interference voltages.

When examining the green line (10-V-limit) it emerges that for this example (20-km parallel course) corrosion relevant voltages of 10 V [9] can in case of the railway interference occur up to horizontal distances of 1500 m. In case of the 400 kV overhead line, interference voltages fall for horizontal distances between approximately 450 m and 580 m under the 10-V-limit.

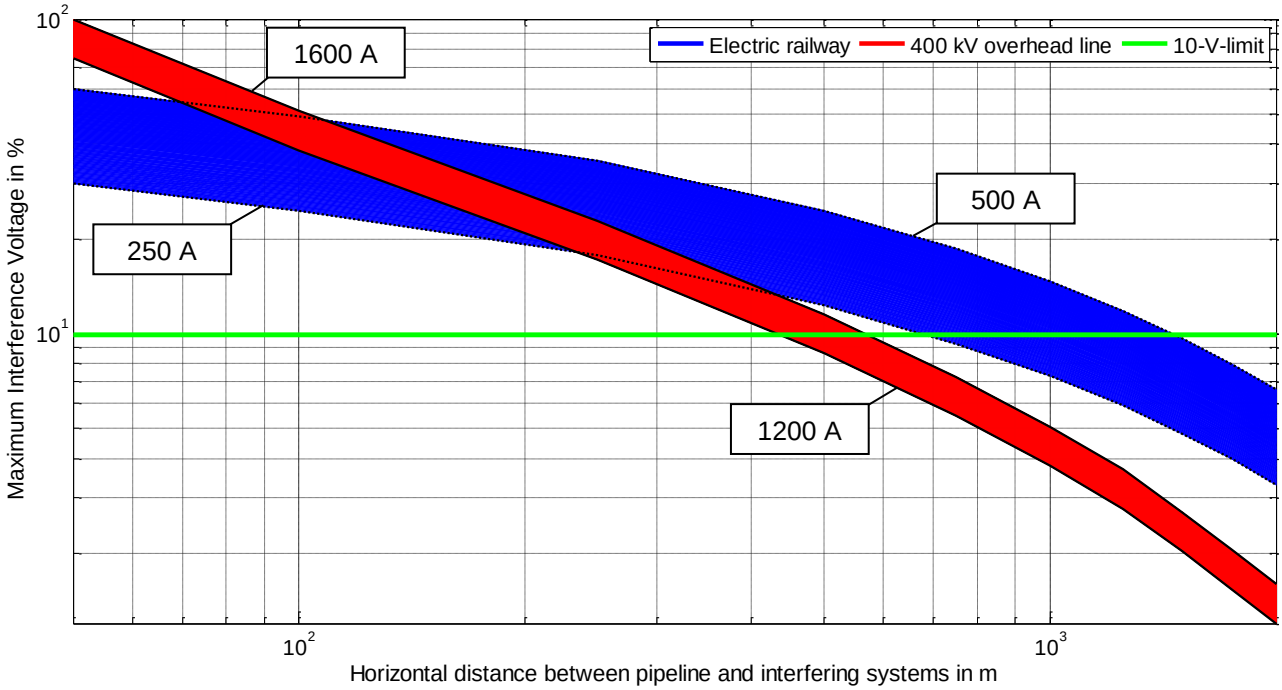

Figure 5.12: Comparison of the Influence of an electric railway system and a 400 kV overhead line for exemplary, practicable operational currents, operational currents over whole interfering section

5.4 Summary

With the help of traction current- and short-circuit diagrams it is possible to evaluate the inductive pipeline interference for all operating- fault and load flow situations. For the investigated 10-km long approach the comparison of the interfering systems show a stronger influence of the electric railway regarding the risk of hazard. When evaluating the AC corrosion likelihood the influence of the 400 kV overhead line is dominant in the vicinity area. In the far area the influence of the electric railway system is greater. For evaluating the AC corrosion likelihood in figure 5.12 the maximum occurring pipeline interference voltages of each horizontal distance is taken account. These values occur at the beginning and the end of the approach (see figures 2.8, 2.10). This is for example interesting if there are coating holidays in these areas. For achieving a profile of the pipeline interference voltage along the pipeline the current traction diagram as shown in the figures 5.2 and 5.3 should be considered.

6 Soil Conditions for AC Earthing systems

This chapter shows measuring results of the specific soil resistivity ρ during the seasons. Within the carried out case study in chapter 7, the impact of a seasonal varying specific soil resistivity ρ on AC earthing systems and accordingly on pipeline interference voltages is investigated.

6.1 Measurements

As already mentioned in the introduction of this thesis a humid soil is beside other things (oxygen in soil, AC currents flowing along pipeline, existence of coating holiday(s)) necessary to start AC corrosion effects.
The humidity and the temperature of the soil are also significant for the specific resistivity of any soil [39]. Therefore between November 2009 and March 2011 monthly measurements of the specific soil resistivity took place [40] on a fixed location.

Figure 6.1: Investigated soil for annual measuring series for two different measuring dates, images by René Braunstein

The above figure 6.1 shows the investigated soil at two different measuring dates. The pylon resistances of the shown 110 kV overhead line were also measured, but are not part of this thesis. For measuring the specific soil resistivity it is important to choose a measuring trace at a sufficient distance from metallic installations such as pylon earthing systems in order to get correct results. Therefore the already mentioned 20-m-saftey radius according to [7] offers an applicable solution.
The specific soil resistivity was measured by the method of Frank Wenner [41]. The method can also be called “4-electrode method” and bases on the measurement of the potential difference of two points inside an electric flow field in earth [39].
In the following figure 6.2 the results of the twelve monthly series is shown. The upper and lower envelope curves are dotted red.

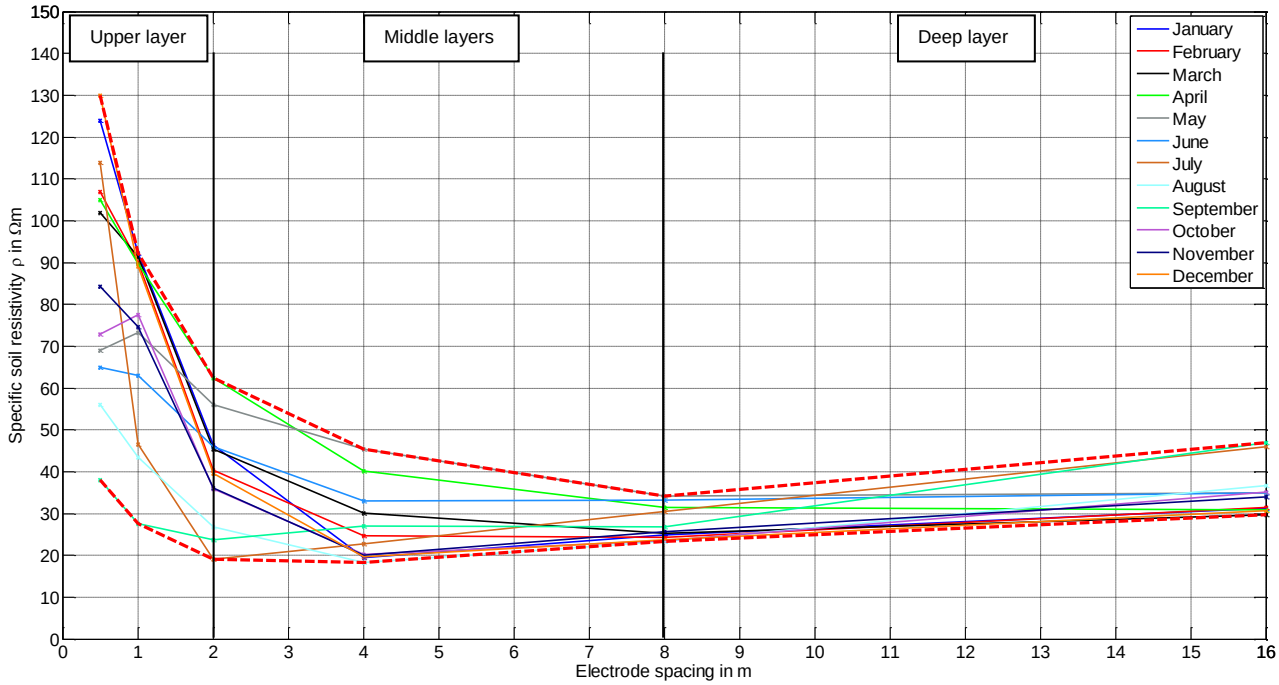

Figure 6.2: Series of specific soil resistivities over one year plotted against electrode spacing

During the measurements, the electrode spacing was varied from 0.5 m to 16 m (0.5 m, 1 m, 2 m, 4 m, 8 m and 16 m[4]).

In praxis the measurement goes until a depth which is almost equivalent to the electrode spacing. The measuring values are average values of all more or less conductive soil layers until the measured depth (electrode spacing) [39].

The above figure 6.2 shows that the investigated soil gets more conductive until an electrode spacing of approximately 8 m. In higher depths a less conductive soil layer follows.

Based on the dependency of the specific soil resistivity on humidity and temperature it is in literature [39] recommended to bury horizontal earthing conductors at least between 0.5 and 1 m. In figure 6.2 a special sensitivity regarding humidity can be seen in the upper soil layers (for example May and October), especially at a depth of 0.5 m. Consequently in some cases it might be useful to install horizontal earthing conductors at least in a depth of 1 m.

Regarding to literature [39] the specific soil resistivity changes up to +- 30% over the season. The lowest values in Central Europe are usually reached in August, the highest values in February [39]. The months with the highest or lowest values don't correlate exactly with the measurements, the "dry" July has in lower depths for example almost similar high values than the "frozen" January or February. Nevertheless the range of possible specific soil resistivities and the dependency on humidity and temperature for different depths is shown.

[4] Based on the prevailing topography and the applied measuring system it was in the investigated case not possible to work with higher electrode spacing than 16 m.

When calculating the arithmetic average of the deviation for low depths between 0.5 m and 2 m, one gets a factor of 3.4. Based on the measurements at the investigated soil horizontal earthing conductors in the worst-case can have a 3.4 times higher impedance than expected. When calculating the arithmetic average of the deviation for greater depths between 8 m and 16 m, one gets a factor of 1.5. Based on the measurements at the investigated soil ground rods in the worst-case can have a 1.5 times higher impedance than expected because of the seasonal changes of the specific soil resistivity.
Consequently safety demands might not be achieved during these seasons. When installing earthing systems, one should take higher impedances in case of frozen or dry soils into account.
Well knowing that the measurement of the specific soil resistivity based on the Wenner method depends on the above mentioned parameters, with the help of the measurement one gets a hint whether a ground rod or a horizontal earthing conductor is to be preferred for the measured soil.
The effective resistivity of a horizontal earthing conductor can be calculated with the following approximation formulas (51) and (52):

$$R_S = \frac{2 \cdot \rho}{l}, \text{ for } l \leq 10\ \text{m} \quad (51)\ [39]$$

$$R_S = \frac{3 \cdot \rho}{l}, \text{ for } l > 10\ \text{m} \quad (52)\ [39]$$

R_S Resistivity of the earthing system in Ω
ρ Specific soil resistivity in Ωm
l Length of installed material (band steel) in m

The effective resistivity of a ground rod can be calculated with the following approximation formula (53):

$$R_S = \frac{\rho}{l} \quad (53)\ [39]$$

R_S Resistivity of the earthing system in Ω
ρ Specific soil resistivity in Ωm
l Depth of installed material (steel) in m

The introduced approximation formulas (52)-(53) show that for the investigated soil, ground rods will offer earthing systems with lower impedance than horizontal earthing conductors.

6.2 Summary

As the measurements show, the investigated specific soil resistivity varies in the upper layers (0.5 m -2 m) by a factor of 3.4 and in the deeper layers (8 m – 16 m) bay a factor of 1.5. More information about the resistivities of layers deeper than 16 m can be obtained by the measuring method of Schlumberger. The impact of the measured soil characteristic on effective AC earthing systems is shown within the case study in the following chapter.

7 Case study

In this chapter the cost effectiveness of the introduced pipeline interference voltage mitigating measures AC earthing systems, isolating joints and compensation conductors is evaluated by a case study. At the end of this chapter the special fields of application for each measure is investigated.

7.1 Situation

The following figure 7.1 shows the approach between the interfered pipeline and the interfering system for the case study. It is here shown a typical example with an approximately 13.3-km-long pipeline (blue), an interfering 400 kV overhead line (red) and an interfering railway system (black). The routes of the pipeline, the railway and the 400 kV overhead line base on practice. The for the AC corrosion relevant operation currents (95 % quantiles) are in the case of the 400 kV overhead line assumed with 1100 A per conductor and in the case of the railway system with 400 A (detailed simulation parameters, see chapter 11). Based on worst-case assumptions the same current is assumed along the whole interfering railway section (see also chapter 5.1.1).

The combination of interfering systems with different operation frequencies (50 Hz and 16.7 Hz) often occurs in practice.

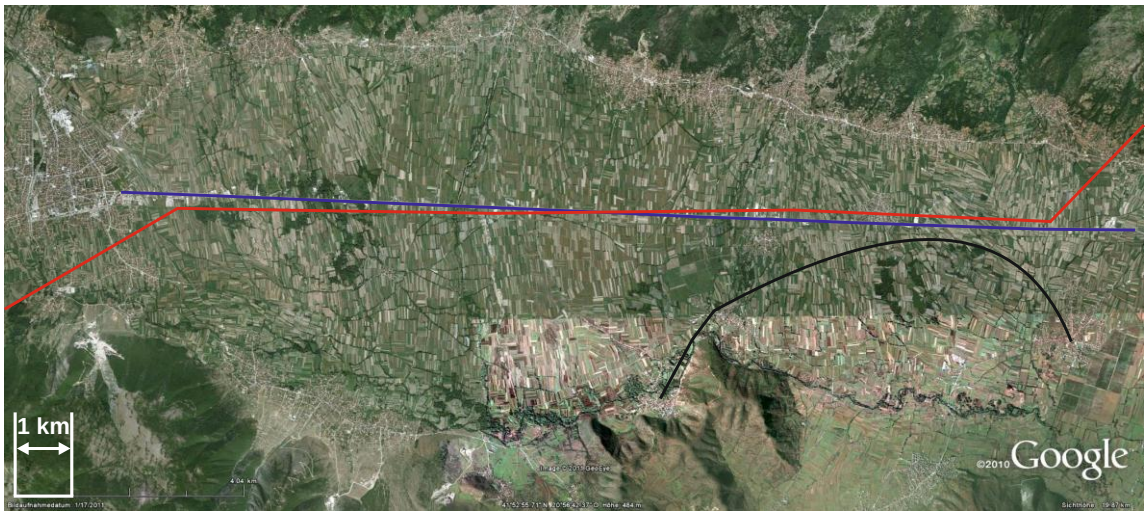

Interfered pipeline system
Interfering 400 kV overhead line (50 Hz)
Interfering Railway system (16.7 Hz)

Figure 7.1: Approach between the interfered pipeline and the interfering system for the carried out case study

At the moment there exists no calculation rule that considers the combination of interfering sources with two different operating frequencies. Therefore it is decided to choose the

approach of superposition. The actual versions of CEN/TS 15280 [9] regarding the AC corrosion likelihood of buried pipelines or prEN 50433 [42] caused by railway systems and/or high voltage lines do not include this calculation procedure at the moment, however it is discussed in the committees for future versions.

The superposition of the pipeline interference voltages of both interfering systems is in the following chapter 7.2 calculated for each pipeline nodal point and plotted in red.

7.2 Solution Scenarios

In this subchapter 4 solutions scenarios to reduce the pipeline interference voltages below the 10-V-limit are investigated. Within the first solution scenario the impact of the seasonal varying specific soil resistivity ρ on AC earthing systems and as a consequence on pipeline interference voltages is discussed.

7.2.1 Solution Scenario 1

The first solution scenario presents a conservative and secure method, the earthing of the pipeline with as much earthing systems as necessary to come below the required limit. The following figure 7.2 shows the scheme of the selected solution scenario 1.

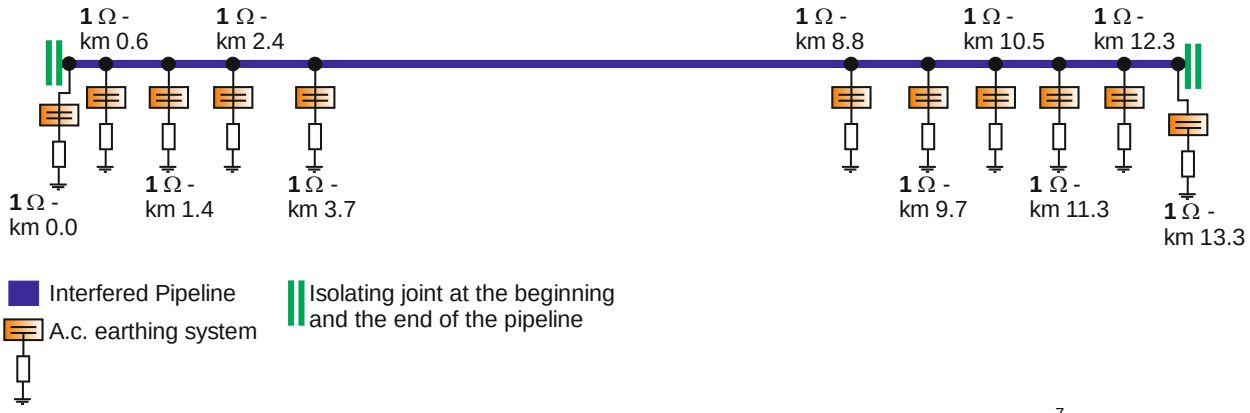

Figure 7.2: Scheme of Solution scenario 1, Installation of11 earthing systems with 1Ω[7]

The following figure 7.2 shows the simulation result for the pipeline interference voltages for the above introduced approaches between pipeline, 400 kV overhead line and electric railway system.

Based on the approaches in it is evident that the 400 kV overhead line has a dominant influence (blue line). Compared with the 400 kV overhead line, the electric railway occurs only at the last third of the pipeline and has less horizontal distances. As can be seen in the figure 7.3, the pipeline interference voltages are much too high for an evaluation of the AC corrosion likelihood based on CEN/TS 15280 [9] (compare also chapter 2.1.2).

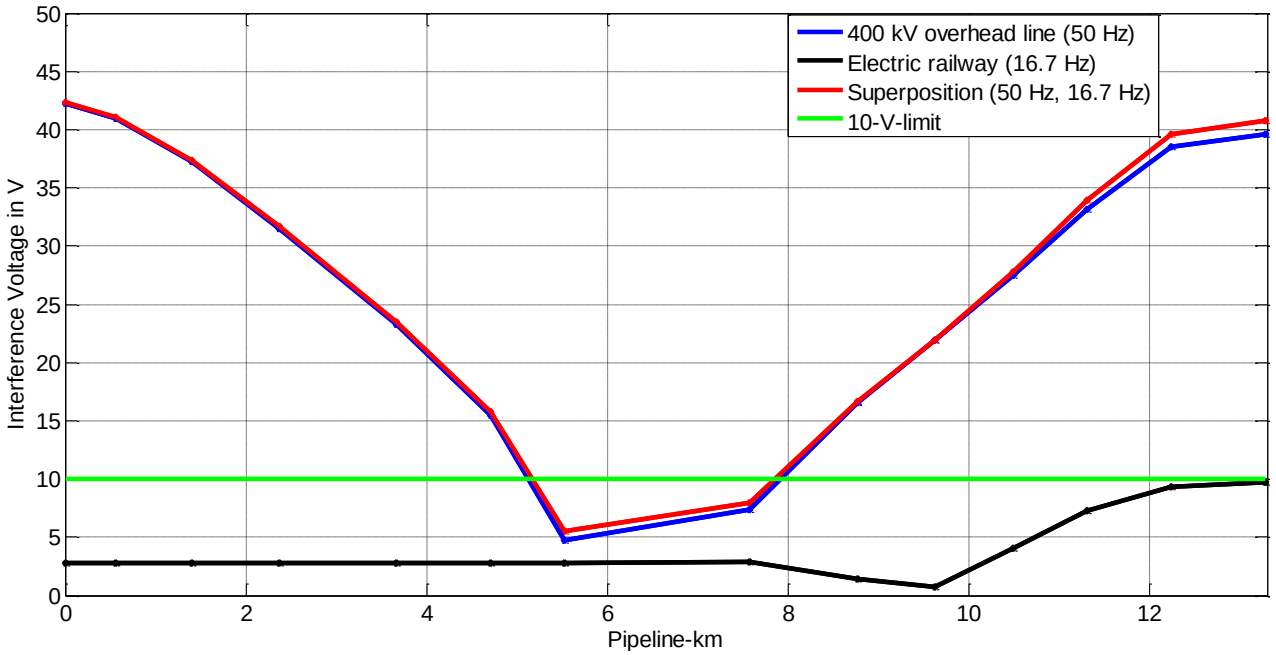

Figure 7.3: Induced pipeline interference voltages without interference voltage mitigating measures

In order to reduce the pipeline interference voltage under the 10-V-limit regarding to [9] interference voltage mitigating measures such as AC earthing systems are necessary. In the following figure 7.4 the impact of 11 AC earthing systems with 1 Ω on pipeline interference voltage is shown. With the help of the 11 AC earthing systems the pipeline interference voltage can be reduced from approximately 42 V below the 10-V-limit. The pipeline interference voltages caused by each interfering system as well as the superposition of both interfering frequencies are under the 10-V-limit.

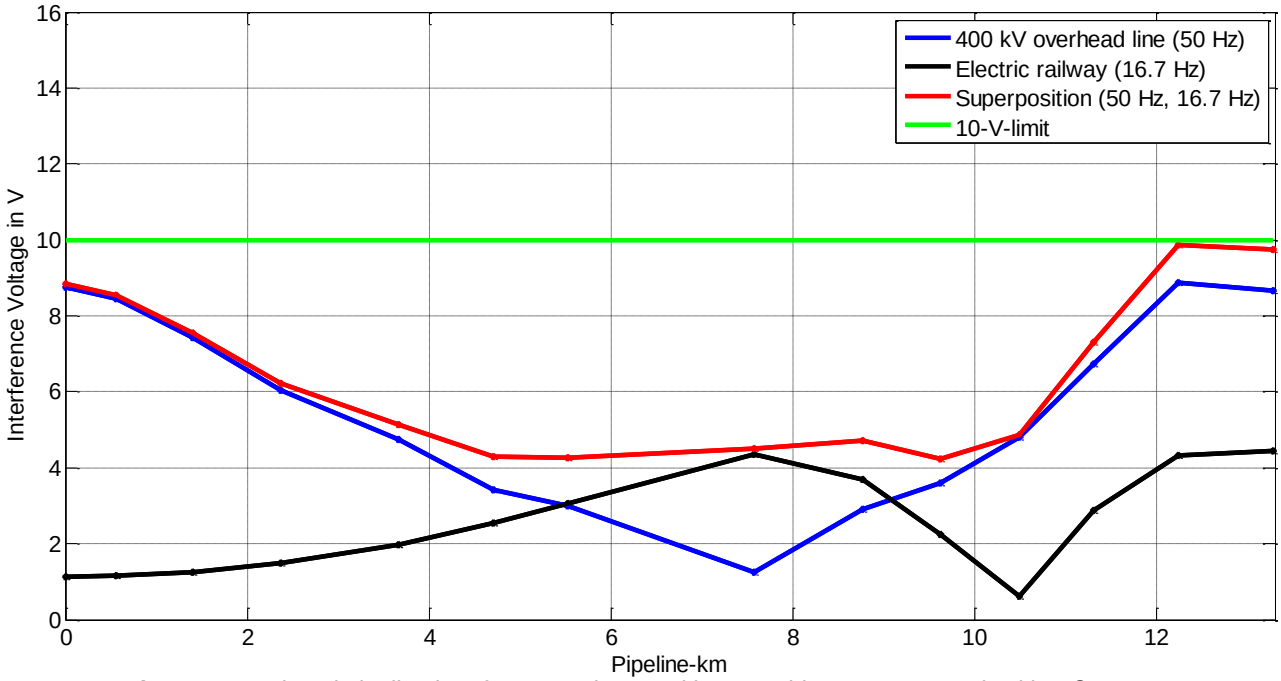

Figure 7.4: Induced pipeline interference voltages with 11 earthing systems, each with 1 Ω

The low impedant 1-Ω-earthing-systems could be implemented by ground rods (investigated soil see chapter 6), because the investigated soil is less practicable for installing horizontal

earthing conductors. Based on the in chapter 6.1 calculated arithmetic average of the deviation in deeper soil layers the following figure 7.5 shows the pipeline interference voltages based on earthing systems with 1.5 times higher resistances.

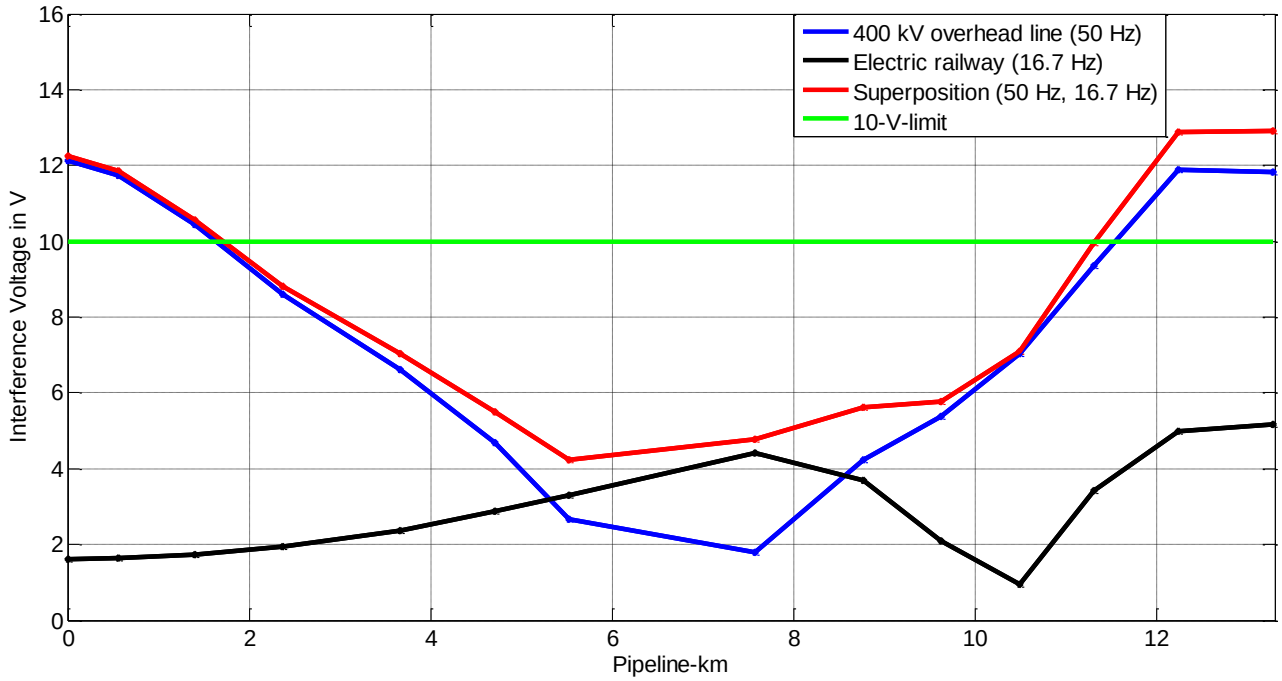

Figure 7.5: Induced pipeline interference voltages with 11 earthing systems, each with 1.5 Ω

As it can be seen in the above figure 7.5, the pipeline interference voltage caused by the 400 kV overhead line and consequently the superposition of both frequencies is above the 10-V-limit. As already mentioned in chapter 2.1.2, practical experiments [11], [24] as well as the analyses in chapter 3 showed that under some circumstances (properly adjusted cathodic protection potentials, high soil resistivities) higher interference voltages than 10 V can be accepted. Nevertheless this case study shows that the seasonal change of the specific soil resistivity could in worst-cases lead to an exceeding of permissible limiting values.

7.2.2 Solution Scenario 2

The combination of isolating joints and earthing systems is to be discussed when thinking about earthing systems directly at the isolating joint. These earthing systems can only be realised either at the left or the right side of the isolating joint. Earthing systems at both sides of the isolating joint could lead to a bridging of the isolating joint through earth. The interference voltage reducing effect of the isolating joint would not be effective any more. The second selected solution scenario is realised by 7 isolating joints exclusively. The following figure 7.6 shows the scheme of the solution scenario 2. Isolating joints can be realised at nodes of the model. Between pipeline-km 10.5 and the end of the pipeline no additional isolating joint is necessary to keep the pipeline interference voltage below the 10-V-limit.

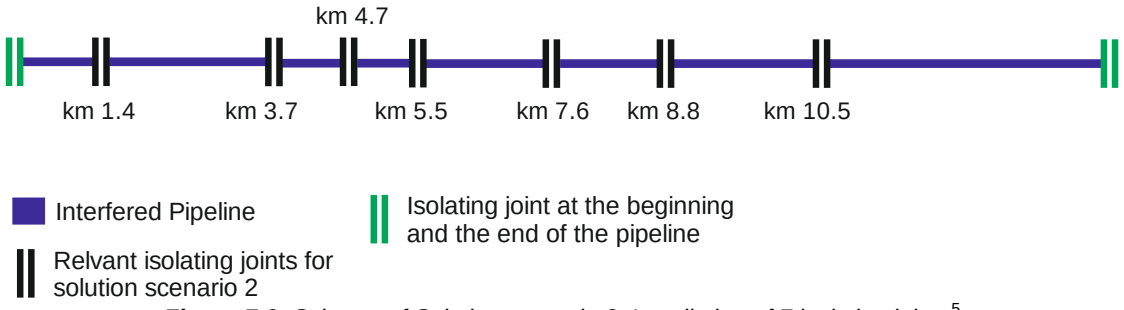

Figure 7.6: Scheme of Solution scenario 2, Installation of 7 isolating joints[5]

Based on the high number of isolating joints it is possible to reduce the induced pipeline interference voltage significantly under the 10-V-limit regarding to [9]. In the following figure 7.7 the impact of 7 isolating joints on pipeline interference voltage is shown. The disadvantage of the installation of isolating joints at every few kilometres is the high economical effort for a separate rectifier for each cathodic corrosion protection area. For longer cathodic corrosion protection areas (for example 20 km … 40 km) a depth drilling is necessary for the protection anode. These expenditures have not to be realised for such small cathodic corrosion protection areas.

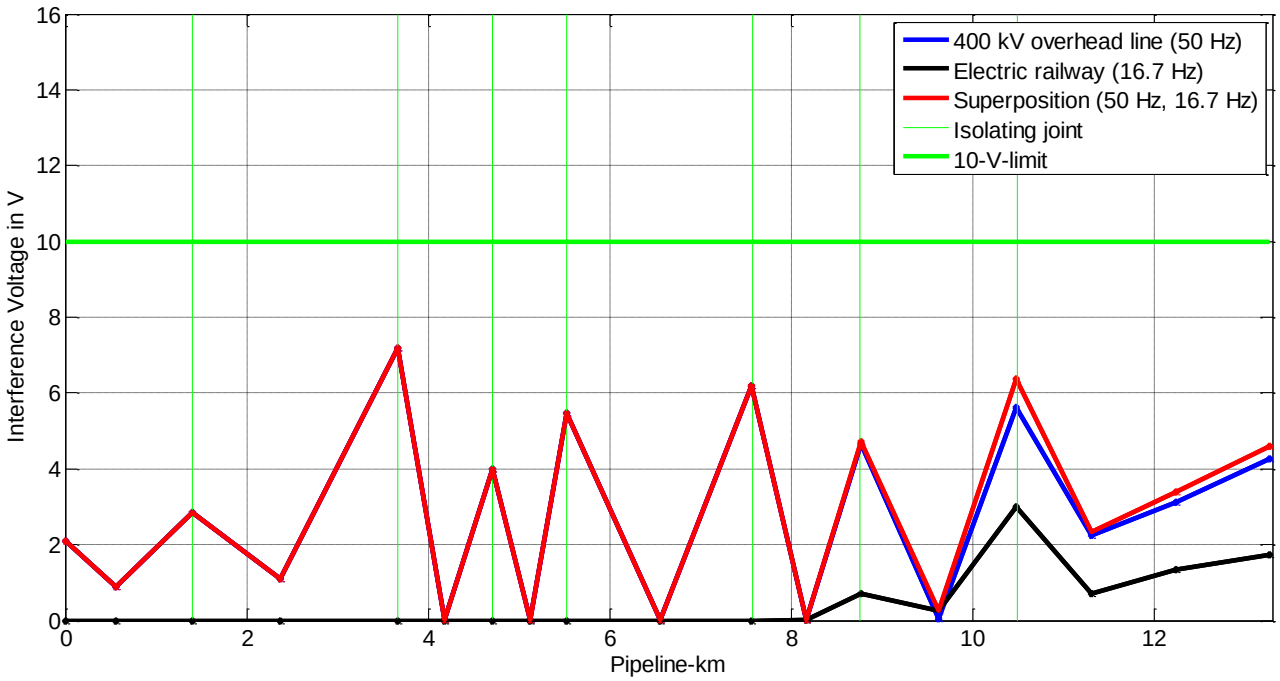

Figure 7.7: Solution scenario 2 - Induced pipeline interference voltages with 7 isolating joints

[5] Isolating joints at the beginning and at the end the pipeline (green) are not part of the case study.

7.2.3 Solution Scenario 3

The next selected solution scenario is realised by 1 isolating joint and two compensation conductors. The following figure 7.8 shows the scheme of the selected solution scenario 3.

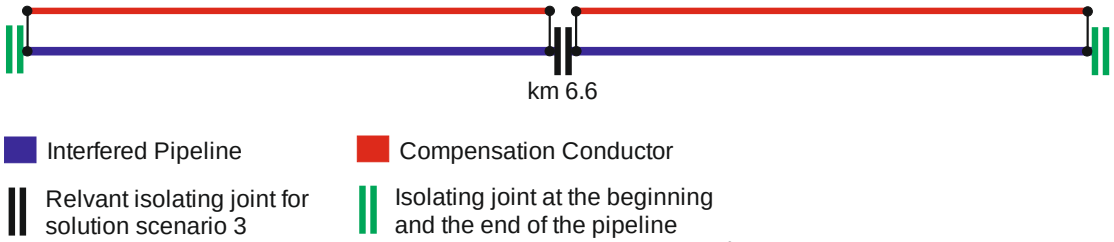

Figure 7.8: Scheme of Solution scenario 3, Installation of 1 isolating joint[6] and two isolated compensation conductors

Based on measurements [37] a pipeline reduction factor R_{FP} (see chapter 4.3.1) of approximately 0.3 can be achieved if the pipeline is connected with the compensation conductor at both ends and there is no additional connection to earthing systems. An additional reduction for the selected solution scenario 3 is achieved by the installation of an isolating joint approximately at the middle of the pipeline. The following figure 7.9 shows the impact of a combination of isolating joints and compensation conductors on pipeline interference voltages.

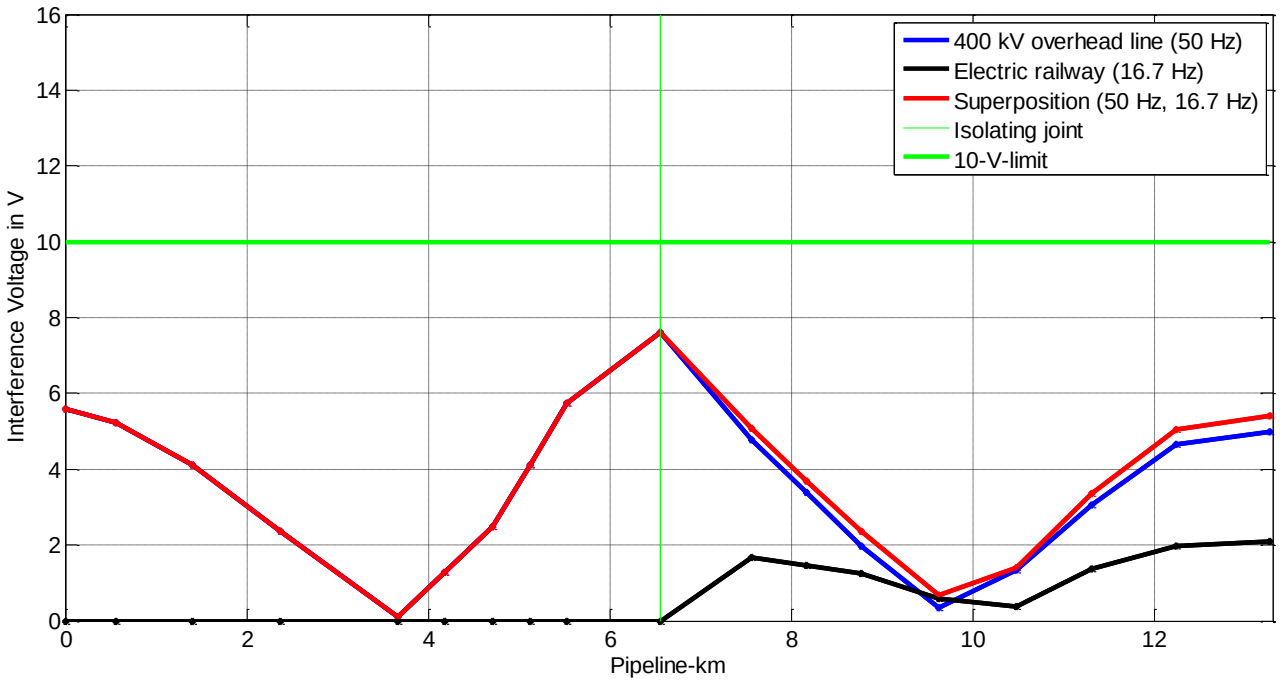

Figure 7.9: Solution scenario 3 - Induced pipeline interference voltages with 1 isolating joint and one compensation conductor

[6] Isolating joints at the beginning and at the end the pipeline (green) are not part of the case study.

7.2.4 Solution Scenario 4

The last selected solution scenario is realised by 2 isolating joints, 4 low impedant earthing systems and two compensation conductors. The following figure 7.10 shows the scheme of the selected solution scenario 4.

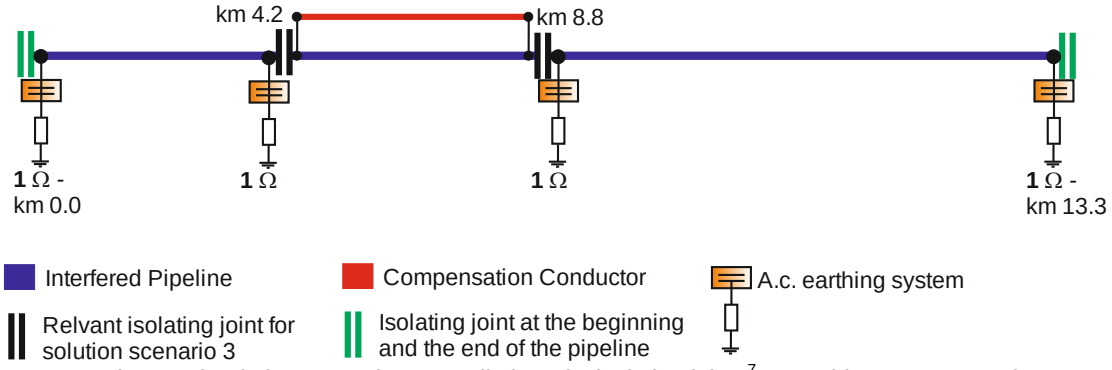

Figure 7.10: Scheme of Solution scenario 4, Installation of 2 isolating joints[7], 4 earthing systems and one compensation conductor

As it can be seen in the following figure 7.11, with the help of the combination of earthing systems, isolating joints and a compensation conductor the induced pipeline interference voltages can be reduced to 10 V. The root mean square value of the pipeline interference voltages of both interfering systems (50 Hz and 16.7 Hz) is in the range of 10 V. This can possibly be tolerated, well knowing that the root mean square value calculation procedure is currently not part of calculation standards and that higher pipeline interference voltages between 12 V… 15 V are discussed to be tolerated for properly adjusted cathodic protection potentials.

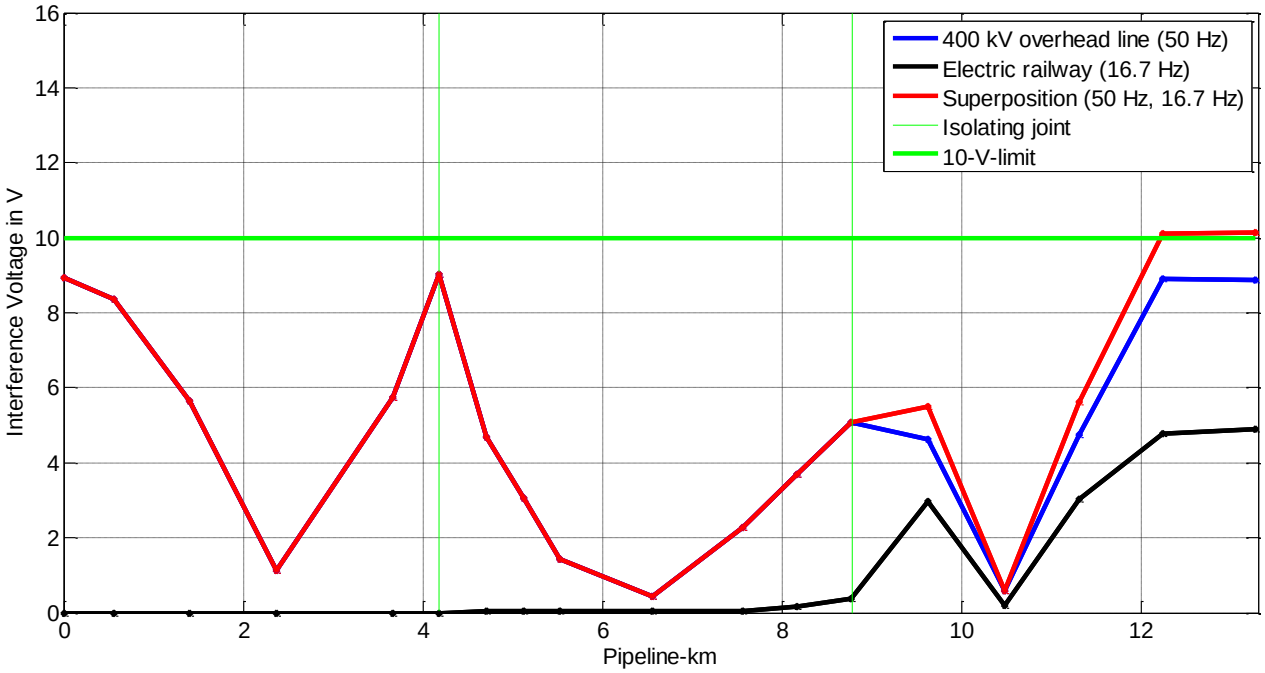

Figure 7.11: Solution scenario 4 - Induced pipeline interference voltages with 2 isolating joints, 4 earthing systems and one compensation conductor

[7] Isolating joints at the beginning and at the end the pipeline (green) are not part of the case study.

7.3 Cost Effectiveness Analysis

In this subchapter cost effectiveness analysis of the four introduced solution scenarios are carried out. The following table 7.1 shows orientation prices for interference voltage mitigating measures and the belonging equipment in €, which base on the experiences of Austrian pipeline operators.

Nr.	Measure/Product	Costs in €
1	Compensation conductor, costs for material and laying (c_{lmc})	8.- per lm[8]
2	Ground rod, mobile site equipment (c_{se})	2.800.-
	Ground rod, costs for material, working hours and depth drilling (c_{dd})	190.- per dm[6]
3	Horizontal earthing conductor, costs for material only, laying in existing trench	2.- per lm
4	Horizontal earthing conductor, costs for material and digging work (c_{lmh})	5.- per lm
5	Power capacitor for cathodic corrosion protection and earthing system (c_{pc})	2.500.-
6	Isolating joint, installation before operation start (c_{ij})	4.000.-
7	Isolating joint, installation after operation start	35.000.-
8	Rectifier for cathodic corrosion protection of a small system (c_r)	15.000.-
9	Rectifier for cathodic corrosion protection including depth drilling	45.000.-

Table 7.1: Orientation prices for pipeline interference voltage mitigating measures

The construction costs (C_c) of the four introduced solution scenarios are calculated with the formula (54):

$$C_c = \eta_1 \cdot \left(c_{dd} \cdot dd + \frac{c_{se}}{\eta_1} + c_{pc} \right) + \eta_2 \cdot \left(c_{lmh} \cdot lm_h + \frac{c_{se}}{\eta_1} + c_{pc} \right) + \eta_3 \cdot \left(c_{lmc} \cdot lm_c \right) + \eta_4 \cdot \left(c_{ij} + c_r + \frac{c_r}{\eta_4} \right) \quad (54)$$

In the following the variables that are not contained in the table 7.1 are described:

η_1 Number of ground rods
dd Drilling depth
η_2 Number of horizontal earthing systems
lm_h Linear meters of horizontal earthing system(s)
η_3 Number of compensation conductors
lm_c Linear meters of compensation conductor(s)
η_4 Number of isolating joints

[8] lm …linear meter, dm … drilling meter

Basis for the calculation is a simplified model of the in chapter 6 investigated soil layers with a specific soil resistivity of approximately 100 Ωm in the upper layers (0 m – 2 m) and 30 Ωm in the underlying layers. Based on the in chapter 6.1 introduced approximation formulas a horizontal extension of 300 m would be necessary for realising a 1 Ω horizontal earthing conductor. When estimating the necessary drill depth for a 1 Ω ground rod it has to be mentioned that if the specific soil resistivity of the upper layers is relatively high, by considering only the upper value for the calculation of the earthing system, a too high system resistance would be calculated if the underlying layers have a lower impedance [16], [43]. The results of the calculation lead to a necessary drilling depth of approximately 35 m for the introduced soil conditions. In the following table 7.2 the investigated scenarios and their construction costs are summarized.

Solution Scenarios	**Costs in €**
Scenario 1a – 11 Ground rods with 1 Ω (see fig. 6.7)	118.450.-
Scenario 1b – 11 Horizontal earthing conductors with 1 Ω (see fig. 6.7)	59.000.-
Scenario 2a – 7 Isolating joints before start of operation (see fig. 6.8)	148.000.-
Scenario 2b – 7 Isolating joints after start of operation (see fig. 6.8)	365.000.-
Scenario 3a – 1 Isolating joint before start of operation and 1 compensation conductor (see fig. 6.10)	140.400.-
Scenario 3b – 1 Isolating joint after start of operation and 1 compensation conductor (see fig. 6.10)	171.400.-
Scenario 4a – 2 Isolating joints before start of operation, 4 ground rods and 1 compensation conductor (see fig. 6.12)	129.200.-
Scenario 4b – 2 Isolating joints after start of operation, 4 horizontal earthing conductors and 1 compensation conductor (see fig. 6.12)	105.800.-
Scenario 4c – 2 Isolating joints before start of operation, 4 ground rods and 1 compensation conductor (see fig. 6.12)	191.200.-
Scenario 4d – 2 Isolating joints after start of operation, 4 horizontal earthing conductors and 1 compensation conductor (see fig. 6.12)	167.800.-

Table 7.2: Selected solution scenarios and their construction costs

In the above table 7.2 for each scenario, additional price variations are listed. The overall prices consist of the following items:

Scenario 1

- Scenario 1a: 11 ground rods including 11 power capacitors and 1 rectifier for cathodic corrosion protection.
- Scenario 1b, same configuration as scenario 1a: 11 horizontal earthing conductors are assumed instead of ground rods.

Scenario 1b includes 11 horizontal earthing conductors. The smallest assumed distance between two systems is 600 m. As already mentioned a horizontal extension of 300 m would be necessary for realising horizontal earthing conductors with 1 Ω. In addition to that the potential gradients of two close horizontal earthing conductors could overlap which could lead to a bridging effect and consequently to the loss of the interfering voltage mitigating functions of two close earthing systems. Not least because of this reason Scenario 1b represents a borderline scenario which is problematical to put in reality. To sum up, it can be said that horizontal earthing conductors would be an impracticable variant for this investigated case, if one thinks about the seasonal changes of the specific soil resistivity ρ of the in chapter 6.1 investigated soil.

Scenario 2

- Scenario 2a: 7 isolating joints and 8 rectifiers for cathodic corrosion protection.
- Scenario 2b, same configuration as scenario 2a: It is assumed that the isolating joints are installed after pipeline operation start. Based on the high costs and expenditures in praxis it should be avoided to install isolating joints after pipeline operation start for interference voltage mitigating reasons.

Scenario 3

- Scenario 3a: 1 Isolating joint and two rectifiers for cathodic corrosion protection. Compensation conductor of 13000 m length.
- Scenario 3b, same configuration as scenario 3a: Assumption that isolating joint is installed after pipeline operation start. The practical procedure regarding the subsequent installation of isolating joints is already mentioned in the description of Scenario 2b.

Scenario 4

- Scenario 4a: 4 ground rods. 2 Isolating joints 3 rectifiers as well as 4 power capacitors for cathodic corrosion protection. Compensation conductor of 4600 m length.
- Scenario 4b, same configuration as scenario 4a: 4 horizontal earthing conductors are assumed instead of ground rods. Based on the above described overlapping effect of

the potential gradients of two close horizontal earthing conductors, scenario 4b would be a practicable variant because they are far enough apart from each other. But when thinking about the above mentioned seasonal changes of the specific soil resistivity ρ of the in chapter 6.1 investigated soil, this variant can be seen as not recommendable.

- Scenario 4c, same configuration as scenario 4a: It is assumed that the isolating joint is installed after pipeline operation start. The practical procedure regarding the subsequent installation of isolating joints is already mentioned in the description of Scenario 2b.
- Scenario 4d, same configuration as scenario 4b: It is assumed that the isolating joint is installed after pipeline operation start. The practical procedure regarding the subsequent installation of isolating joints is already mentioned in the description of Scenario 2b. The disadvantages of horizontal earthing conductors in this case have already been mentioned.

The following figure 7.12 shows the voltage reduction of the 4 introduced solution scenarios. Therefore the superposition of the pipeline interference voltages (50 Hz, 16.7 Hz) of the solutions scenarios are subtracted from the pipeline interference voltages of the reference case without any interference voltage mitigating measures (see figure 7.3).

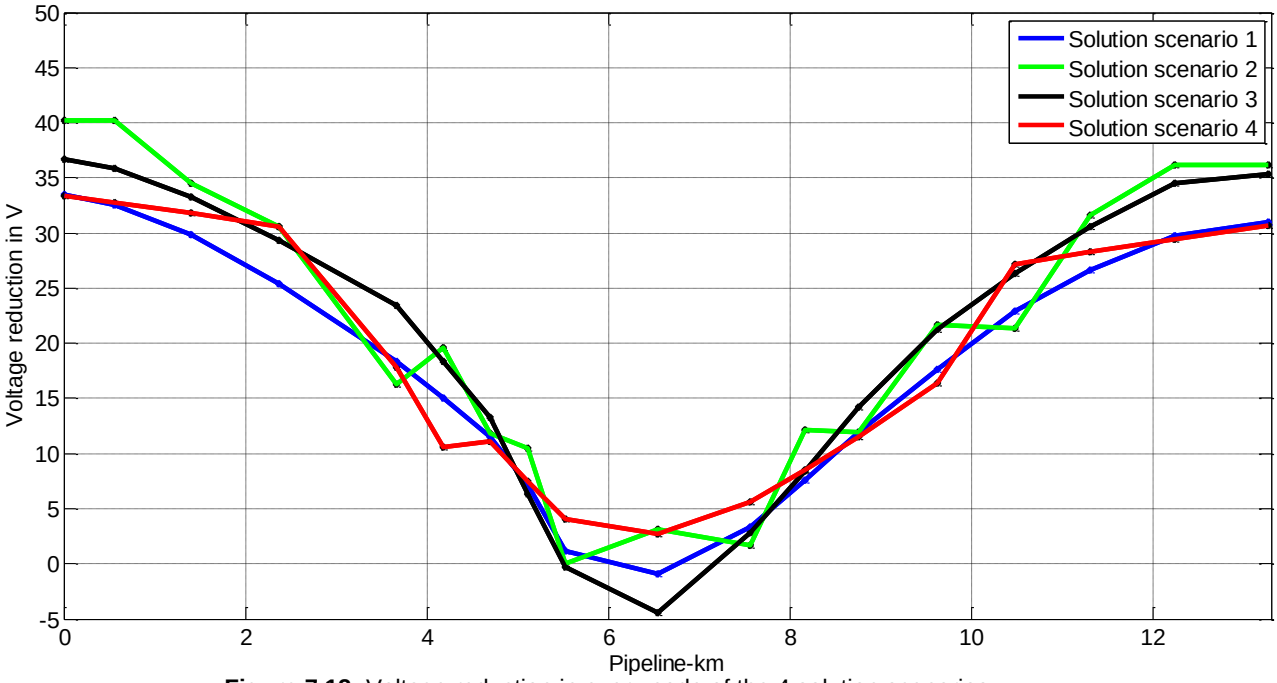

Figure 7.12: Voltage reduction in every node of the 4 solution scenarios

In the above figure 7.12 it is evident that some mitigating scenarios lead to small voltages rises in areas where the pipeline is at least interfered. For classical parallel courses this area is located in the middle of the pipeline. In the case of solution scenario 1, the earthing systems lead to a voltage reduction at relevant nodes and to a, considering AC corrosion, small and uncritical increase at nodes with low interference. In the case of solution scenario 3 the isolating joint at the node with the lowest interference (pipeline-km 6.60) leads to an uncritically increase of the pipeline interference voltage directly at the isolating joint. Principally all reduction curves have a shape similar to the initial curve (see figure 7.3, root mean square value without interference voltage mitigating measures).

The following table 7.3 shows a benefit-cost analysis of the investigated scenarios. The for the assumed circumstances non-practicable scenarios 1b, 2b, 3b, 4b, 4c and 4d are still taken into account in order to cover the range of specific costs and to demonstrate the impact of possible planning errors.

In column 2 the minimum voltage reduction, in column 3 the maximum interference voltage reduction of all nodes is shown. Column 4 shows the arithmetical average of the interference voltage reduction over all nodes. The last column shows to whole numbers rounded € per V of the averaged voltage reduction.

Solution Scenarios	Min (V)	Max (V)	AVG (V)	€ per V of averaged voltage reduction
Scenario 1a	- 0.95	33.48	18.03	6.570.-
Scenario 1b	- 0.95	33.48	18.03	3.272.-
Scenario 2a	0.04	40.24	21.10	7.014.-
Scenario 2b	0.04	40.24	21.10	17.299.-
Scenario 3a	- 4.47	36.72	20.31	6.913.-
Scenario 3b	- 4.47	36.72	20.31	8.439.-
Scenario 4a	2.70	33.37	18.88	6.843.-
Scenario 4b	2.70	33.37	18.88	5.604.-
Scenario 4c	2.70	33.37	18.88	10.127.-
Scenario 4d	2.70	33.37	18.88	8.888.-

Table 7.3: Overview of the interference voltage reduction for each scenario

One result of the above table is that the investigated case scenario 1a (ground rods exclusively) shows the best cost-benefit ratio. The installation of horizontal earthing conductors (scenario 1b) is cheaper but based on the seasonal changes of the specific soil resistivity much more uncertain. Scenarios 3a and 4a offer tolerable alternatives with higher expenditures.

7.4 Fields of application

Based on the findings obtained in this thesis it is possible to verify the crucial impact of two parameters for the cost- and technical effectivity of pipeline interference voltage mitigating measures. The first one is the specific soil resistivity ρ and the soil arrangement in layers and the second one is the length of the influenced pipeline or pipeline segment. In the following the main characteristics of earthing systems, isolating joints and compensation conductors are summarised.

- Earthing systems: The carried out cost effective analysis are based on the measured relatively low impedant soil. Earthing systems are directly dependent on the specific soil resistivity. For relatively low specific soil resistivities earthing systems offer a solid method. For higher soil resistivities they are uneconomical and respectively because of the hardness of soils with high resistances almost impossible to realise. Ground rods should be preferred to horizontal earthing conductors because their system resistivities fluctuate less during the season. The length of the interfered pipeline or pipeline segment has no influence on the principal effectivity of earthing systems.

- Isolating joints: Nowadays they are generally used for defining cathodic corrosion protection areas. The selection of these areas is usually already customised to the interference situation. The realisation of more cathodic protection areas in order to reduce pipeline interference voltages could be taken into account more often, especially in areas with high specific soil resistivities. The length of the interfered pipeline or pipeline segment has no influence on the principal effectivity of isolating joints.

- Compensation conductors: The preferred field of application of the compensation conductor are pure parallel and narrow routes between interfering systems and pipelines over some kilometres. The carried out investigations are bases on an approximately 7 km long isolated copper test compensation conductor with a cross section of 50 mm^2. As within the case study shown one can imagine that longer compensation conductors present a cost-intensive measure if one considers a higher cross section in order to keep a low conductibility. The measurements show that the compensation conductor should be installed over the whole length of the interfered pipeline or pipeline segment. Pipeline segments with lower interference or with installed earthing systems should be separated by isolating joints.

Nevertheless compensation conductors show an alternative in regions with high specific soil resistivities.

7.5 Summary

Based on the findings in this chapter, the numerous possibilities and combinations of measures to mitigate pipeline interference voltages are shown and economically evaluated. The optimisation of these measures can be viewed as a target in order to reduce the workload for pipeline interference investigations.

The in Austria up to now preferred measure is the installation of AC earthing systems. The following chapter presents algorithms for the optimum placement of AC earthing systems along inductively interfered pipelines.

8 Optimisation Procedures

This chapter describes present simulation and optimisation procedures as well as two algorithms for the optimal location of pipeline interference voltage mitigating AC earthing systems.

8.1 Practical Procedures

The following figure 8.1 enables a holistic view of the calculation- and optimisation procedures to minimise pipeline interference voltages.

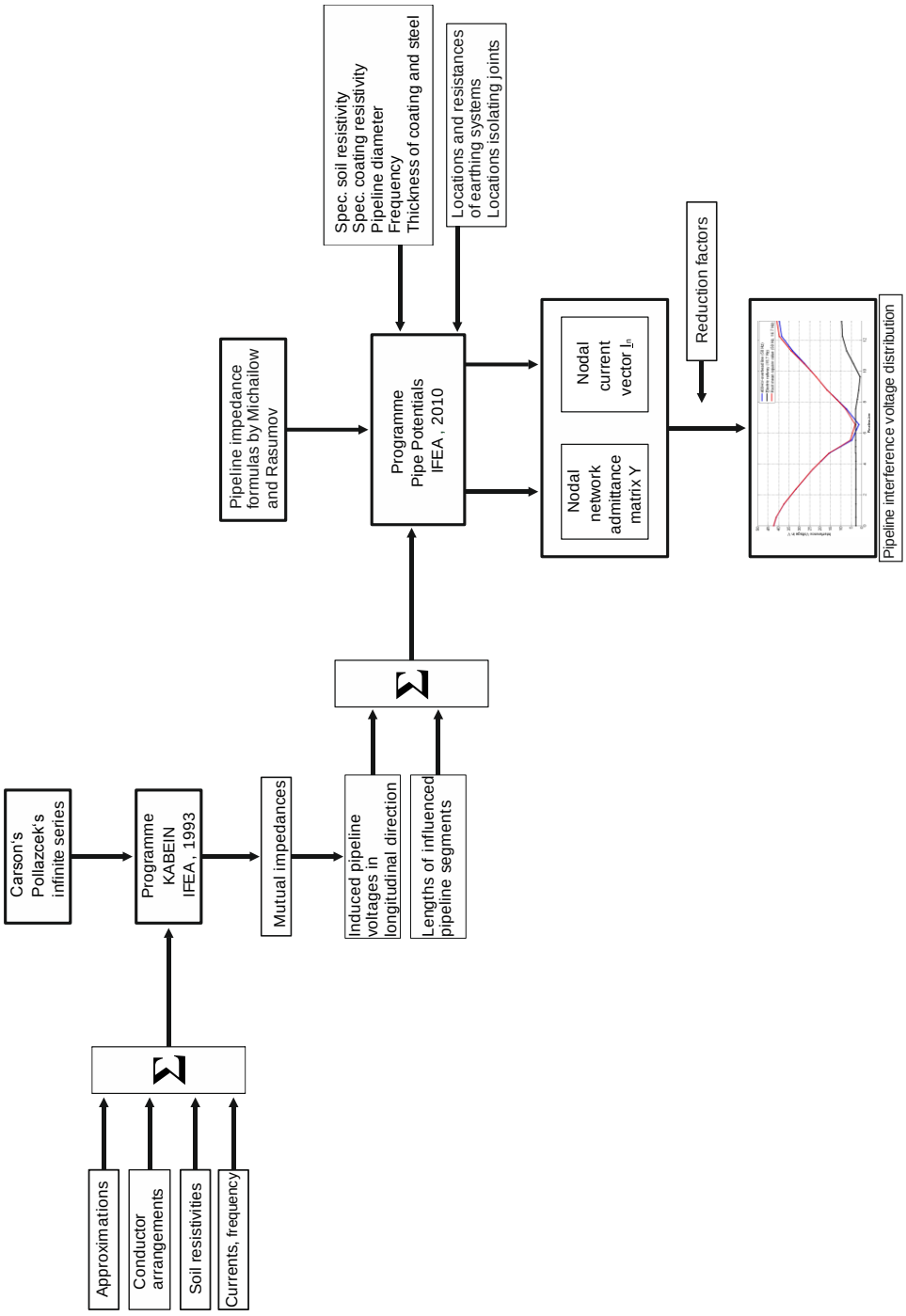

Figure 8.1: Holistic view of present simulation- and optimisation procedures, important input- and output parameters

The mutual impedances for any approach between the interfering systems and the interfered pipelines are calculated with the help of the programme KABEIN which was developed within the scope of a previous work [3] at the Institute of Electrical Powers Systems of Graz University of Technology. The most important input parameters for calculating the mutual impedances between interfering and interfered systems are the geometrical approaches, the conductor arrangements, the specific soil resistivity ρ, the interfering currents (absolute values and phase angles) and the interfering system-frequency. The calculation procedures for pure parallel approaches are shown in the chapters 2.2.2 and 4.3 of this thesis.

The output parameters are the induced pipeline voltages in direct axis and the lengths of the influenced pipeline segments. With the help of the in chapter 2.2.3 of this thesis described formulas of Michailow and Rasumov [5] the pipeline impedances in longitudinal direction and the pipeline shunt-admittances are calculated for each pipeline segment with the Programme PipePotentials.

In a following step the setup of the nodal admittance-matrix is solved in order to calculate the pipeline interfering voltages along an inductively interfered pipeline (see chapter 2.2.4). The locations and the values of possible AC earthing systems (see chapter 4.1, earthing systems) are in the programme PipePotentials taken into consideration. Also possible locations of isolating joints (see chapter 3.3, isolating joints) are taken into account. Possible reduction factors either obtained by the operational management of the interfering system operators or calculated by the in chapter 4.2 (compensation conductors) described procedures. The reduction factors are be multiplied with the pipeline interfering voltages within the programme.

The output of the programme PipePotentials is a diagram of pipeline interference voltage along the interfered pipeline for the selected input parameters.

Practical experiences show that a successively supplementation of AC earthing systems at locations, where peaks of the pipeline interference voltage occur, is necessary in order to reach practicable and secure values for the pipeline interference voltage. Within this process it must be ensured that the AC earthing systems attain practicable values. As introduced in the previous chapter one can imagine that extremely low earthing system resistances as for example 0.1 Ω can be hardly achieved in praxis.

The following chapter describes algorithms that simulate practical optimisation procedures of an expert to achieve optimal locations of AC earthing system.

8.2 Expert system algorithms

The following figure 8.2 shows a flowchart of an algorithm realised in Matlab® [44]. The language of the flowchart is written in pseudocode containing some Matlab®-elements.

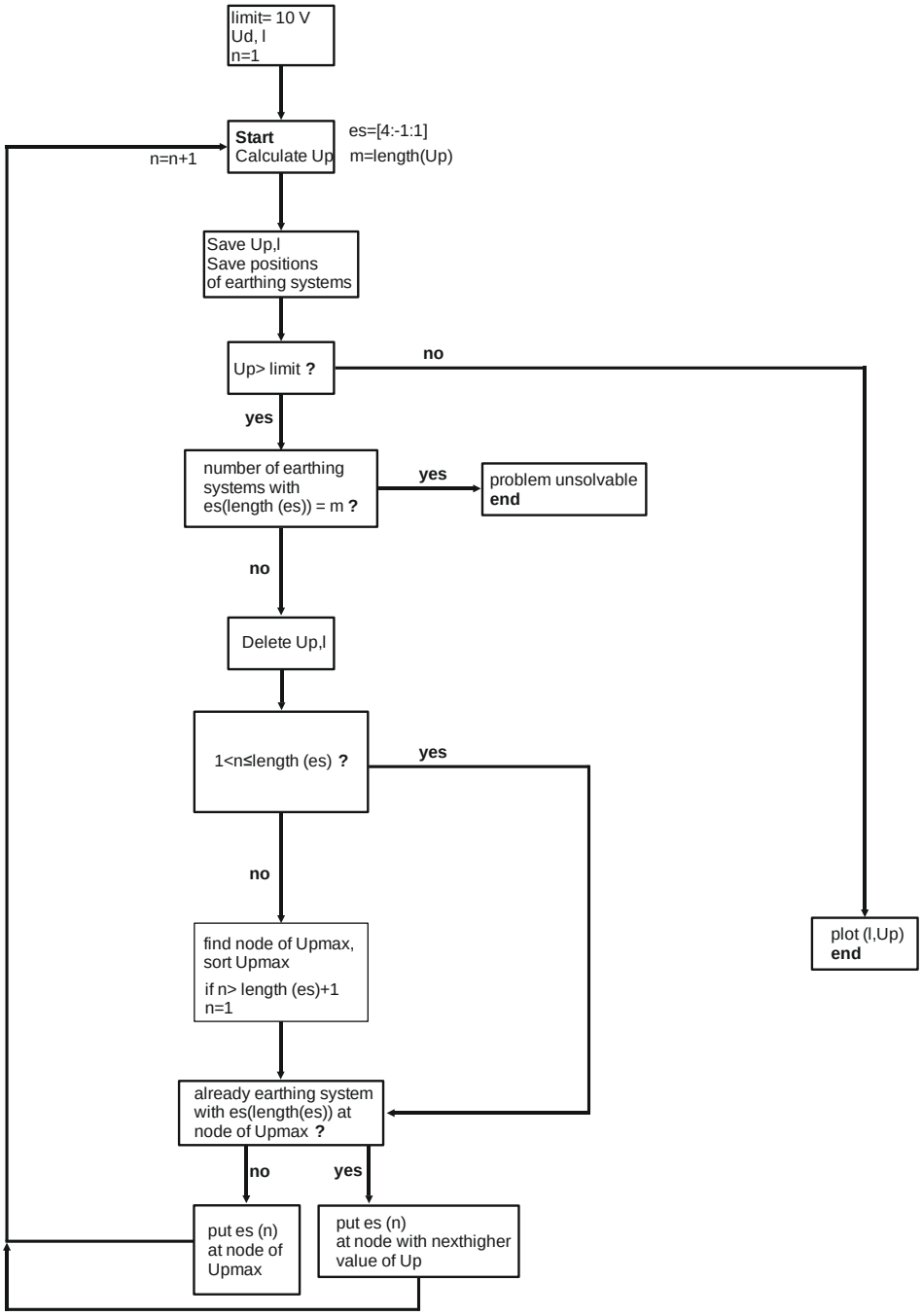

Figure 8.2: Flowchart of the expert system algorithm no. 1

The input parameters of the algorithm are the requesting voltage limit- in this case 10 V, the voltages in longitudinal direction (Ud), the lengths of the pipeline segments (l) and a control variable which is in this case called n. The calculation of the pipeline interference voltage distribution is performed as described with the programme PipePotentials. Possible resistances of earthing systems can in Matlab® be specified in the form of a vector, in decreasing order. So the vector es represents a list of possible earthing system resistances in decreasing order.

In the example of the flowchart in figure 8.2 the resistances decrease from 4 Ω to 1 Ω in steps of 1 Ω (vector es). The length of the pipeline interference vector Up corresponds to the number of nodes of the equivalent pi-circuit of an inductively interfered pipeline.

The algorithm is denominated with the help of a 10-km-long pipeline, divided into 20 pipeline segments with a single length of 0.5 km. An interfering voltage in longitudinal direction (Ud) of 1.80 V is assumed in each pipeline pi-segment.

The following basic example in figure 8.3 facilitates the principle description of the algorithm.

The blue plotted line shows the initial voltage distribution that has to be optimised below 10 V.

In the first 4 optimisation steps (red lines in figure 8.3) earthing systems with 4 Ω, 3 Ω, 2 Ω and 1 Ω are assumed at the node with the initially highest pipeline interference voltage. In the represented example the highest voltages appear at two nodes, at the beginning and the end of the pipeline (see figure 8.3 and table 8.1). In this case the algorithm begins at the node with the lower pipeline kilometre.

In the optimisation steps 5-8 (black lines in figure 8.3) the 1-Ω earthing system (step 4) remains at the beginning of the pipeline and 4 Ω, 3 Ω, 2 Ω and 1 Ω are assumed at the node with the highest pipeline interference voltage, which in this case is at the end of the pipeline. After optimisation step 8 the pipeline is grounded with 1 Ω at both ends. The pipeline interference voltage is marginally above the requested 10-V-limit.

Therefore for the optimisation steps 9-12 (grey line in figure 8.3) additional earthing systems with 4 Ω, 3 Ω, 2 Ω and 1 Ω are assumed at the next highest node at pipeline-km 0.5.

In the course of the last optimisations step where 1-Ω earthing systems are fixed at pipeline-km 0.0, 0.5 and 10.0, an additional earthing system with 4 Ω is assumed at pipeline-km 9.5 (at km 10.0 there is already an earthing system with the lowest possible value), which leads to the solution of this problem. After this optimisation step, the pipeline interference voltage is below the 10-V-limit (9.92 V).

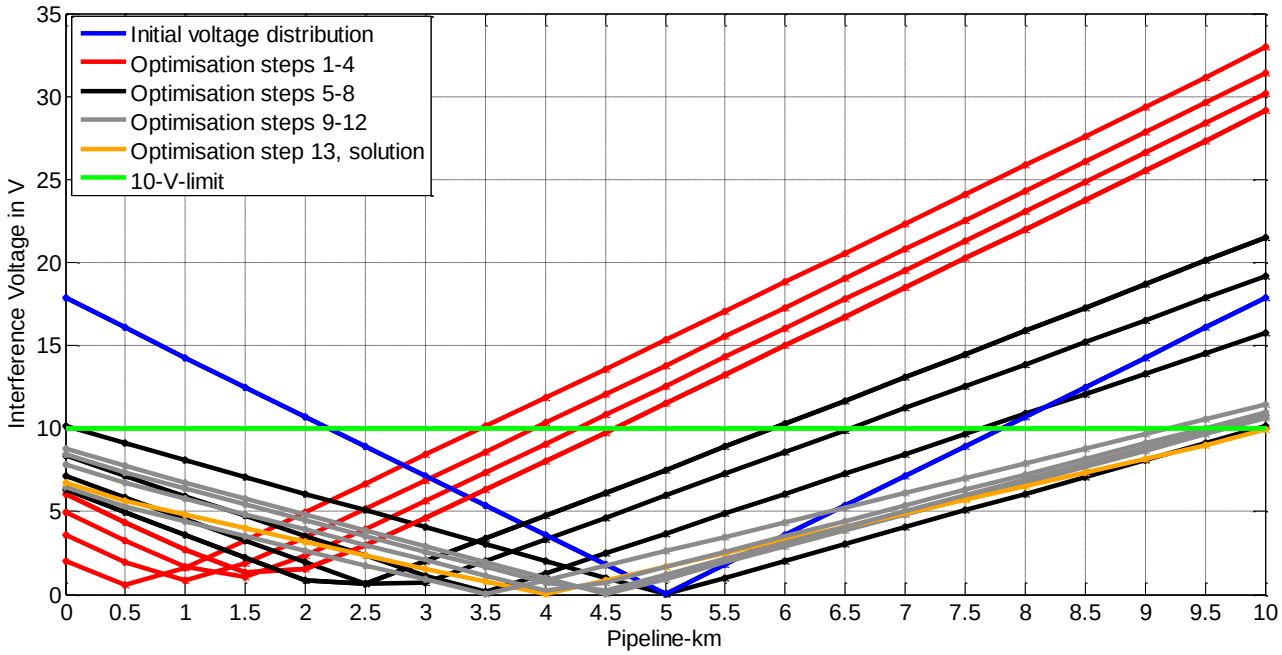

Figure 8.3: Optimisation steps of the expert system algorithm no. 1

The following table 8.1 corresponds to the above described optimisation steps in figure 8.3.

Optimisation step	Earthing system(s) at km	Ui_{max} (V) at km
Step 0	-	17.87 (km 0.0, km 10.0)
Step 1	4 Ω, km 0.0	29.13 (km 10.0)
Step 2	3 Ω, km 0.0	30.17 (km 10.0)
Step 3	2 Ω, km 0.0	31.43 (km 10.0)
Step 4	1 Ω, km 0.0	32.96 (km 10.0)
Step 5	1 Ω, km 0.0, 4 Ω, km 10.0	21.53 (km 10.0)
Step 6	1 Ω, km 0.0, 3 Ω, km 10.0	19.20 (km 10.0)
Step 7	1 Ω, km 0.0, 2 Ω, km 10.0	15.75 (km 10.0)
Step 8	1 Ω, km 0.0, 1 Ω, km 10.0	10.15 (km 0.0, km 10.0)
Step 9	1 Ω, km 0.0, 1 Ω, km 10.0, 4 Ω, km 0.5	10.63 (km 10.0)
Step 10	1 Ω, km 0.0, 1 Ω, km 10.0, 3 Ω, km 0.5	10.75 (km 10.0)
Step 11	1 Ω, km 0.0, 1 Ω, km 10.0, 2Ω, km 0.5	10.97 (km 10.0)
Step 12	1 Ω, km 0.0, 1 Ω, km 10.0, 1 Ω, km 0.5	11.42 (km 10.0)
Solution	1 Ω, km 0.0, 1 Ω, km 10.0, 1Ω, km 0.5, 4 Ω, km 9.5	9.92 (km 10.0)

Table 8.1: Optimisation steps of the expert system algorithm no.1, corresponding to figure 8.3

The introduced expert system algorithm no.1 is not suitable for interference situations where only one earthing system is sufficient to keep the pipeline interference voltage below the requested limit. Therefore a complete search- and sorting algorithm could go through first. However, this would increase the simulation time significantly, because the impact of earthing systems is successively calculated for every node.

In addition to that, it has to be said that nowadays a lot of limits have to be observed, as for instance 500 V in short-circuit cases and 65 V in normal operation mode regarding personal safety, as well as 10 V regarding AC corrosion (see chapter 2.1). Furthermore the pipeline interference voltage has to be optimised for multiple interference sources (16.7 Hz, 50 Hz). Because of these facts, nowadays only one single earthing system is rarely sufficient.

In [44] the algorithm is compared with a random based Las-Vegas-algorithm and a complete search and sorting algorithm by runtime-analysis of different examples. The results are that the random-based-algorithm and the complete search and sorting algorithm are at most suitable for shorter pipelines (few nodes). The developed expert system algorithm no.1 is characterised by acceptable results at constantly quick run-times.

As already described in chapter 6, earthing systems are certainly connected to specific costs. In principle, the lower the impedance of an earthing system, the higher are the costs. The following figure 8.4 shows the flowchart of an upgraded expert system algorithm in order to reduce the costs of possible earthing systems as well as to improve the pipeline interference voltage distribution.

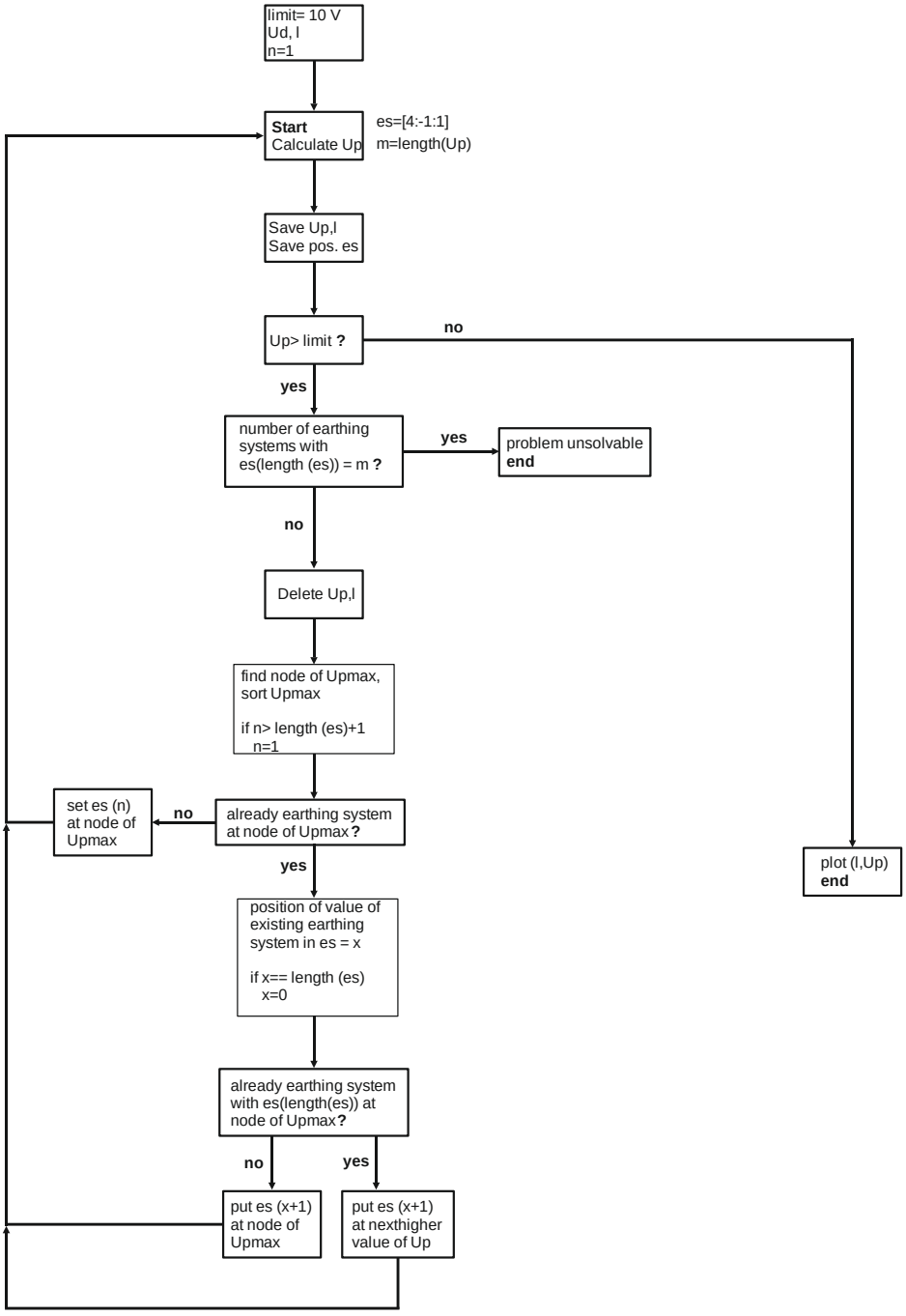

Figure 8.4: Flowchart of the expert system algorithm no. 2

The input parameters of the expert system algorithm no.2 are again the requested voltage limit, the voltages in direct axis (Ud), the length of the pipeline segments (l) and a variable n. In this case the variable n is only responsible for setting an earthing system at a node for the first time with the highest possible resistance (position 1 of vector es.). The vector es is again assumed with 4 Ω, 3 Ω, 2 Ω and 1 Ω. The same basic example configuration as introduced for expert system algorithm no.1 facilitates the principle description of expert system algorithm no.2.

The blue plotted line shows again the initial voltage distribution that has to be optimised below 10 V.

In the first optimisation step (red line in figure 8.5) an earthing systems with 4 Ω is assumed at the node with the initially highest pipeline interference voltage.

In the optimisation steps 2-8 (black lines in figure 8.5) every occurring peak is reduced by an earthing system at its node. If there because of a previous optimisation step already an earthing system was assumed, the next lower value of the vector es is taken.

If the peak is already reduced by an earthing system with the lowest possible resistance of the vector es, the highest possible value of es is taken at the node with the next higher value of the pipeline interference voltage Ui. This happens in the optimisation step 9 (grey line in figure 8.5) and within the final optimisation step (orange solution line in figure 8.5).

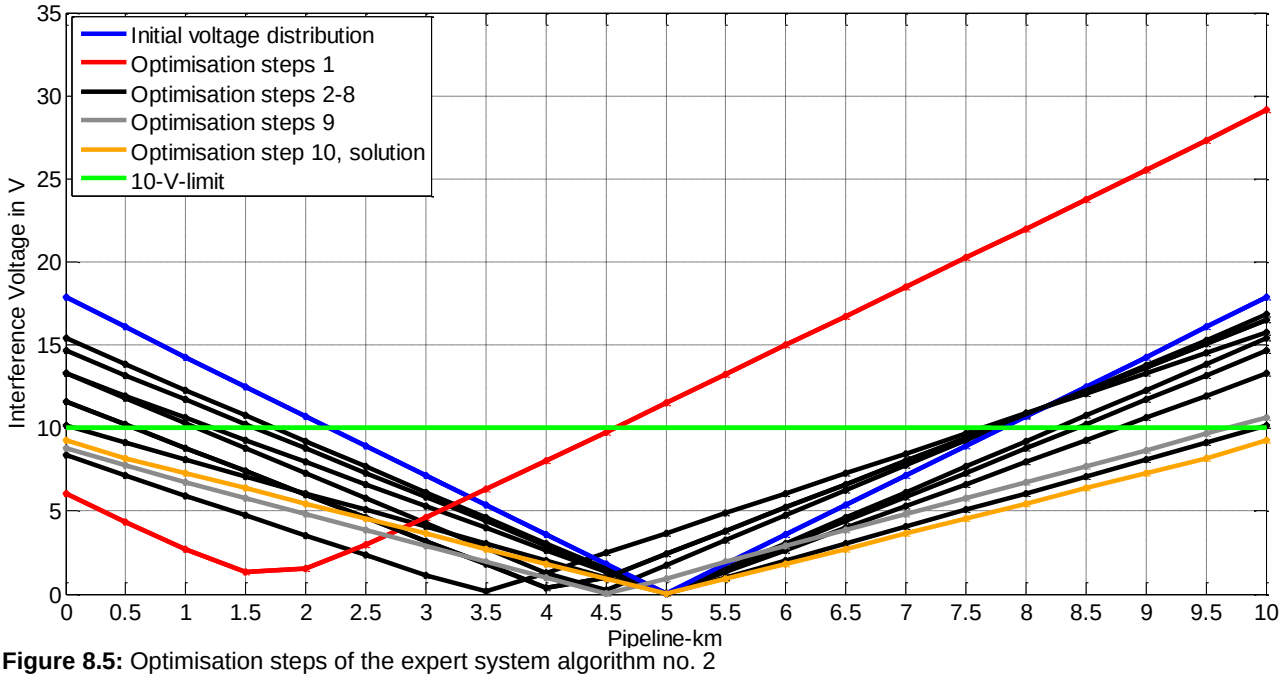

Figure 8.5: Optimisation steps of the expert system algorithm no. 2

The following table 8.2 corresponds to the above described optimisation steps in figure 8.5.

Optimisation step	Earthing system(s) at km	Ui_{max} (V) at km
Step 0	-	17.87 (km 0.0, km 10.0)
Step 1	4 Ω, km 0.0	29.13 (km 10.0)
Step 2	4 Ω, km 0.0, 4 Ω, km 10.0	15.39 (km 0.0, km 10.0)
Step 3	3 Ω, km 0.0, 4 Ω, km 10.0	16.83 (km 10.0)
Step 4	3 Ω, km 0.0, 3 Ω, km 10.0	14.64 (km 0.0, km 10.0)
Step 5	2 Ω, km 0.0, 3 Ω, km 10.0	16.50 (km 10.0)
Step 6	2 Ω, km 0.0, 2 Ω, km 10.0	13.27 (km 0.0, km 10.0)
Step 7	1 Ω, km 0.0, 2 Ω, km 10.0	15.75 (km 10.0)
Step 8	1 Ω, km 0.0, 1 Ω, km 10.0	10.15 (km 0.0, km 10.0)
Step 9	1 Ω, km 0.0, 1 Ω, km 10.0, 4 Ω, km 0.5	10.63 (km 10.0)
Solution	1 Ω, km 0.0, 1 Ω, km 10.0, 4Ω, km 0.5, 4 Ω, km 9.5	9.23 (km 10.0)

Table 8.2: Optimisation steps of the expert system algorithm no.1, corresponding to figure 8.5

8.3 Summary

As the findings in this chapter show, the introduced expert system algorithm no.1 and expert system algorithm no.2 act for the most part similar. The difference is that expert system algorithm no.2 prefers a successive pairwise modification of earthing systems at nodes of different peaks. Therefore in the investigated case less optimisation steps are necessary, which leads to shorter runtimes.

Another advantage is, that in the investigated case less installation effort is necessary (2 earthing systems with 1 Ω and 2 earthing systems with 4 Ω instead of 3 earthing systems with 1 Ω and 1 earthing systems with 4 Ω), which leads to lower costs and to a more homogeneous voltage distribution.

To sum up expert system algorithm no.2 leads compared to expert system algorithm no. 1 at shorter runtimes to a lower pipeline interference voltage distribution at lower costs.

9 Conclusion and Outlook

In this thesis pipeline interference voltage mitigating measures such as AC earthing systems, isolating joints and compensation conductors are investigated in detail from a technical and an economical point of view.

In this thesis the possibility to calculate pipeline interference voltages with the help of differential equations is demonstrated. For the programme „PipePotentials“ (developed within this thesis) a numerical approach is preferred which bases on the interaction of the mutual impedances, the electrical pipeline parameters, the equivalent ladder network and the solution of the nodal admittance matrix.

Within this thesis an approach to model coating holidays as circular plate earthing systems of the pipeline was chosen. The sensitivity analysis of all interesting parameters concerning current densities at coating holidays show, that regarding AC corrosion likelihood for higher soil resistivities, higher pipeline interference voltages than 10 V could be allowed. In future works these effects could be approved by electrochemical measurements, whereas it could be a topic for future guidelines and standards.

The technical effectiveness of AC earthing systems, isolating joints and compensation conductors is shown with the help of examples. A developed tool enables to determine reduction factors such as the pipeline reduction factor („R_{FP}”) and the railway reduction factor („R_{FR}”). For higher soil resistivities it is difficult and expensive to install low impedant earthing systems, therefore the installation of compensation conductors shows an alternative, which is in Austria starts to be applied at the moment.

Additionally to calculations and theoretical considerations measurements were carried out within the context of this PhD thesis. These measurements at a pipeline with an existing compensation conductor show advantageous compensation conductor switching conditions. The comparison between measurements and simulations show the longitudinal decrement of the interfering current and consequently the pipeline interference voltage along a parallel one side fed railway section, because different vehicle positions have to be considered.

The investigations of the impact of different compensation conductor locations show that there are two principle possibilities to install compensation conductors either close to the pipeline or close to the interfering system. If the compensation conductor is close to the interfering system, effects based on the phase position may worsen the situation; therefore a better option is installing the compensation conductor close to the pipeline. Additionally it is shown, that the pipeline reduction factor „R_{FP}” depends on the distances between the pipeline, interfering system and compensation conductor. Therefore in future the established constant reduction factors should be mentioned with a corresponding distance.

The developed tool helps to carry out future analyses regarding the implementation of additional and/or high conductive earth wires. A new tool considering the inductive coupling between interfering system, interfered pipeline and a conductive coupled compensation conductor could be developed and verified by measurements.

The investigation of different phase conductor arrangements shows that a simple modification of the phase conductor arrangements is in many cases an effective measure which has also been optimised within the context of this PhD thesis.

The analysis of the impact of an increasing distance between interfering line and pipeline shows the importance of the pipeline route planning phase. The economic analysis of the main investigated pipeline interference voltage mitigating measures demonstrates among other things the disadvantage of a later isolating joint installation. These facts show that in future AC interference problems should be much more taken into account during planning phases.

Within this PhD thesis a comparison between the impact of 400 kV overhead lines and electric railway systems on pipeline interference voltages is carried out. Assuming thermal currents along the whole interfering section, railways show a stronger influence regarding the risk of hazard. The analysis of the influence on the AC corrosion likelihood shows different results for the vicinity and the far area. In the vicinity area (up to 100 m) the 400 kV overhead lines have a bigger influence than the electric railway systems, because of the characteristic load flow. With higher horizontal distances, the influence of the railway system is bigger. This hint can be useful for planning future pipeline routes.

As it is shown with the examples of one- and both side fed railway lines, the assumption of the maximum current over the whole approach is a worst-case assumption. Based on measured data a future model taking relevant load flows and feeding situations into account could be developed.

The annual measuring series of the specific soil resistivity gives an interesting sight on the seasonal changes of the investigated soil in the upper and the lower layers. The investigation of the impact of the seasonal varying soil resistivity on earthing systems shows the need for a safety margin for AC earthing systems resistances. This could also be a topic for future guidelines and standards. The annual measuring series of the specific soil resistivity could be repeated for different soil types in order to derive additional conclusions.

Within the carried out case study the approach of superposing the influence of interfering systems with different frequencies is selected. Within electrochemical analysis this approach could be verified or a more representative calculation rule can be worked out.

The cost effective analysis of the solution scenarios shows useful benchmarks to compare the efficiency of different pipelines or pipeline operators.

At the end of this PhD thesis two algorithms are designed in order to simulate the practical optimisation procedures of an expert. The second of these algorithms can be seen as an improvement which leads to lower pipeline interference voltages at lower costs.

In the following time the algorithms will be applied for a large national inductive pipeline interference project. Based on these upcoming practical experiences there could be new suggestions to develop the expert system algorithm further.

10 References

[1] CIGRÉ: *AC corrosion on metallic pipelines due to interference from AC power lines-Phenomenon, Modelling and Countermeasures*, Cigré Technical Brochure No. 290, April 2006.

[2] R. Braunstein, E. Schmautzer, G. Propst: *Comparison and Discussion on Potential Mitigating Measures Regarding Inductive Interference of Metallic Pipelines.* In: IEEE ESARS International Conference on Electrical Systems for Aircraft, Railway and Ship Propulsion, Bologna, Italy, 2010, ISBN 978-1-4244-9093-6, p.1-4.

[3] E. Schmautzer: *Ein Beitrag zur Berechnung der induktiven Beeinflussung von Rohrleitungsnetzen,* PhD thesis, Institute of Electrical Power Systems, Graz University of Technology, 1990.

[4] R. Braunstein, M. Lindinger, E. Schmautzer, L. Fickert: *Approaches to the reduction of the AC corrosion likelihood along interfered pipelines due to operation and short-circuit currents of high voltage lines and electric railways.* In: 2nd International Youth Conference on Energetics, IYCE, Budapest, Hungary, 2009, ISBN 978-963-420-983-6, p.1-6.

[5] Michailow, M., Rasumov, Z.D.: *Electrical parameters of metallic pipelines in earth*, Èlektričestvo, Journal 5, p. 60-63, 1963.

[6] E. Schmautzer, R. Braunstein: *Lösungsansätze zur Reduktion der Wechselstrom-korrosionswahrscheinlichkeit von induktiv beeinflussten Rohrleitungen durch Traktionsströme elektrischer Bahnanlagen.* In: e&i, Elektrotechnik und Informationstechnik- journal, „Bahntechnik“, vol. 6, June 2009, p.221-226.

[7] TE 30: (Technische Empfehlung Nr. 30): *Maßnahmen beim Bau und Betrieb von Rohrleitungen im Einflussbereich von Starkstromanlagen mit Nennspannungen über 1 kV.* Technical committee for interference (ÖVE), April 1987.

[8] AfK-Empfehlung Nr. 3: *Maßnahmen beim Bau und Betrieb von Rohrleitungen im Einflussbereich von Hochspannungs-Drehstromanlagen und Wechselstrom-Bahnanlagen*. Working group DVGW/VDE for corrosion (AfK), October 2006.

[9] Prestandard CEN/TS 15280: *Evaluation of AC corrosion likelihood of buried pipelines-Application to cathodically protected pipelines.* CEN, March 2006.

[10] CENELEC prEN 50351: *Basic standard for the calculation and measurement methods relating to the influence of electric power supply and traction systems on telecommunication systems*. CENELEC, Januar 2003.

[11] M. Büchler, C-H.Voûte, H.G. Schöneich: *Der Einfluss der Betriebsbedingungen des kathodischen Korrosionsschutzes auf die Wechselstromkorrosion und Schutzmaßnahmen*, Schweizerische Gesellschaft für Korrosionsschutz - SGK, 2008.

[12] K. Friedl, E. Schmautzer: *Impact of the Phase Positions on the Electric and Magnetic Field of High-Voltage Overhead Lines.* In: Congrès International des Réseaux Electriques de Distribution, Cired, Prague, Czech Republic, 978-1-84919126-5, p.1-4, June 2009.

[13] K. Budnik, W. Machczynski: *AC Corrosion Computer Simulation as an Element of Pipeline System Integrity Process*. In: 24th World Gas Conference, Buenos Aires, Argentinia, 2009, http://www.igu.org/html/wgc2009/, 08.2010.

[14] R. Braunstein, E. Schmautzer, M. Ölz: *Impacts of inductive and Conductive Interference due to High Voltage Lines on Coating Holidays of Isolated Metallic Pipelines.* In: Congrès International des Réseaux Electriques de Distribution, Cired, Frankfurt, Germany, ISSN 2032-9644, p.1-4, June 2011

[15] E. Schmautzer, W. Friedl, P. Linhardt, G. Ball: *Wechselstromkorrosion an Rohrleitungen- Modellbildung und elektrochemische Analysen.* Technical report by order of the Austrian Association for Gas and Water (OVGW).October 2004.

[16] W. Koch: *Erdungen in Wechselstromanlagen über 1 kV- Berechnung und Ausführung*, published by Springer, 1961.

[17] J. Carson: *Wave propagation in overhead wires with ground return*, Bell System Technical Journal, vol. 5, p. 539-554, 1926.

[18] F. Pollaczek: *Über die Induktionswirkung einer Wechselstromeinfachleitung*, Elektrische Nachrichtentechnik, vol. 4, p. 539-554, 1927.

[19] U. Bette, M. Büchler: *Taschenbuch für den kathodischen Korrosionsschutz,* published by Vulkan, ISBN 978-3-8027-2556-2, 2010.

[20] U. Bette, G. Schell: *Einfluss der Fehlstellengeometrie auf die lokale Stromdichte,* 3R International, vol. 6/7, p. 352-357, 2010.

[21] E. Wendler-Kalsch, H. Gräfen: *Korrosionsschadenkunde*, published by Springer, ISBN 978-3-5406-3377-8, p. 27, 1998.

[22] H.-J. Haubrich, B.A. Flechner, W. Machczynski: *A Universal Modell for the computation of the electromagnetic interference on earth return circuits*, IEEE Transactions on Power Delivery, Vol. 9, No 3, 1994.

[23] B.R. Oswald: *Knotenorientierte Verfahren in der Netzberechnung*, Leipziger Universitätsverlag, ISBN 3-934565-51-4, 2000.

[24] M. Büchler, C-H.Voûte, H.G, D. Joos: *Feldversuche zur Wechselstromkorrosion*, Energie Wasser-Praxis, Vol.7/8, p.30-38, 2010.

[25] AfK-Empfehlung Nr.11: *Wechselstromkorrosion- Beurteilung der Verhältnisse bei Stahlrohrleitungen und Schutzmaßnahmen*, Working group DVGW/VDE for corrosion (AfK), January 2003.

[26] H. Biesenack, G. George, G. Hofmann, A. Schmieder et al. : *Energieversorgung elektrischer Bahnen,* published by Teubner, ISBN 3-519-06249-6, September 2006.

[27] DIN VDE 0228, Teil 3: *Maßnahmen bei Beeinflussung von Fernmeldeanlagen durch Starkstromanlagen – Beeinflussung durch Wechselstrom-Bahnanlagen.*
German Standardisation Institute (DIN), September 1988.

[28] S. Jank: *Beeinflussung von Anlagen der Leit- und Sicherungstechnik durch Bahnströme.* In: BahnPraxis E, Zeitschrift für Elektrofachkräfte zur Förderung der Betriebssicherheit und der Arbeitssicherheit bei der DB AG- Journal, Vol. 2/2007, p.7.

[29] D. Oeding, B. R. Oswald: *Elektrische Kraftwerke und Netze,* published by Springer, ISBN: 3-540-00863-2, 2004.

[30] A. A. Hossam-Eldin, W. Mokhtar: *Interference between HV Transmission Line and nearby Pipelines*. In: IEEE MEPCON, International Middle-East Power System Conference, Aswan, Egypt, 2008, ISBN 978-1-4244-1933-3, p.218-223.

[31] R. Muckenhuber: *Einflussgrößen bei der Berechnung induktiver und ohmscher Beeinflussungen*, Symposium „Starkstrombeeinflussung von Fernmeldeanlagen“, 1966

[32] R. Muckenhuber: *Die Fehlerströme in einem elektrischem Netz als Funktion des Fehlerortes*, ÖZE, vol. 12, p. 679-684, 1960.

[33] R. Muckenhuber: *Die induktive Beeinflussung von Rohrleitungen durch Hochspannungsleitungen*, ÖZE, vol. 6, p. 273-280, 1968.

[34] W. Friedl: *Berechnung niederfrequenter Beeinflussung von Rohrleitungen,* Diploma Thesis, Institute of Electrical Power Systems, Graz University of Technology, 2004.

[35] E. Schmautzer: *Die kartografische Aufnahme und Berechnung von induktiven Einfach- und Mehrfachbeeinflussungen durch Hochspannungsfreileitungen und -kabel,* Technical report No. 119, Institute of Electrical Power Systems, Graz University of Technology, 1990.

[36] S. Schmidt, D. Martin: *Wechselstrombeeinflussung kathodisch geschützter Rohrleitungen durch Hochspannungsfreileitungen.* In: 3R international journal, vol. 45, November 2006, p.653-656.

[37] M. Ölz: *Messtechnische Ermittlung von Rohrleitungsparametern unter Berücksichtigung von Erdern,* Diploma thesis, Institute of Electrical Power Systems, Graz University of Technology, 2011.

[38] E. Schmautzer, R. Braunstein, M. Ölz: *Simulation and optimised Reduction of induced Pipeline Voltages caused by High-voltage Lines on inductively interfered pipelines.* In: Congrès International des Réseaux Electriques de Distribution, Cired, Frankfurt, Germany, ISSN 2032-9644, p.1-4, June 2011.

[39] G. Biegelmeier, G. Kiefer, K.-H. Kreft: *Schutz in elektrischen Anlagen, Band 2: Erdungen, Berechnung, Ausführung und Messung,* published by VDE, ISBN: 3-8007-2049-3, 1996.

[40] M. Muffat: *Der spezifische Erdwiderstand im jahreszeitlichen Verlauf,* Bachelor thesis, Institute of Electrical Power Systems, Graz University of Technology, 2012.

[41] F. Wenner: *A Method of Measuring Earth Resistivity,* Bull, National Bureau of Standards, Bull 12(4), 1915/16.

[42] prEN 50443: *Effects of electromagnetic interference on pipelines caused high voltage AC railway systems and/or high voltage AC power supply systems.* CEN, March 2009.

[43] M. Lindinger: *Nachweis globaler Erdungssysteme durch Messung und Berechnung von verteilten Erdungsanlagen*, working title, PhD thesis, Institute of Electrical Power Systems, Graz University of Technology, 2012.

[44] C. Wahl: *Implementierung von Algorithmen zur optimalen Verortung von Erdungsanlagen entlang induktiv beeinflusster Rohrleitungen,* Diploma thesis, Institute of Electrical Power Systems, Graz University of Technology, 2011.

[45] ÖVE/ÖNORM EN 50163, *Railway applications – Supply voltages of traction systems.* Austrian Electrotechnical Association (ÖVE), April 2008.

[46] ITU: *Directives concerning the production of telecommunication lines against harmful effects from electric power and electrified railway lines.* International Telecommunication Union, “ITU-T”, 1998.

11 Lists of Figures and Tables

11.1 Figures

11.2 Tables

12 Appendix

12.1 Pipeline Parameters

Network Element or derived term	**Bitumen-Coating** ru = 10 kΩm^2			**PE-Coating** ru = 100 kΩm^2			
	1 kHz	**10 kHz**	**50 kHz**	**1 kHz**	**10 kHz**	**50 kHz**	**Most Determining Factors**
r_{L0} (Ω/km)	0.23	0.72	1.60	0.023	0.72	1.60	f,R_L
r_e (Ω/km)	0.99	9.87	49.35	0.99	9.87	49.35	f
x_L(Ω/km)	0.23	16.76	134.36	0.23	16.76	134.36	f, R_L, ρ
x_{iL0} (Ω/km)	0.23	0.72	1.60	0.23	0.72	1.60	f, R_L
Z_L'(Ω/km)	1.21+ 0.0029 j	10.59+ 16.04 j	50.95+ 132.76 j	1.21+ 0.0029 j	10,59+ 16.04 j	50.95+ 132.76 j	f, R_L, ρ
|Z_L'|(Ω/km)	1.21	19.22	142.20	1.21	19.22	142.20	f, R_L, ρ
$r_{L\ 1km}$ (Ω)	1.21	10.58	50.95	1.21	10.58	50.95	f, R_L
$l_{L\ 1km}$ (µH)	45.04	255.34	422.58	45.04	255.34	422.58	f, R_L, ρ
g_L(mS/km)	157.1	157.1	157.1	15.71	15.71	15.71	r_u, R_L
b_L(mS/km)	146.5	1465.2	7325.9	146.5	1465.2	7325.9	f, R_L
Y_L'(mS/km)	157.1+ 146.5 j	157.1+ 1565.2 j	157.1+ 7325.9 j	15.71+ 146.5 j	15.71+ 1465.2 j	15.71+ 7325.9 j	r_u, f, R_L
$r_{p\ 1km}$ (Ω)	6.37	6.37	6.37	63.66	63.66	63.66	r_u, R_L
$c_{p\ 1km}$ (µF)	23.32	23.32	23.32	23.32	23.32	23.32	R_L
|$Z_{Pipeline}$|$_{1km}$ (Ω)	4.88	1.28	0.27	6.84	1.29	0.27	f, ru

Table 12.1: Sensitivity table for elements of pipeline equivalent network for high frequencies

12.2 Coating Holidays

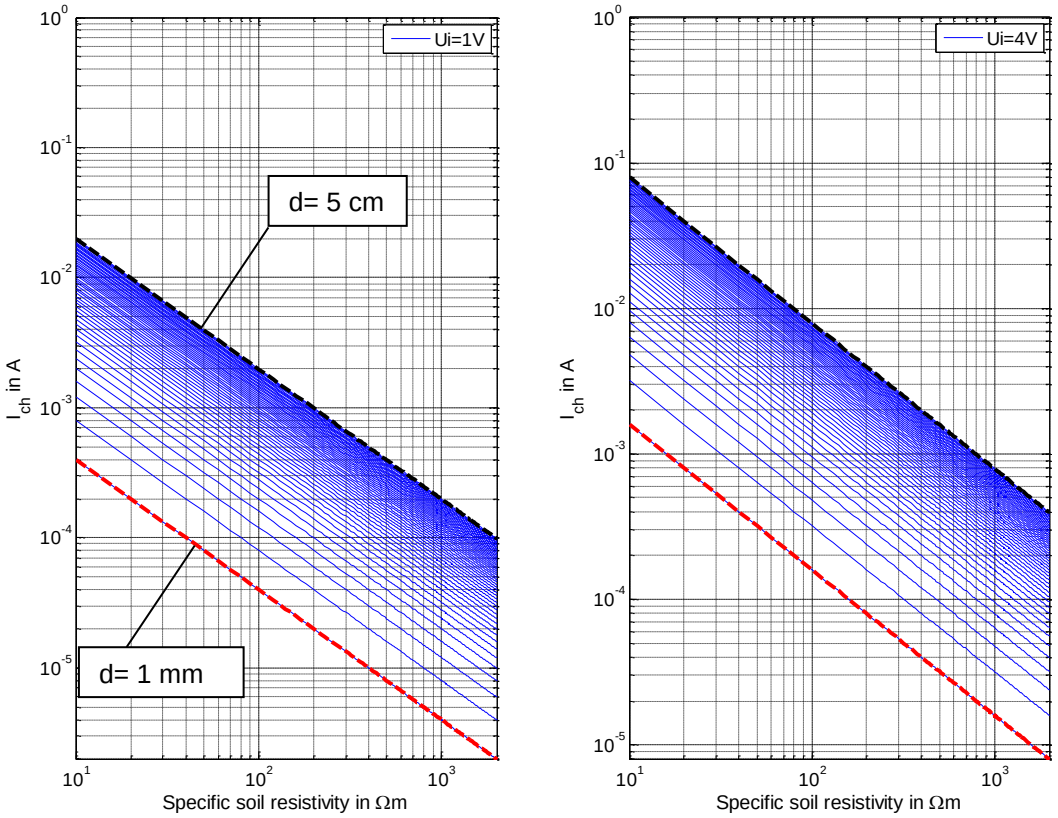

Figure 12.1: Coating holiday current I_{ch} plotted against ρ for variable coating holiday diameters and the selected pipeline interference voltages 1 V and 4 V

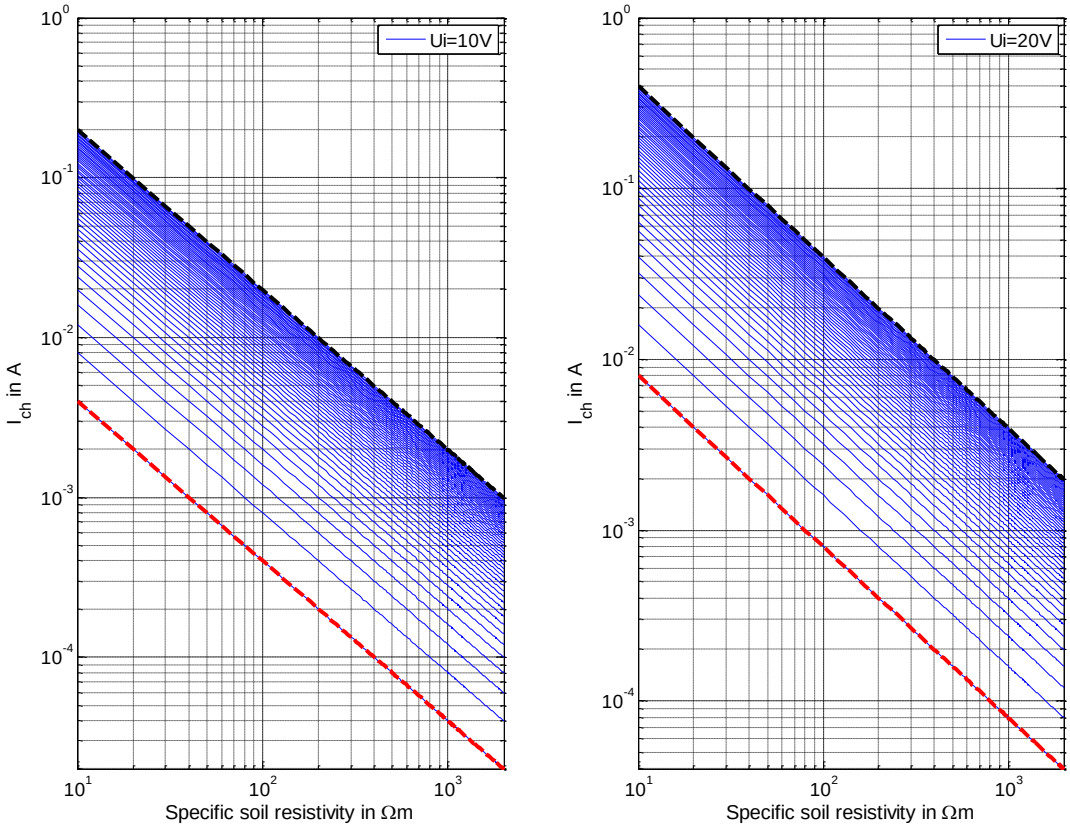

Figure 12.2: Coating holiday current I_{ch} plotted against ρ for variable coating holiday diameters and the selected pipeline interference voltages 10 V and 20 V

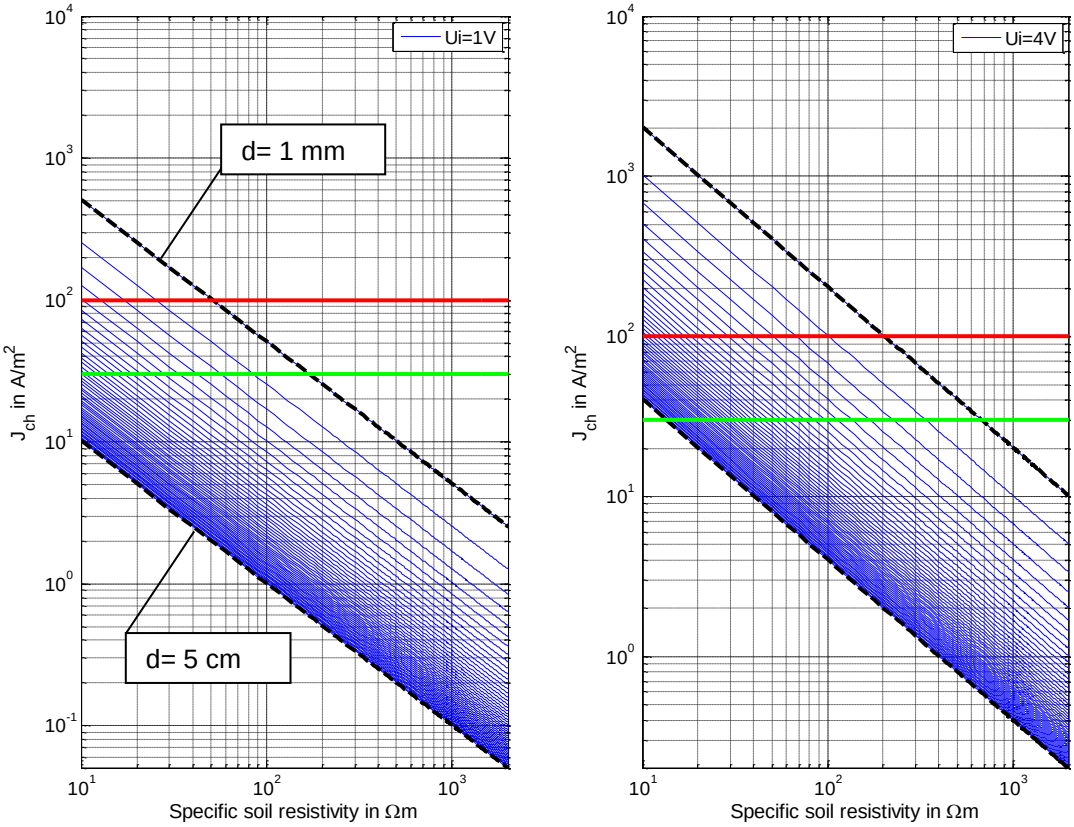

Figure 12.3: Current density at coating holidays J_{ch} plotted against ρ for variable coating holiday diameters and the selected pipeline interference voltages 1 V and 4 V, red line: 100 A/m^2 limit, green line: 30 A/m^2-limit

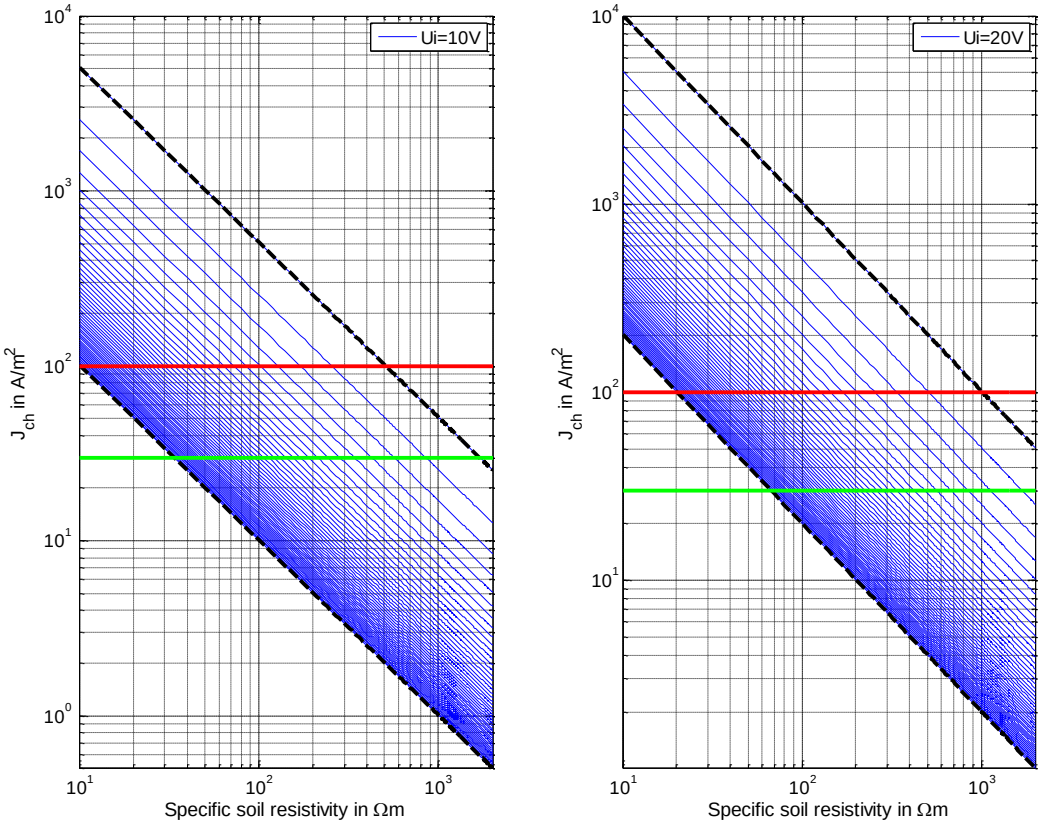

Figure 12.4: Current density at coating holidays J_{ch} plotted against ρ for variable coating holiday diameters and the selected pipeline interference voltages 10 V and 20 V, red line: 100 A/m^2 limit, green line: 30 A/m^2-limit

12.3 Simulation Parameters

If the assumed simulation parameters are not included in the full text of this thesis, they are listed below:

Figure 2.8: Length if the pipeline l=100 %, 50 pipeline segments with a constant length of 2 %, constant interference voltages in longitudinal direction for every pipeline segments between 20 % and 80%, no interference voltages from 0 % - 20% and 80% - 100 %, pipeline covering resistivity r_u = 100000 Ωm^2, specific soil resistivity ρ= 100 Ωm, pipeline diameter d= 400 mm. Interfering frequency f=50 Hz.

Figure 2.10: Length if the pipeline l=100 %, 50 pipeline segments with a constant length of 2 %, constant interference voltages in longitudinal direction for every pipeline segments between 20 % and 50%, no interference voltages from 0 % - 20% and 50% - 100 %, pipeline covering resistivity r_u = 100000 Ωm^2, specific soil resistivity ρ= 100 Ωm, pipeline diameter d= 400 mm. Interfering frequency f=50 Hz.

Figure 4.3: Length if the pipeline l=20 km, 40 pipeline segments with 500 m, constant interference of 10 V in longitudinal direction for every pipeline segment, railway reduction factor = 0.5, pipeline covering resistivity r_u = 100000 Ωm^2, specific soil resistivity ρ= 100 Ωm, pipeline diameter d= 800 mm. Interfering frequency f=16.7 Hz.

Figure 4.6: Length if the pipeline l=20 km, 40 pipeline segments with 500 m, constant interference 10 V in longitudinal direction for every pipeline segment, railway reduction factor = 0.5, pipeline covering resistivity r_u = 100000 Ωm^2, specific soil resistivity ρ= 100 Ωm, pipeline diameter d= 800 mm. Interfering frequency f=16.7 Hz.

Figure 4.8: Length if the pipeline l=20 km, 40 pipeline segments with 500 m, inconstantly interference: 0 V in longitudinal direction for pipeline segments 1-10 and 22-41, 15 V in direct axis for pipeline segments 11-21, railway reduction factor R_{FR} = 0.5, pipeline covering resistivity r_u = 100000 Ωm^2, specific soil resistivity ρ= 100 Ωm, pipeline diameter d= 800 mm. Interfering frequency f=16.7 Hz.

Figure 4.10: Phase conductor diameter d= 32.2 mm, Earth wire diameter d= 21.4 mm, pipeline diameter d= 800 mm, compensation conductor diameter= 21.4 mm, phase currents = 1000 A with 0°, 120° and 240°. Phase coordinates (x/y) of overhead line: Phase 1: -3.5 m/ 20 m, Phase 2: 0 m/20 m, Phase 3: 3.5 m/ 20 m. Earth wire coordinates (x/y): 0 m/25 m, Pipeline coordinates (x/y): -50 m/ -1 m, Compensation conductor coordinates (x/y): variable/ -- 1 m. Interfering frequency f=50 Hz.

Figure 4.11: Phase conductor diameter d= 32.2 mm, Earth wire diameter d= 21.4 mm, pipeline diameter d= 800 mm, compensation conductor diameter= 21.4 mm, phase currents = 1000 A with 0°, 120° and 240°. Phase coordinates (x/y) of overhead line: Phase 1: -3.5 m/ 20 m, Phase 2: 0 m/20 m, Phase 3: 3.5 m/ 20 m. Earth wire coordinates (x/y): 0 m/25 m, Pipeline coordinates (x/y): -50 m/ -1 m, Compensation conductor coordinates (x/y): variable/ between- 0.5 m and -2 m. Interfering frequency f=50 Hz.

Figure 4.19: Simulation curve: 31 pipeline segments with an average length of 300 m, average voltage in longitudinal direction 17 V for every pipeline segment, railway reduction factor R_{FR} = 0.32, pipeline covering resistivity r_u = 100000 Ωm^2, specific soil resistivity ρ= 100 Ωm, pipeline diameter d= 150 mm. Interfering frequency f=16.7 Hz.

Figure 4.20: Length if the pipeline 10 km, 20 pipeline segments with an average length of 500 m, railway reduction factor R_{FR} = 0.25, pipeline covering resistivity r_u = 100000 Ωm^2 and 30000 Ωm^2 , specific soil resistivity ρ= 100 Ωm, pipeline diameter d= 800 mm. Interfering frequency f=50 Hz.

Figure 4.22: Length if the pipeline 10 km, 20 pipeline segments with a length of 500 m, pipeline covering resistivity r_u = 100000 Ωm^2 , specific soil resistivity ρ= 100 Ωm, pipeline diameter d= 1000 mm. Interfering frequency f=50 Hz.

Figure 5.2: Length if the pipeline 20 km, 40 pipeline segments with a length of 500 m, pipeline covering resistivity r_u = 100000 Ωm^2 , specific soil resistivity ρ= 100 Ωm, pipeline diameter d= 800 mm. Interfering frequency f=16.7 Hz.

Figure 5.3: Length if the pipeline 20 km, 40 pipeline segments with a length of 500 m, pipeline covering resistivity r_u = 100000 Ωm^2 , specific soil resistivity ρ= 100 Ωm, pipeline diameter d= 800 mm. Interfering frequency f=16.7 Hz.

Figure 5.11: specific soil resistivity ρ= 100 Ωm, railway reduction factor R_{FR} = 0.35, 10-km-approach between pipeline and interfering system, variable horizontal distances. Only maximum values of pipeline interference voltage of each approach are relevant for this figure. Interfering frequency f=16.7 Hz.

Figure 5.12: specific soil resistivity ρ= 100 Ωm, railway reduction factor R_{FR} = 0.35, 10-km-approach between pipeline and interfering system, variable horizontal distances. Only maximum values of pipeline interference voltage of each approach are relevant for this figure. Interfering frequency f=16.7 Hz.

Figure 7.3: Length if the pipeline 13.28 km, 13 pipeline segments with an average length of 1 km, specific soil resistivity ρ= 100 Ωm, railway reduction factor R_{FR} = 0.25, pipeline diameter d= 400 mm. Interfering frequencies f=16.7 Hz and 50 Hz.

Figure 7.4: Length if the pipeline 13.28 km, 13 pipeline segments with an average length of 1 km, specific soil resistivity ρ= 100 Ωm, railway reduction factor R_{FR} = 0.25, pipeline diameter d= 400 mm. Interfering frequencies f=16.7 Hz and 50 Hz.

Figure 7.5: Length if the pipeline 13.28 km, 13 pipeline segments with an average length of 1 km, specific soil resistivity ρ= 100 Ωm, railway reduction factor R_{FR} = 0.25, pipeline diameter d= 400 mm. Interfering frequencies f=16.7 Hz and 50 Hz.

Figure 7.7: Length if the pipeline 13.28 km, 13 pipeline segments with an average length of 1 km, specific soil resistivity ρ= 100 Ωm, railway reduction factor R_{FR} = 0.25, pipeline diameter d= 400 mm. Interfering frequencies f=16.7 Hz and 50 Hz.

Figure 7.9: Length if the pipeline 13.28 km, 13 pipeline segments with an average length of 1 km, specific soil resistivity ρ= 100 Ωm, railway reduction factor R_{FR} = 0.25, pipeline diameter d= 400 mm. Interfering frequencies f=16.7 Hz and 50 Hz.

Figure 7.11: Length if the pipeline 13.28 km, 13 pipeline segments with an average length of 1 km, specific soil resistivity ρ= 100 Ωm, railway reduction factor R_{FR} = 0.25, pipeline diameter d= 400 mm. Interfering frequencies f=16.7 Hz and 50 Hz.

Figure 8.3: Length if the pipeline 10 km, 20 pipeline segments with a length of 500 m, constant interference of 1.8 V in longitudinal direction for every pipeline segment specific soil resistivity ρ= 100 Ωm, pipeline diameter d= 400 mm. Interfering frequency f=50Hz.

Figure 8.5: Length if the pipeline 10 km, 20 pipeline segments with a length of 500 m, constant interference of 1.8 V in longitudinal direction for every pipeline segment specific soil resistivity ρ= 100 Ωm, pipeline diameter d= 400 mm. Interfering frequency f=50Hz.